Non-perturbative phenomena in gauge theory on S^3

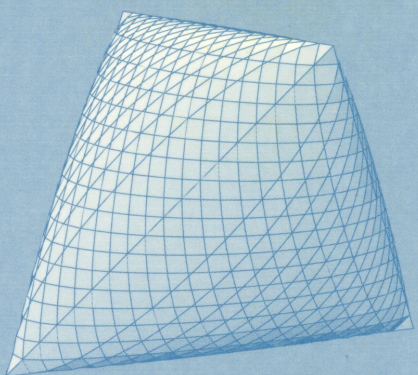

B.M. van den Heuvel

Kast dissertaties

Non-perturbative phenomena in gauge theory on S^3

Non-perturbative phenomena in gauge theory on S^3

PROEFSCHRIFT

TER VERKRIJGING VAN DE GRAAD VAN DOCTOR
AAN DE RIJKSUNIVERSITEIT TE LEIDEN, OP GEZAG
VAN DE RECTOR MAGNIFICUS DR. L. LEERTOUWER,
HOOGLERAAR IN DE FACULTEIT DER GODGELEERDHEID,
VOLGENS BESLUIT VAN HET COLLEGE VAN DEKANEN
TE VERDEDIGEN OP WOENSDAG 11 SEPTEMBER 1996
TE KLOKKE 16.15 UUR

DOOR

Bastiaan Matthijs van den Heuvel

GEBOREN TE DUBBELDAM OP 4 NOVEMBER 1969

Promotiecommissie:

Promotor:	Prof.dr. P.J. van Baal
Referent:	Dr. W.L.G.A.M. van Neerven
Overige leden:	Prof.dr. F.A. Bais (Universiteit van Amsterdam)
	Prof.dr. C.W.J. Beenakker
	Prof.dr. G. 't Hooft (Rijksuniversiteit Utrecht)
	Prof.dr. L.J. de Jongh

. . . und über die Metaphysik der Leberwurst
ist selten Gehaltvolleres gesagt worden, als
ich es in meiner Dissertation zu Leyden tat.
Hermann Hesse

Contents

1 Introduction

1.1 Perspective

High-energy physics is that branch of science that seeks to explain the interactions between the elementary constituents of matter. In order of rising strength, the four fundamental forces in nature are the gravitational, weak, electromagnetic and strong force. The particles that carry these forces are respectively the gravitons, the W and Z bosons, the photons and the gluons. All other matter consists of force-feeling particles. These can be divided in leptons and hadrons: the hadrons are by definition sensitive to the strong force, the leptons (e.g. electrons, neutrinos) are not. The leptons are believed to be elementary particles, whereas the hadrons are composed of quarks. Thus mesons (e.g. pions) consist of a quark-antiquark pair and the heavier baryons (e.g. protons, neutrons) consist of three quarks. There are six different quarks. These are the flavours up, down, strange, charm, top (or truth) and bottom (or beauty).

The biggest issue in the theory of strong interaction is the problem of confinement. This is the observation that the quarks, contrary to the leptons, do not exist as free particles, but are always locked up in hadrons. When constructing hadron states in the spectrum from quarks, a new quantum number is needed in order to obey the Pauli exclusion principle. This quantum number is colour which takes the 'values' red, green and blue. The confinement property can now be rephrased by stating that only colourless states can occur as physical particles.

Quantum chromodynamics (QCD) is generally assumed to be the correct theory of the strong interactions. It is a generalization of quantum electrodynamics (QED) which describes electromagnetism. In both theories, the fundamental matter fields are fermion fields (electrons respectively quarks) that interact through a minimal coupling with the bosonic gauge fields (photons, gluons) that are associated with a local symmetry. In QED the local symmetry group is U(1) and corresponds to electric charge. In QCD the local symmetry group is SU(3) and corresponds to the three colours of the quarks.

One way of extracting predictions from QCD relies on perturbation theory. This is the method that was extremely successful in QED. One assumes the coupling between gluons and quarks to be small and performs perturbation theory around free quarks and gluons. Although quarks and gluons do not occur as free particles, it is still possible to obtain in this way accurate predictions for high-energetic collisions with hadrons. This is due to the property of non-abelian interactions called asymptotic freedom: at high energies the coupling goes to zero, i.e. the quarks become asymptotically free. However, the confinement problem or the calculation of the hadronic spectrum are issues that cannot be resolved within perturbative QCD.

A truly non-perturbative way of attacking QCD is the lattice method. It consists of using a lattice regularization for space-time. This renders the euclidean path integral for the theory well-defined and one can study the properties of the spectrum using methods from statistical mechanics. In view of the confinement problem, the quark-antiquark potential for static sources can be found to rise linearly with distance, thus strongly hinting at confinement. The picture that emerges is of a string of gluonic field between the two quarks, with an energy per length or string tension σ. When the distance becomes too large, the string breaks, but at the breaking point a new quark-antiquark pair is formed, thus ensuring that the final states will again be colourless.

In the last decade lattice QCD has had a lot of successes, but many problems still remain. For instance, to simulate the full theory (i.e. with dynamical fermions) is still extremely expensive in terms of computer time. When applying the lattice method to electroweak processes, one faces the problem that a satisfactory, simple description of chiral fermions has not yet been found.

The non-abelian nature of the gauge group in QCD leads to self-interactions of the gluons. This is in sharp contrast with the abelian theory of QED where the photons have no (direct) self-interaction. The interaction of gluons among themselves opens the possibility of a bound state of gluons, a so-called glueball. Another way of saying that gluons interact among themselves is by saying that they too carry colour charge. Hence, an appropriate combination of gluons can form a colourless object and be a physical particle or resonance. The existence of glueballs is thus also a manifestation of colour confinement. Although some resonances in the hadronic spectrum are good candidates for glueballs, one cannot claim yet that glueballs really exist in nature.

As indicated by for instance the linearly rising quark-antiquark potential, one assumes that confinement is caused by the pure gauge part of QCD. In order to understand this mechanism better one can start by removing the quark fields from the theory altogether: one retains only the purely gluonic part of QCD. This means that one studies the dynamics of just the non-abelian gauge field (or Yang-Mills field). This is the approach we shall adopt in this thesis, where we will investigate the dynamics of the pure SU(2) Yang-Mills field in a finite spatial volume. In particular, we will calculate the glueball masses within an effective model, where this effective model incorporates (for a certain range of coupling constants) the relevant non-perturbative phenomena of QCD in a new way. Changing the gauge group from SU(3) to SU(2) gives technical simplications. As compared to the more numerical lattice results, finite-volume studies can provide complementary insights. Restricting ourselves to a finite volume gives us analytic tools to investigate the onset of non-perturbative behaviour of the theory.

1.2 Gauge theory in a finite volume

The mechanism of asymptotic freedom [1] renders the coupling constant small at high energies or, equivalently, at small distances. This gives us a handle on the coupling

constant. Taking the finite volume to be small results in a small coupling constant: one can use perturbation theory. Gradually increasing the volume then allows one to study the onset of non-perturbative phenomena and to see, hopefully, the setting in of confinement. In this regime one can employ a hamiltonian formulation [2] of the problem. Our strategy in studying the dynamics of the Yang-Mills field is based on two observations. First, quantum field theory can in a sense be regarded as ordinary quantum mechanics, but with an infinite number of degrees of freedom. For the case of non-abelian gauge field theory, the configuration space of this quantum mechanical problem is complicated, which gives rise to non-perturbative behaviour. Second, coming from the perturbative regime, these complications first show up in the low-energy modes of the gauge field: one can capture the influence of the topology of the configuration space by studying the effective theory of the finite number of affected modes.

Let us first reformulate quantum field theory as quantum mechanics. For this the restriction to a finite volume is not essential: this only renders the degrees of freedom discrete. In the hamiltonian picture we are dealing with wave functionals in the configuration space. Speaking generally, each point in the configuration space corresponds to a configuration of the fields $\varphi(\vec{x})$ (one can think of ordinary φ^4 theory as an example). This means we have fields $\varphi(\vec{x})$, conjugated momenta $\Pi(\vec{x})$, a hamiltonian $H[\varphi, \Pi]$ and wave functionals $\Psi[\varphi]$. To write this in a more familiar form, we decompose the fields $\varphi(\vec{x})$ in orthogonal modes, like ordinary Fourier modes in the case of flat space. We can reformulate the hamiltonian problem in terms of the generalized Fourier coefficients q_k and their conjugate momenta p_k. This leads to a hamiltonian $H[q_k, p_k]$ and wave functionals $\Psi[q_k]$. A typical hamiltonian would look like

$$H[q_k, p_k] = \sum_k \left(p_k^2 + \omega_k q_k^2\right) + \text{interaction terms.} \tag{1.2.1}$$

At small coupling, the modes will not interact and the potential will rise quadratically in all directions. As a consequence, the wave functions will be the familiar harmonic oscillator wave functions. One subsequently uses perturbation theory to take the interactions between this infinity of modes into account. What we have just described is the ordinary perturbative approach to quantum field theory. The hamiltonian formulation for the perturbative regime is cumbersome, and the covariant path integral approach of Feynman is to be preferred. However, the perturbation scheme breaks down when at larger coupling the behaviour of the wave function for some of the modes is dictated by the properties of the configuration space, as explained below. We then have to replace these wave functions by functions that have the behaviour required by the configuration space. In this regime the hamiltonian method is superior.

An essential feature of the non-perturbative behaviour is that the wave functional spreads out and becomes sensitive to the global features of the configuration space. This spreading out of the wave functional will occur first in those directions of the configuration space where the potential energy is lowest, i.e. in the direction of the

low-energy modes of the gauge field (small ω_k). If the configuration space has non-contractable circles, the wave functionals are drastically affected by the topology when the support of the wave functional extends over the entire circle (i.e. bites in its own tail). This is what typically happens in non-abelian gauge theories. The Yang-Mills configuration space is the space of gauge orbits $\mathcal{A}/\mathcal{G}$ ($\mathcal{A}$ is the collection of gauge fields or connections, $\mathcal{G}$ the group of local gauge transformations). We know from Singer [3] that the topology of this configuration space is highly non-trivial when $\mathcal{G}$ is non-abelian. The configuration space also has a Riemannian geometry [4] that can be made explicit, once explicit coordinates are chosen on $\mathcal{A}/\mathcal{G}$. This geometry also leads to non-perturbative effects: if wave functionals are no longer localized within regions much smaller than the inverse curvature of the field space, this curvature influences the wave functionals.

One of the most prominent properties of a non-abelian gauge theory, as compared to an abelian gauge theory like QED, is the multiple vacuum structure. This means that the gauge degrees of freedom cannot be completely removed [5] by imposing a simple condition like the Coulomb gauge. After gauge fixing there will remain Gribov copies, that is, gauge equivalent gauge field configurations that all satisfy the gauge fixing condition. Intimately related to this is the existence of instantons [6]. Instantons are gauge field configurations that are solutions of the euclidean equations of motion. They can be shown to describe tunnelling between gauge copies of the vacuum, that is, tunnelling from one Gribov copy to another. The configuration sitting at the top of the tunnelling path with lowest energy barrier is called the sphaleron [7]: it is a saddle-point of the potential with one unstable mode. Let us suppose that the potential energy in the direction of the sphaleron(s) grows slowly. This means that at increasing volume the wave functionals around the different gauge copies of the vacuum will start to flow out over the instanton barriers and will develop a substantial overlap with each other. We then have the situation described above of probing the non-contractable loops in configuration space. See fig. 3-3 on page 34 to get an idea of how the potential landscape might look. This figure displays gauge copies, sphalerons and the potential in a two-dimensional subspace (consisting of low-energy modes) of the configuration space.

The use of the hamiltonian formulation is especially fruitful when the non-perturbative effects manifest themselves appreciably only in a small number of the modes of the gauge field. For this limited number of modes one defines an effective hamiltonian that takes the perturbative effect of all the other modes into account [8]. By studying the resulting ordinary quantum mechanical problem, one can go beyond purely perturbative results [9].

Apart from offering the possibility to go beyond perturbation theory, the finite-volume approach sketched above, which is sometimes called 'analytical', has the merit of being directly comparable to the numerical results of lattice calculations. For this the finite volume of the analytic approach must be chosen to be the finite volume of the lattice calculations. Putting a theory on a finite lattice necessarily means that it is put in a finite volume with certain boundary conditions. For the standard lattice

geometry, this finite volume is cubic with periodic boundary conditions, i.e. a torus.

To make the reduction of an infinite to a finite number of degrees of freedom, we use the Born-Oppenheimer approximation, which has its origin in the quantum mechanical treatment of molecules. To be specific, one can consider the hydrogen molecule, which has two electrons and two protons. Since the electrons are much lighter than the protons, one can separate the time scales. One first solves the Schrödinger problem for the electrons in the potential caused by the static protons. The obtained energy levels depend parametrically on the coordinates of the protons. These energy levels contribute to the potential of the Schrödinger problem for the protons. One says that the fast modes (the positions of the electrons) have been integrated out, and that we are left with an effective problem in the slow modes (the positions of the protons). The phrase 'integrated out' stems from the formulation of quantum mechanics using path integrals.

One can use the Born-Oppenheimer approximation in field theory to obtain an effective hamiltonian in a finite number of slow modes. Using these methods in the intermediate-volume regime for SU(2) gauge theory on the torus resulted in good agreement with the lattice results [9, 10]. However one would like to extend these results to larger volumes in an attempt to get as close as possible to the confinement domain, and in this way get some intuition about how confinement sets in. The first thing to do, as argued above, is to include contributions coming from instantons: one wants to take into account the sphaleron directions in configuration space, because there the potential will show the strongest deviation from gaussian behaviour. This is not an easy task first of all because the instanton solutions on a torus are only known numerically [11].

To avoid this problem, we have shifted our attention to the case where the finite volume is S^3, (the surface of) a three-sphere [12]. Here the instantons are known analytically, and the tunnelling paths that connect gauge copies of the vacuum lie within the space of low-energy modes. Another simplification is that the structure of the perturbative vacuum is much simpler than in the case of the torus: there is no vacuum valley, that is, there is no continuous set of minima of the classical potential. A drawback of the three-sphere is that we lose the possibility to check against lattice results. Also, the approach to infinite-volume results will go as powers of $1/R$ as compared to the exponential behaviour in L for the torus [13]. Thus, due to the intrinsic curvature of S^3, it will be even less easy to derive infinite-volume results from our calculations. Nevertheless, within this model one can study non-perturbative phenomena like the effects of large gauge transformations and especially of the θ angle on the glueball spectrum. A gauge transformation is called 'large' if it cannot be continuously deformed into the identity. Typically, two Gribov copies of the vacuum are related by a large gauge transformation. The θ angle, which will be properly defined in chapter 2, is a free parameter of the theory that one has to allow when one implements gauge invariance under large gauge transformations. Previous research into gauge theory on S^3 [14] did not include the study of the effects of large gauge transformations.

1.3 Outline

Here we will give a short description of the contents of this thesis. We study pure SU(2) gauge theory on the three-sphere. As in the torus case, the strategy is to reduce the full problem to an effective theory consisting of a hamiltonian and a set of boundary conditions in the (finite-dimensional) configuration space. These boundary conditions incorporate the non-perturbative effects of the non-contractable loops in the full configuration space.

In chapter 2 we develop the necessary machinery for the analysis on S^3. We isolate the slow modes of the theory, investigate the homotopy properties of gauge transformations on S^3, introduce the θ angle, and we show how the instanton degrees of freedom are embedded in the space of slow modes. We derive the lowest order effective hamiltonian (or truncated hamiltonian) by simply truncating the full theory to the slow modes and we indicate how to obtain the one-loop effective hamiltonian, i.e. how to integrate out the fast modes.

In chapter 3 we will describe our investigations into the configuration space for SU(2) gauge theory on S^3. We perform the gauge fixing by restricting the gauge fields to a so-called fundamental domain [15, 16]. This is a convex subset of the space of all gauge field configurations that is in one-to-one correspondence (modulo constant gauge transformations) with the space of gauge orbits $\mathcal{A}/\mathcal{G}$. The latter is precisely the physical configuration space on which we want to study the dynamics. For some parts of the configuration space one can find the boundary of the fundamental domain exactly, whereas for other parts we were able to derive upper and lower bounds on its position. Restricting the dynamics to the fundamental domain raises the need for boundary conditions to be imposed on the wave functional. These boundary conditions will depend on the θ angle.

In chapter 4 we explicitly integrate out the high-energy modes using a background field method. This not only gives us the renormalization of the coupling constant, but also the one-loop correction to the effective potential.

In chapter 5 we will use dynamical arguments to show that the boundary conditions at the sphalerons (which are on the boundary of the fundamental domain) will be most important when the wave functional starts to spread out over the full configuration space. Using this we first impose the correct boundary conditions on the space of low-energy modes and then construct a basis of functions that respect these (θ-dependent) boundary conditions. Using this basis we perform a Rayleigh-Ritz analysis to approximate the spectra of both the lowest order hamiltonian and of the one-loop corrected hamiltonian. From the eigenvalues one can obtain the masses of the different excitations (the glueballs) in this model.

Chapter 6 contains a summary and a discussion of the results. We argue that the effect of the instantons is large, but calculable. We determine the range of validity of the effective model and show that the results are in reasonable agreement with results on the torus.

2 Preliminaries

2.1 Introduction

In this chapter the necessary machinery needed for the analysis on S^3 is developed. In particular, we will write down bases of functions for scalar and vector functions on S^3. These bases of functions will be used in chapter 4 for the evaluation of various functional determinants. These functions will also allow us to isolate the space of low-energy modes on which the effective theory will be defined. After this we will familiarize ourselves with some of the topological properties of SU(2) gauge theory on the three-sphere; we will also show the intimate relation between the space of low-energy modes and the instantons. Next we will describe the derivation of the effective hamiltonian, and discuss the validity of the adiabatic approximation. In the appendix we relate our bases of functions to other descriptions of functions on S^3 [14], and we give some group theoretical background to these bases.

2.2 Low-energy modes

We begin by introducing two framings on S^3. These will lead to a basis of scalar functions. By taking tensor products of these scalar modes with eigenfunctions of the spin operator, we will construct vector functions on S^3. By a similar method we will also construct su(2)-valued functions, where su(2) denotes the Lie algebra corresponding to the Lie group SU(2). After this we will write down the space of low-energy modes for SU(2) gauge theory on S^3.

2.2.1 Two framings on the three-sphere

Let τ_a be the Pauli matrices. We introduce the unit quaternions σ_μ and their conjugates $\bar{\sigma}_\mu = \sigma_\mu^\dagger$ by

$$\sigma_\mu = (\mathbb{1}, i\vec{\tau}), \quad \bar{\sigma}_\mu = (\mathbb{1}, -i\vec{\tau}). \tag{2.2.1}$$

They satisfy the multiplication rules

$$\sigma_\mu \bar{\sigma}_\nu = \eta^a_{\mu\nu}\sigma_a, \quad \bar{\sigma}_\mu \sigma_\nu = \bar{\eta}^a_{\mu\nu}\sigma_a, \tag{2.2.2}$$

where we used the 't Hooft η symbols [17], generalized slightly to include a component symmetric in μ and ν for $\alpha = 0$. The η^i and $\bar{\eta}^i$ form bases for respectively the self-dual and anti-self-dual four by four matrices. The η symbols enjoy the following contraction identities

$$\eta^a_{\mu\nu}\eta^b_{\rho\nu} = \eta^\nu_{ab}\eta^\nu_{\mu\rho}, \quad \bar{\eta}^a_{\nu\mu}\bar{\eta}^b_{\nu\rho} = \bar{\eta}^\nu_{ab}\bar{\eta}^\nu_{\mu\rho}. \tag{2.2.3}$$

Another useful relation is

$$\eta^{\alpha}_{\beta\gamma} = \bar{\eta}^{\gamma}_{\alpha\beta}. \tag{2.2.4}$$

We can use η and $\bar{\eta}$ to define orthonormal framings of S^3, which were motivated by the particularly simple form of the instanton vector potentials in these framings (see section 2.3). We embed S^3 in $\mathbb{R}^4$ by considering the unit sphere parametrized by a unit vector n_μ. Using the scale-invariance of the classical hamiltonian, we can make the restriction to a sphere of radius $R = 1$. The R dependence can be reinstated on dimensional grounds. The framing for S^3 is obtained from the framing of $\mathbb{R}^4$ by restricting in the following equation the four-index α to a three-index a (for $a = 0$ one obtains the normal n_μ on S^3):

$$e^{a}_{\mu} = \eta^{a}_{\mu\nu} n_\nu, \quad \bar{e}^{a}_{\mu} = \bar{\eta}^{a}_{\mu\nu} n_\nu. \tag{2.2.5}$$

The orthogonal matrix V that relates these two frames is given by

$$V^{i}_{j} = \bar{e}^{i}_{\mu} e^{j}_{\mu} = \tfrac{1}{2} \operatorname{tr}((n \cdot \sigma)\sigma_i(n \cdot \bar{\sigma})\sigma_j). \tag{2.2.6}$$

Note that e and $\bar{e}$ have opposite orientations. The parity operation $\mathcal{P}$ defined by

$$\mathcal{P} : (n_0, \vec{n}) \to (n_0, -\vec{n}), \tag{2.2.7}$$

interchanges the e and the $\bar{e}$ framing.

A vector field A_μ can be written with respect to either framing (2.2.5). From now on we will, unless stated otherwise, use the framing e^{i}_{μ} and write

$$A_\mu = A_i e^{i}_{\mu}. \tag{2.2.8}$$

Since we want vector fields to be tangent to S^3 we have that $n_\mu A_\mu = 0$ and the sum over i runs from 1 to 3. Latin indices refer to this framing, while Greek indices will refer to the embedding space $\mathbb{R}^4$.

2.2.2 Scalar and vector modes on S^3

Each of the framings (2.2.5) defines a differential operator

$$\partial^{i} = e^{i}_{\mu} \frac{\partial}{\partial x^\mu}, \quad \bar{\partial}^{i} = \bar{e}^{i}_{\mu} \frac{\partial}{\partial x^\mu}, \tag{2.2.9}$$

to which belong su(2) angular momentum operators, which for historical reasons will be denoted by $\vec{L}_1$ and $\vec{L}_2$:

$$L^{i}_{1} = \tfrac{i}{2} \partial^{i}, \quad L^{i}_{2} = \tfrac{i}{2} \bar{\partial}^{i}. \tag{2.2.10}$$

They are easily seen to commute and to satisfy the condition

$$\vec{L}^2 \equiv \vec{L}_1^2 = \vec{L}_2^2. \tag{2.2.11}$$

The manifold S^3 is isomorphic to the Lie group SU(2). The spatial symmetries of S^3 correspond to the left and right action of SU(2) on itself: $so(4) = su(2) \oplus su(2)$. In the appendix we will show explicitly that $\vec{L}_1$ and $\vec{L}_2$ correspond to the generators of the left and right symmetries on SU(2).

A basis of scalar functions on S^3 is given by the set of eigenfunctions of the commuting operators $\{\vec{L}^2, L_{1z}, L_{2z}\}$:

$$|l\, m_L\, m_R\rangle, \qquad l = 0, \tfrac{1}{2}, 1, \ldots, \quad m_L, m_R = -l, \ldots, l. \tag{2.2.12}$$

Since the laplacian on S^3 is given by $\partial_i \partial_i = -4\vec{L}^2$, these modes are eigenfunctions of the spherical laplacian with eigenvalue $-4l(l+1)$ and degeneracy $(2l+1)^2$.

To classify vector fields A_i on S^3, we introduce a spin operator $\vec{S}$ by $(S^a A)_i = -i\varepsilon_{aij} A_j$. This is an su(2) angular momentum operator that commutes with $\vec{L}_1$ and $\vec{L}_2$. We also define $\vec{K} = \vec{L} + \vec{S}$, which is shorthand for $\vec{K}_{ij} = \vec{L}\,\delta_{ij} + \vec{S}_{ij}$. When there is no confusion possible, we will write $\vec{L}$ for $\vec{L}_1$. The fact that we single out $\vec{L}_1$ is related to the fact that we chose e^i_μ as the preferred framing for expressing vector fields. A basis of vector fields can be obtained by taking tensor products of the scalar functions (2.2.12) with the basis functions $|1\, m_s\rangle$ of the spin operator. In the standard way one obtains eigenfunctions of the set $\{\vec{K}, \vec{L}_2\}$:

$$|l\, m_R; k\, m_k\rangle, \qquad l = 0, \tfrac{1}{2}, 1, \ldots, \quad k = |l-1|, \ldots, l+1. \tag{2.2.13}$$

The three modes with $(l,k) = (0,1)$ are the three vector fields e^i_μ. The three vector fields $\bar{e}^j_\mu = V^j_i e^i_\mu$ correspond to the modes with $(l,k) = (1,0)$, as can be seen from $L^k_1 V^j_i = i\varepsilon_{kim} V^j_m$. To identify transversal and longitudinal modes, first note that $\partial_\mu A_\mu = \partial_i A_i$. Next we introduce the operator Q via $Q_{ij} = L_i L_j$. Note that $QA = 0$ for A in the Coulomb gauge. Using the identity

$$\left(\vec{L}\cdot\vec{S}\right)^2 = \vec{L}^2 - \vec{L}\cdot\vec{S} - Q, \tag{2.2.14}$$

one concludes that the modes with $k = l \pm 1$ are transverse, whereas the modes with $k = l$ are purely longitudinal.

To deal with su(2)-valued functions, we introduce the isospin operator $\vec{T}$ by $T^a = \mathrm{ad}\,(\frac{1}{2}\tau_a)$, where $\mathrm{ad}\,(X)(Y) \equiv [X,Y]$. This operator is yet another su(2) angular momentum operator that commutes with all operators defined before. By taking tensor products of the functions obtained so far with the basis functions $|1\, m_t\rangle$ of $\vec{T}$, we can construct scalar and vector modes that take their values in su(2). Introducing $\vec{J} = \vec{L} + \vec{T}$ we obtain for the su(2)-valued scalar functions (e.g. infinitesimal gauge transformations on S^3)

$$|l\, m_R; j\, m_j\rangle, \qquad l = 0, \tfrac{1}{2}, 1, \ldots, \quad j = |l-1|, \ldots, l+1. \tag{2.2.15}$$

For the vector functions (e.g. gauge fields on S^3) we define $\vec{J} = \vec{K} + \vec{T}$ and obtain

$$\begin{aligned} &|l\, m_R; k; j\, m_j\rangle, \qquad l = 0, \tfrac{1}{2}, 1, \ldots, \quad k = |l-1|, \ldots, l+1, \\ &\qquad\qquad\qquad\qquad\quad j = |k-1|, \ldots, k+1. \end{aligned} \tag{2.2.16}$$

Generalizing to the case where $\vec{S}$ and $\vec{T}$ correspond to respectively a spin-s and a spin-t representation, we obtain (suppressing the m_R dependence)

$$|t;(ls)k;j\,m_j\rangle, \qquad \begin{array}{l} l=0,\frac{1}{2},1,\ldots, \quad k=|l-s|,\ldots,l+s, \\ j=|k-t|,\ldots,k+t. \end{array} \tag{2.2.17}$$

The scalar modes are recovered by the choice $s=0$, $t=1$, the vector modes correspond to the choice $s=1$, $t=1$.

The functions defined so far will be used extensively in chapter 4 for the evaluation of functional determinants and traces. In chapter 3 we will also make use of the operator $\vec{J}=\vec{L}_1+\vec{L}_2+\vec{T}$ and of the corresponding eigenfunctions.

2.2.3 The quadratic fluctuation operator

An SU(2) gauge field on the three-sphere can be written as

$$A_\mu = A_i e^i_\mu = A^a_i e^i_\mu \frac{\sigma_a}{2}. \tag{2.2.18}$$

The field strength F is given by

$$F_{ij} = \partial_i A_j - \partial_j A_i + [A_i, A_j] - 2\varepsilon_{ijk}A_k, \tag{2.2.19}$$

where the last term is the so-called spin-connection: it is a consequence of the fact that we used a framing on the curved manifold S^3. Reinstating the radius R would lead to a factor $1/R$ for this last term, which shows that this term vanishes in the limit of no curvature, i.e. for $R\to\infty$. A gauge transformation $g: S^3\times\mathbb{R}\to SU(2)$ acts as follows:

$$({}^gA)_i = g^{-1}A_i g + g^{-1}\partial_i g = g^{-1}D_i(A)g, \tag{2.2.20}$$

where $D(A)$ denotes the covariant derivative in the fundamental representation. As usual, the field strength F transform under the adjoint representation

$$({}^gF)_{ij} = g^{-1}F_{ij}g. \tag{2.2.21}$$

In order to isolate the lowest energy levels, we examine the potential energy

$$V(A) = -\frac{1}{2\pi^2}\int_{S^3}\tfrac{1}{2}\,\mathrm{tr}(F^2_{ij}). \tag{2.2.22}$$

Note the factor $2\pi^2$ that we absorbed in the potential. We define the quadratic fluctuation operator $\mathcal{M}$ by

$$V(A) = -\frac{1}{2\pi^2}\int_{S^3}\mathrm{tr}(A_i\mathcal{M}_{ij}A_j) + \mathcal{O}\left(A^3\right). \tag{2.2.23}$$

This gives

$$\mathcal{M}_{ij} = 2\vec{L}^2\delta_{ij} + 2\vec{K}^2_{ij} - 4Q_{ij}. \tag{2.2.24}$$

Using $\vec{S}^2 = 2$ and eq. (2.2.14) one rewrites

$$\mathcal{M}_{ij} = \left(\vec{K}^2 - \vec{L}^2\right)^2_{ij}. \tag{2.2.25}$$

Now focus on the modes (2.2.16). For $l = 0$, we have $k = 1$ and $\mathcal{M} = 4$. The 9 eigenmodes are $A^a_i = c^a_i$ with c^a_i constant. For $l = \frac{1}{2}$, the modes with $k = \frac{1}{2}$ are pure gauge ($\mathcal{M} = 0$ and $Q \neq 0$), whereas the modes with $k = \frac{3}{2}$ are physical with $\mathcal{M} = 9$. For $l \geq 1$, the modes with $k = l - 1$ have $\mathcal{M} = (2l)^2$, the modes with $k = l + 1$ have $\mathcal{M} = (2(l+1))^2$ and the modes with $k = l$ are again pure gauge. In particular the 9 modes with $l = 1$, $k = 0$ have $\mathcal{M} = 4$ and are given by $A^a_i = d^a_m V^m_i$ with d^a_m constant. The lowest eigenspace of $\mathcal{M}$ is thus 18 dimensional and given by

$$A_\mu(c,d) = \left(c^a_i + d^a_j V^j_i\right) e^i_\mu \frac{\sigma_a}{2} = \left(c^a_i e^i_\mu + d^a_j \bar{e}^j_\mu\right) \frac{\sigma_a}{2}. \tag{2.2.26}$$

This is the space on which we will build the effective theory.

If we introduce the symmetric matrices $X = cc^T$ and $Y = dd^T$, we obtain the following form for the potential energy V of eq. (2.2.22) in the (c,d) space:

$$V(c,d) = V(c) + V(d) + \tfrac{1}{3}(\mathrm{tr}(X)\,\mathrm{tr}(Y) - \mathrm{tr}(XY)), \tag{2.2.27}$$

$$V(c) = 2\,\mathrm{tr}(X) + 6\det c + \tfrac{1}{4}\left(\mathrm{tr}^2(X) - \mathrm{tr}(X^2)\right). \tag{2.2.28}$$

2.3 Winding numbers and instantons

Before writing down the instantons, we first introduce the notions of winding number and topological charge. The reader is referred to [18] for more details.

In the $A_0 = 0$ gauge, the set of gauge transformations $\mathcal{G}$ consists of mappings

$$g : S^3 \to SU(2) \cong S^3. \tag{2.3.1}$$

As a consequence, $\mathcal{G}$ splits up in distinct classes that can be labelled by the winding number of the gauge transformations in that class:

$$n[g] = \frac{-1}{24\pi^2} \int_{S^3} \varepsilon_{ijk}\,\mathrm{tr}\left((g^{-1}\partial_i g)(g^{-1}\partial_j g)(g^{-1}\partial_k g)\right). \tag{2.3.2}$$

Gauge transformations with zero winding number can be continuously deformed into the identity mapping, whereas mappings with non-zero winding number cannot. The latter mappings are sometimes referred to as 'large' or 'homotopically non-trivial' gauge transformations.

Related to this, we define the standard Chern-Simons functional that measures the topological charge of a gauge field configuration:

$$Q[A] = \frac{1}{16\pi^2} \int_{S^3} \varepsilon_{ijk}\,\mathrm{tr}\left(A_i F_{jk} - \tfrac{2}{3} A_i A_j A_k\right). \tag{2.3.3}$$

The sign of $n[g]$ was chosen such that we have $Q[{}^g A] = Q[A] + n[g]$.

In the hamiltonian picture, gauge invariance is implemented through Gauss' law, which implies invariance of the wave functional under small gauge transformations. For large gauge transformations, we have to allow for a possible θ angle:

$$\psi[{}^g A] = e^{in[g]\theta}\psi[A]. \tag{2.3.4}$$

The (anti-)instantons [6] in the framings (2.2.5), obtained from those on $\mathbb{R}^4$ by interpreting the radius in $\mathbb{R}^4$ as the exponential of the time t in the geometry $S^3 \times \mathbb{R}$, become ($\vec{\varepsilon}$ and $\vec{A}$ are defined with respect to the framing e^a_μ for instantons and with respect to the framing $\bar{e}^a_\mu$ for anti-instantons)

$$A_0 = \frac{\vec{\varepsilon}\cdot\vec{\sigma}}{2(1+\varepsilon\cdot n)}, \qquad A_a = \frac{\vec{\sigma}\wedge\vec{\varepsilon} - (u+\varepsilon\cdot n)\vec{\sigma}}{2(1+\varepsilon\cdot n)}, \tag{2.3.5}$$

where

$$u = \frac{2s^2}{1+b^2+s^2}, \qquad \varepsilon_\mu = \frac{2sb_\mu}{1+b^2+s^2}, \qquad s = \lambda e^t. \tag{2.3.6}$$

The instanton describes tunnelling from $A = 0$ (Q=0) at $t = -\infty$ to $A_a = -\sigma_a$ (Q=1) at $t = \infty$, over a potential barrier that is lowest when $b_\mu \equiv 0$. This configuration (with $b_\mu = 0$, $u = 1$) corresponds to a sphaleron [7], i.e. the vector potential $A_a = \frac{-\sigma_a}{2}$ is a saddle point of the energy functional with one unstable mode, corresponding to the direction (u) of tunnelling. At $t = \infty$, $A_a = -\sigma_a$ has zero energy and is a gauge copy of $A_a = 0$ by a gauge transformation $g = n\cdot\bar{\sigma}$ with winding number one, since

$$n\cdot\sigma\partial_a n\cdot\bar{\sigma} = -\sigma_a. \tag{2.3.7}$$

We will be concentrating our attention to the c and d modes of eq. (2.2.26). These modes are degenerate in energy to lowest order with the modes that describe tunnelling through the sphaleron and "anti-sphaleron". The latter corresponds to the configuration with the minimal barrier height separating $A = 0$ from its gauge copy by a gauge transformation $g = n\cdot\sigma$ with winding number -1. The anti-sphaleron is actually a copy of the sphaleron under this gauge transformation, as can be seen from eq. (2.3.5), since

$$n\cdot\bar{\sigma}e^a_\mu\sigma_a n\cdot\sigma = -\bar{e}^a_\mu\sigma_a. \tag{2.3.8}$$

The two-dimensional space containing the tunnelling paths through the sphalerons is consequently parametrized by u and v through

$$A_\mu(u,v) = \left(-ue^a_\mu - v\bar{e}^a_\mu\right)\frac{\sigma_a}{2} = A_i(u,v)e^i_\mu, \tag{2.3.9}$$

$$A_i(u,v) = \left(-u\delta^a_i - vV^a_i\right)\frac{\sigma_a}{2} = -u\frac{\sigma_i}{2} + v\,n\cdot\bar{\sigma}\frac{\sigma_i}{2}n\cdot\sigma. \tag{2.3.10}$$

The gauge transformation with winding number -1 is easily seen to map $(u,v) = (w,0)$ into $(u,v) = (0,2-w)$. In particular, as discussed above, it maps the sphaleron $(1,0)$ to the anti-sphaleron $(0,1)$. Comparing with eq. (2.2.26) shows that we obtain the (u,v) space from the (c,d) space by the choice $c^a_i = -u\delta^a_i$ and $d^a_i = -v\delta^a_i$.

2.4 Reduction to a quantum mechanical problem

Let us start with the naive derivation of the hamiltonian for the (c,d) modes. From the lagrangian

$$L = -\frac{1}{4g^2}\int_{S^3} F^a_{\mu\nu}F^{a\mu\nu} = \frac{1}{2g^2}\int_{S^3} F^a_{0i}F^a_{0i} - \frac{2\pi^2}{g^2}V(A), \tag{2.4.1}$$

we obtain for the (c,d) space

$$L = \frac{2\pi^2}{2g^2}\left(\dot{c}^a_i\dot{c}^a_i + \dot{d}^a_i\dot{d}^a_i\right) - \frac{2\pi^2}{g^2}V(c,d). \tag{2.4.2}$$

This leads to the hamiltonian

$$\mathcal{H} = -\frac{f}{2}\left(\frac{\partial^2}{\partial c^a_i \partial c^a_i} + \frac{\partial^2}{\partial d^a_i \partial d^a_i}\right) + \frac{1}{f}V(c,d), \quad f = \frac{g^2}{2\pi^2}, \tag{2.4.3}$$

with the potential $V(c,d) = V_{\rm CJ}(c,d)$ given by eq. (2.2.27).

The correct way to obtain the effective hamiltonian for the (c,d) modes must start from the full theory. In the case where the finite volume is the three-torus all zero momentum states become degenerate with the ground state at $g = 0$. This infinite degeneracy allows one to derive an effective hamiltonian for these states using degenerate hamiltonian perturbation theory starting from the full hamiltonian $\widehat{\mathcal{H}}$ [8]. This full hamiltonian in the Coulomb gauge is given in [2]. Proceeding to higher order in this way is complicated, mainly due to the non-abelian Coulomb Green function that occurs in the kinetic part of the hamiltonian, but it can be done [19].

For the case of the three-sphere however, the ground state at $g = 0$ is non-degenerate. The (c,d) modes are in this respect not the analogue of the zero momentum modes on the torus, but are singled out just because of the fact that they are the slow modes of the system. To calculate the effective hamiltonian for these modes, we compute the effective action for the (c,d) degrees of freedom using a background field method. This explicit calculation will be performed in chapter 4.

We will use the hamiltonian formulation of the full problem for the discussion of the validity of restricting ourselves to the (c,d) space. Let x denote the 18 (c,d) modes and q all the transverse modes orthogonal to the (c,d) space. We use p_x and p_q to denote the conjugate momenta. The full hamiltonian in the Coulomb gauge [2] is a function of x, p_x, q and p_q. We define

$$\mathcal{H}_{[x]} = \widehat{\mathcal{H}}(x, p_x = 0, q, p_q). \tag{2.4.4}$$

Consider the following decomposition of the full wave function

$$\Psi = \sum_{n=1}^{\infty} \varphi^{(n)}(x)\chi^{(n)}_{[x]}(q), \tag{2.4.5}$$

where the functions $|n\rangle = \chi^{(n)}_{[x]}(q)$ are chosen to be eigenstates of $\mathcal{H}_{[x]}$:

$$\mathcal{H}_{[x]}\chi^{(n)}_{[x]}(q) = V^{(n)}(x)\chi^{(n)}_{[x]}(q). \tag{2.4.6}$$

The Schrödinger equation $\widehat{\mathcal{H}}\Psi = E\Psi$ is equivalent to the following set of equations:

$$\langle n|\widehat{\mathcal{H}}(x,p_x,q,p_q)\left(\sum_{m=1}^{\infty}\varphi^{(m)}(x)|m\rangle\right) = E\varphi^{(n)}(x) \quad \forall n. \tag{2.4.7}$$

As an example we assume the following form for the full hamiltonian,

$$\widehat{\mathcal{H}} = -\frac{f}{2}\frac{\partial^2}{\partial x_i^2} + \frac{1}{f}V_{\rm cl}(x) + \mathcal{H}_{[x]}(q,p_q). \tag{2.4.8}$$

This would be the form of the full hamiltonian if we neglect the complications of the non-abelian Coulomb Green function. The Schrödinger equation for this case leads to

$$-\frac{f}{2}\sum_m \vec{\nabla}^2_{nm}\varphi^{(m)}(x) + (\frac{1}{f}V_{\rm cl}(x) + V^{(n)}(x))\varphi^{(n)}(x) = E\varphi^{(n)}(x) \quad \forall n. \tag{2.4.9}$$

Here we introduced the covariant derivative ∇ by

$$\nabla^i_{nm} = \frac{\partial}{\partial x_i}\delta_{nm} + \langle n|\frac{\partial}{\partial x_i}|m\rangle = \frac{\partial}{\partial x_i}\delta_{nm} - A^i_{nm}. \tag{2.4.10}$$

The adiabatic approximation consists of truncating this equation to $\varphi^{(1)}$, that is, we assume the transverse wave function to be in its ground state and we assume this ground state to decouple dynamically from the excited states. This approximation is valid if either the coefficients A^i_{nm} are small, or if we are in the region where the energy difference $V^{(2)}(x) - V^{(1)}(x)$ is large compared to the excitation energies of the states we are interested in.

Returning to the general problem, the equations for the functions $\varphi^{(n)}(x)$ will not just contain the functions A_{nm} defined above, but more general matrix elements of the form

$$\langle n|f(p_x,q,p_q)|m\rangle. \tag{2.4.11}$$

Still, if the excitation energies are small compared to $V^{(2)}(x) - V^{(1)}(x)$, the higher φ's will be small and we can restrict eq. (2.4.7) to $\varphi^{(1)}$.

Appendix A: Details on the basis

In this appendix we will exploit the relation between S^3 and SU(2) to rederive the basis (2.2.12). After this we will make the link with the definition of functions on S^n in terms of homogeneous polynomials in the coordinates of the embedding space. This last method will also be used when we come to construct a variational basis in configuration space for the effective model. We will also describe an alternative to (2.2.13) which is due to Cutkosky [14].

A.1 The SU(2) group structure of S^3

There is a one-to-one correspondence between points of S^3 and SU(2) given by $g = n \cdot \sigma$. For instance, the matrix V_j^i of eq. (2.2.6) can in this light be seen as the adjoint representation of SU(2). The group of spatial symmetries of S^3 is SO(4). These symmetries correspond to the left and right symmetries on SU(2). Let ψ be a function on SU(2) or equivalently on S^3. SU(2) can now act on this function by left or right multiplication:

$$\left(\mathcal{D}^L(g_1)\psi\right)(g) = \psi(g_1^{-1}g), \quad \left(\mathcal{D}^R(g_2)\psi\right)(g) = \psi(gg_2), \quad g, g_1, g_2 \in \mathrm{SU}(2). \tag{A.1}$$

These infinite-dimensional representations of the group SU(2) induce representations of the Lie algebra su(2). We will show that the generators $\mathcal{L}$ of these representations correspond to $\vec{L}_1$ and $\vec{L}_2$:

$$\begin{aligned}
\left(i\mathcal{L}_j^L\psi\right)(g) &= \frac{d}{dt}\psi(\exp(-it\tfrac{1}{2}\tau_j)g)|_{t=0} \\
&= \frac{d}{dt}\psi(n\cdot\sigma + \tfrac{1}{2}t\bar{\sigma}_j n\cdot\sigma)|_{t=0} \\
&= \frac{d}{dt}\psi((n_\alpha + \tfrac{1}{2}t\bar{\eta}^\alpha_{j\mu}n_\mu)\sigma_\alpha)|_{t=0} \\
&= \tfrac{1}{2}\eta^j_{\mu\alpha}n_\mu\frac{\partial}{\partial x_\alpha}\psi(n) = \left(iL_1^j\psi\right)(n).
\end{aligned} \tag{A.2}$$

According to the Peter-Weyl theorem [20], a basis of functions on SU(2) is provided by the collection of matrix elements of all the finite-dimensional unitary irreducible representations of SU(2). Let D^j denote the standard $(2j+1)$-dimensional representation of su(2):

$$D^j_{mm'}(\tfrac{1}{2}\tau_3) = m\,\delta_{mm'}, \tag{A.3}$$

$$D^j_{mm'}(\tfrac{1}{2}\tau_+) = \sqrt{j(j+1) - m'(m'+1)}\,\delta_{m\,m'+1}, \tag{A.4}$$

$$D^j_{mm'}(\tfrac{1}{2}\tau_-) = \sqrt{j(j+1) - m(m+1)}\,\delta_{m'\,m+1}, \tag{A.5}$$

with $j = 0, \frac{1}{2}, 1, \ldots$ and $m, m' = -j, \ldots, j$. We obtain an irreducible, unitary representation D^j by exponentiation. The matrix elements of these irreps satisfy the following completeness and orthogonality relations:

$$\int_{\mathrm{SU}(2)} dg\, D^j_{mn}(g)\left(D^{j'}_{m'n'}(g)\right)^* = \frac{1}{d_j}\delta_{jj'}\delta_{mm'}\delta_{nn'}, \tag{A.6}$$

$$\sum_{jmn} d_j D^j_{mn}(g) D^j_{mn}(g') = \delta(g, g'), \tag{A.7}$$

with $d_j = 2j+1$ the dimension of the irrep and dg the normalized Haar measure on SU(2). Writing $g = \exp(i\vec{\alpha}\cdot\vec{\tau}/2)$, it is given by

$$dg = \frac{d\vec{\alpha}}{16\pi^2}\left(\frac{\sin(\frac{\alpha}{2})}{\frac{\alpha}{2}}\right)^2 = \frac{1}{2\pi^2}\sin^2(\tfrac{\alpha}{2})\sin(\theta)\,d(\tfrac{\alpha}{2})\,d\theta\,d\varphi, \tag{A.8}$$

where $\alpha = |\vec{\alpha}| \leq 2\pi$. The last equation shows that this measure corresponds precisely to the standard measure on S^3. Using the well-known properties of the representations D^j of su(2), one can show

$$\mathcal{L}_3^L D^j_{mn}(g) = -m\, D^j_{mn}(g), \tag{A.9}$$

$$\mathcal{L}_+^L D^j_{mn}(g) = -\sqrt{j(j+1) - m(m-1)}\, D^j_{m-1\,n}(g), \tag{A.10}$$

$$\mathcal{L}_-^L D^j_{mn}(g) = -\sqrt{j(j+1) - m(m+1)}\, D^j_{m+1\,n}(g), \tag{A.11}$$

$$\mathcal{L}_3^R D^j_{mn}(g) = n\, D^j_{mn}(g), \tag{A.12}$$

$$\mathcal{L}_+^R D^j_{mn}(g) = \sqrt{j(j+1) - n(n+1)}\, D^j_{m\,n+1}(g), \tag{A.13}$$

$$\mathcal{L}_-^R D^j_{mn}(g) = \sqrt{j(j+1) - n(n-1)}\, D^j_{m\,n-1}(g). \tag{A.14}$$

To obtain functions with standard normalization and behaviour under the angular momentum operators, we define

$$\langle g | j\, m_L\, m_R \rangle = (-1)^{m_L} \sqrt{2j+1}\, D^j_{-m_L m_R}(g). \tag{A.15}$$

This is the basis (2.2.12).

A.2 The eigenfunctions of the laplacian on S^n

In this section we summarize some well-known facts about the spectrum of the laplacian on a n-dimensional sphere. This allows us to identify the functions (2.2.12) with explicit functions on S^3. Let $x_0, \ldots, x_n$ be coordinates in $\mathbb{R}^{n+1}$. Using radial coordinates $r, \theta_1, \ldots, \theta_n$ one can explicitly solve for the eigenfunctions of the spherical laplacian $\bar{\Delta}_n$, using separation of variables and recursion in n. The result of this calculation (cf. e.g. [20]) is that the spectrum is given by

$$\{-l(l+n-1)\}_{l=0,1,2,\ldots}, \tag{A.16}$$

and the degeneracy of the level l is given by

$$\binom{l+n}{n} - \binom{l-2+n}{n}. \tag{A.17}$$

We will relate these eigenfunctions to polynomials in x_μ. Let V^l be the set of polynomials in x_μ that are homogeneous of degree l. This means that $p \in V^l$ can be written as

$$p(x) = t^{\mu_1 \cdots \mu_l} x_{\mu_1} \cdots x_{\mu_l}, \tag{A.18}$$

where t is a completely symmetric tensor. To such a polynomial p corresponds a function Y on S^n defined by

$$p(x_0, \ldots, x_n) = r^l\, Y(\hat{x}_0, \ldots, \hat{x}_n). \tag{A.19}$$

Suppose that p is a harmonic polynomial, i.e. $\Delta p = 0$. We then have

$$0 = \left(\frac{1}{r^n}\frac{\partial}{\partial r} r^n \frac{\partial}{\partial r} + \frac{1}{r^2}\hat{\Delta}_n\right)\left(r^l Y\right) = l(l+n-1)\, r^{l-2}\, Y + r^{l-2}\,\hat{\Delta}_n Y. \tag{A.20}$$

We have found that every harmonic polynomial of degree l corresponds to a function on the n-sphere that is an eigenfunction of the spherical laplacian with eigenvalue $-l(l+n-1)$. The number of monomials of degree l in the variables $x_0, \ldots, x_n$ can easily be computed. It is

$$\dim\left(V^l\right) = \left(\begin{array}{c} l+n \\ n \end{array}\right). \tag{A.21}$$

Hence we have

$$\begin{aligned} \dim\left(\mathrm{Ker}\,(\Delta)\right) &= \dim\left(V^l\right) - \dim\left(\mathrm{Im}\,(\Delta)\right) \\ &\geq \dim\left(V^l\right) - \dim\left(V^{l-2}\right) \\ &= \left(\begin{array}{c} l+n \\ n \end{array}\right) - \left(\begin{array}{c} l-2+n \\ n \end{array}\right). \end{aligned} \tag{A.22}$$

Since we know the degeneracy of the eigenvalue $-l(l+n-1)$, we have shown that all the eigenfunctions of the spherical laplacian correspond to harmonic polynomials. Moreover, the inequality in the last equation is actually an equality.

For the case of S^2 the eigenfunctions are the well-known spherical harmonics Y_m^l. For the case S^3 the spectrum becomes $\{-l(l+2)\}_{l=0,1,2,\ldots}$ with the degeneracy given by

$$\left(\begin{array}{c} l+3 \\ 3 \end{array}\right) - \left(\begin{array}{c} l+1 \\ 3 \end{array}\right) = (l+1)^2. \tag{A.23}$$

When comparing this with the results (A.15), we see that $l = 2j$. The four $j = \frac{1}{2}$ modes $\langle x|\frac{1}{2}\, m_L\, m_R\rangle$ are linear combinations of the four scalar functions x_μ, $(\mu = 0, \ldots, 3)$, whereas the nine $j = 1$ modes $\langle x|1\, m_L\, m_R\rangle$ correspond to the nine components of V_j^l.

We will now derive a useful triangular condition. Let Y_i $(i = 1, 2, 3)$ be three spherical functions that correspond to harmonic polynomials of degree l_i. We will show that the integral

$$\int_{S^n} d\hat{x}\, Y_1(x)\, Y_2(x)\, Y_3(x) \tag{A.24}$$

is zero if the l_i do not satisfy the triangular condition. This is most easily proved by writing Y_i in the form of eq. (A.18). The condition that the polynomials are harmonic implies that the tensors t_i are traceless. We now have

$$\int_{S^n} d\hat{x}\, Y_1(x)\, Y_2(x)\, Y_3(x) = \\ i_1^{\mu_1 \cdots \mu_{l_1}}\, i_2^{\mu_{l_1+1} \cdots \mu_{l_1+l_2}}\, i_3^{\mu_{l_1+l_2+1} \cdots \mu_{l_1+l_2+l_3}} \int_{S^n} d\hat{x}\, x_{\mu_1} \cdots x_{\mu_{l_1+l_2+l_3}}. \tag{A.25}$$

The integral over S^n will be a sum of products of Kronecker δ-functions. If, say, $l_3 > l_1 + l_2$, not all of the indices on t_3 can be contracted with indices on t_1 and t_2. The necessary contraction of two indices on t_3 will then make the result vanish.

A.3 Cutkosky's method

The construction of the basis (2.2.13) relied on the use of an explicit framing on S^3. Cutkosky has given another way [14] of obtaining a basis of vector functions. With a vector field $A_\mu(n)$ on S^3 corresponds the function $\psi(n,n') = n'_\mu A_\mu(n)$ on $S^3 \times S^3$. All vector fields on S^3 (not necessarily satisfying $n_\mu A_\mu(n) = 0$) can hence be expressed with the help of the set

$$\langle n|j\, m_L\, m_R\rangle \otimes \langle n'|\tfrac{1}{2}\, m'_L\, m'_R\rangle. \tag{A.26}$$

Using Clebsch-Gordan coefficients one can define functions

$$\langle n,n'|(j,\tfrac{1}{2})J_L\, M_L;(j,\tfrac{1}{2})J_R\, M_R\rangle, \tag{A.27}$$

where $\vec{J}_L = \vec{L}_1 + \vec{L}'_1$ and $\vec{J}_R = \vec{L}_2 + \vec{L}'_2$. Imposing the conditions $n_\mu A_\mu(n) = 0$ and $\partial_\mu A_\mu(n) = 0$ leads to a basis for transverse vector fields on S^3 given by

$$V^{j+}_{M_L M_R} = \langle n,n'|(j,\tfrac{1}{2})j+\tfrac{1}{2},-M_L;(j,\tfrac{1}{2})j-\tfrac{1}{2},M_R\rangle, \tag{A.28}$$

$$V^{j-}_{M_L M_R} = \langle n,n'|(j,\tfrac{1}{2})j-\tfrac{1}{2},-M_L;(j,\tfrac{1}{2})j+\tfrac{1}{2},M_R\rangle. \tag{A.29}$$

As an example, to the three vector fields e^i_μ belong the functions $\psi^i = \eta^i_{\mu\nu} n'_\mu n_\nu$. One easily shows that these modes have $J_L = 1$ and $J_R = 0$ and hence correspond to $V^{1/2+}_{M_L 0}$. Analogously, the three vector fields $\bar{e}^i_\mu$ can be expressed in $V^{1/2-}_{0 M_R}$.

The potential $V(A)$ of eq. (2.2.22) is to lowest order in A proportional to the square of the curl of A integrated over space. This means that the quadratic fluctuation operator of eq. (2:2.24) equals the square of the curl. The curl operator on S^3 is given by

$$(\operatorname{curl} A(n))_\mu = \varepsilon_{\mu\nu\rho\sigma} n_\nu \partial_\rho A_\sigma. \tag{A.30}$$

With the help of the SO(4) generators

$$M_{\mu\nu} = -\tfrac{i}{2}(x_\mu\partial_\nu - x_\nu\partial_\mu) = \tfrac{1}{2}(\eta^k_{\mu\nu} L^k_1 + \bar{\eta}^k_{\mu\nu} L^k_2), \tag{A.31}$$

we obtain

$$\operatorname{curl}\psi = -\varepsilon_{\mu\nu\rho\sigma} M'_{\mu\nu} M_{\rho\sigma}\psi = \left(\vec{J}^2_R - \vec{J}^2_L\right)\psi, \tag{A.32}$$

and hence

$$\operatorname{curl} V^{j\pm}_{M_L M_R} = \mp(2j+1) V^{j\pm}_{M_L M_R}. \tag{A.33}$$

3 Gauge fixing and the fundamental domain

3.1 Introduction

The configuration space of Yang-Mills gauge theory is the space of gauge orbits $\mathcal{A}/\mathcal{G}$, where $\mathcal{A}$ is the set of all configurations of the gauge field and $\mathcal{G}$ is the group of local gauge transformations. The geometry of the finite volume on which the Yang-Mills theory is defined, is the one of the three-sphere. When studying the configuration space, many of the arguments are independent of this geometry in which case we will denote (compactified) three-space by M. Nevertheless, the details of the way $\mathcal{A}/\mathcal{G}$ is parametrized will crucially depend on M. This is already evident from Singer's argument [3] as the topology of $\mathcal{A}/\mathcal{G}$ does depend on M. We will come back to the consequences of this for the physics of the problem at the end of this chapter.

The physical interpretation of a hamiltonian [2] is clearest in the Coulomb gauge, $\partial_i A_i = 0$. But it has been known since Gribov's work [5] that this does not uniquely fix the gauge. Furthermore, there are coordinate "singularities" where the Faddeev-Popov determinant vanishes. Here the mapping between $\mathcal{A}/\mathcal{G}$ and the transverse vector potentials becomes degenerate.

In this chapter we will first develop the general theory of gauge fixing with the help of a fundamental domain, after which we analyse the Gribov horizon and the boundary of the fundamental domain in the (c, d) space, that is, in the space of slow modes. We prove that parts of this boundary coincide with the Gribov horizon with the help of bounds on the fundamental modular domain.

3.2 Gribov and fundamental regions

We will now try to find suitable coordinates for the Yang-Mills configuration space. Like using stereographic coordinates for a sphere, which leads to a coordinate singularity at one of the poles, coordinate singularities can be removed at the price of having different coordinate patches with transition functions at the overlaps. In gauge theory, these different coordinate patches can simply be seen as different gauge choices [9, 21]. But this is somewhat cumbersome to formulate and most, but (as we shall see) not all coordinate singularities can be avoided if one restricts the set of transverse vector potentials to a fundamental region which constitutes a one to one mapping with $\mathcal{A}/\mathcal{G}$. One obtains a fundamental region by minimizing the L^2 norm of the vector potential along the gauge orbit [15, 22]

$$\|{}^g A\|^2 \equiv -\int_M d^3x \ \mathrm{tr}\left(\left(g^{-1}A_i g + g^{-1}\partial_i g\right)^2\right). \tag{3.2.1}$$

where the vector potential is taken anti-hermitian. For SU(2) one has:

$$A_i(x) = A_i^a(x)\frac{\sigma_a}{2}, \tag{3.2.2}$$

$$g(x) = \exp\left(X(x)\right),\ X(x) = X^a(x)\frac{\sigma_a}{2}. \tag{3.2.3}$$

The connection with the Coulomb gauge condition and the Gribov horizon becomes clear from expanding eq. (3.2.1) around $g = \mathbb{1}$:

$$\begin{aligned}\|{}^g A\|^2 &= \|A\|^2 + 2\int_M \mathrm{tr}(X\partial_i A_i) + \int_M \mathrm{tr}(X^\dagger \mathrm{FP}(A)X) \\ &\quad + \tfrac{1}{3}\int_M \mathrm{tr}\left(X\left[[A_i, X], \partial_i X\right]\right) + \tfrac{1}{12}\int_M \mathrm{tr}\left([D_i X, X][\partial_i X, X]\right) \\ &\quad + \mathcal{O}\left(X^5\right).\end{aligned} \tag{3.2.4}$$

Here $\mathrm{FP}(A)$ is the Faddeev-Popov operator ($\mathrm{ad}\,(A)X \equiv [A, X]$)

$$\mathrm{FP}(A) = -\partial_i D_i(A) = -\partial_i^2 - \partial_i\,\mathrm{ad}\,(A_i). \tag{3.2.5}$$

At the absolute minimum of eq. (3.2.4) the vector potential is hence transverse, $\partial_i A_i = 0$, and $\mathrm{FP}(A)$ is a positive operator. We denote the set of transverse vector potentials by Γ. The set of all transverse vector potentials with positive Faddeev-Popov operator is by definition the Gribov region Ω. It is a convex subspace of Γ, with a boundary $\partial\Omega$ that is called the Gribov horizon (see fig. 3-1). At the Gribov horizon, the lowest eigenvalue of the Faddeev-Popov operator vanishes, and points on $\partial\Omega$ are hence associated with coordinate singularities.

The Gribov region is the set of *local* minima of the norm functional (3.2.4) and needs to be further restricted to the absolute minima to form a fundamental domain, which will be denoted by Λ. The fundamental domain is clearly contained within the Gribov region and can easily be shown to also be convex [15,22]. Its interior is devoid of gauge copies, whereas its boundary $\partial\Lambda$ will in general contain gauge copies, which are associated to those vector potentials where the absolute minima of the norm functional are degenerate [23]. If this degeneracy is continuous one necessarily has at least one zero eigenvalue for $\mathrm{FP}(A)$ and the Gribov horizon will touch the boundary of the fundamental domain at these so-called singular boundary points. By singular we mean here a coordinate singularity. There are so-called reducible connections [24], and $A = 0$ is the most important example, which are left invariant by a subgroup of $\mathcal{G}$. As here $\mathcal{G}$ does not act transitively, $\mathcal{A}/\mathcal{G}$ has curvature singularities at these reducible connections. They can be "blown-up" by not dividing by their stabilizer. For S^3 one can proof $A = 0$ is the only such a reducible connection in Λ. (Note $\mathcal{G}$ is the set of all gauge transformations, *including* those that are homotopically non-trivial). The stabilizer of $A = 0$ is the group $G(= SU(2))$ of constant gauge transformation. This gauge degree of freedom is *not* fixed by the Coulomb gauge condition and therefore one still needs to divide by G to get the proper identification

$$\Lambda/G = \mathcal{A}/\mathcal{G}. \tag{3.2.6}$$

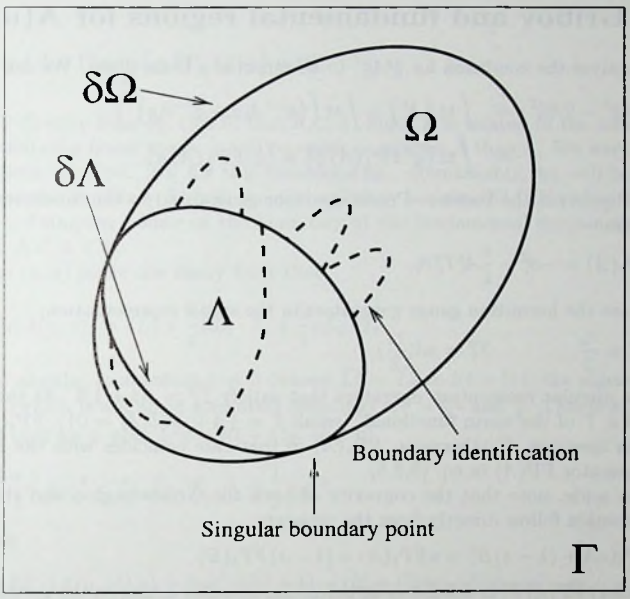

Figure 3-1. Different subsets of $\mathcal{A}$. The set of transverse vector fields is denoted by Γ: $\partial_i A_i = 0$. The Gribov region is Ω: $\mathrm{FP}(A) = -\partial_i D_i^{(A)} \geq 0$. The would-be fundamental domain is Λ: $||{}^g\!A|| \geq ||A|| \quad \forall g \in \mathcal{G}$.

Here Λ is considered to be the set of absolute minima modulo the boundary identifications, where the absolute minimum might be degenerate. It is these boundary identifications that restore the non-trivial topology of $\mathcal{A}/\mathcal{G}$. Furthermore, the existence of non-contractable spheres makes it plausible that singular boundary points cannot be avoided [23]. However, not all singular boundary points, even those associated with continuous degeneracies, need to be associated with non-contractable spheres. Note that absolute minima of the norm functional are degenerate along the constant gauge transformations, this is a trivial degeneracy, also giving rise to trivial zero-modes for the Faddeev-Popov operator, which we ignore. The action of G is essential to remove the curvature singularities mentioned above and also greatly facilitates the standard hamiltonian formulation of the theory [2]. There is no problem in dividing out G by demanding wave functionals to be gauge singlets (colourless states) with respect to G. In practice this means effectively that one minimizes the norm functional over $\mathcal{G}/G$.

3.3 Gribov and fundamental regions for A(u,v)

Let us analyse the condition for $\|{}^g A\|^2$ to be minimal a little closer. We can write

$$\begin{aligned} \|{}^g A\|^2 - \|A\|^2 &= \int \mathrm{tr}\left(A_i^2\right) - \int \mathrm{tr}\left(\left(g^{-1}A_i g + g^{-1}\partial_i g\right)^2\right) \\ &= \int \mathrm{tr}\left(g^\dagger \, \mathrm{FP}_{\frac{1}{2}}(A)\, g\right) \equiv \left\langle g, \mathrm{FP}_{\frac{1}{2}}(A)\, g\right\rangle, \end{aligned} \tag{3.3.1}$$

where $\mathrm{FP}_{1/2}(A)$ is the Faddeev-Popov operator generalized to the fundamental representation:

$$\mathrm{FP}_t(A) = -\partial_i^2 - \frac{i}{t} A_i^a T_t^a \partial_i. \tag{3.3.2}$$

Here $\vec{T}_t$ are the hermitian gauge generators in the spin-t representation:

$$T_{\frac{1}{2}}^a = \frac{\tau_a}{2}, \qquad T_1^a = \mathrm{ad}(\frac{\tau_a}{2}). \tag{3.3.3}$$

They are angular momentum operators that satisfy $\vec{T}_t^2 = t(t+1)\mathbb{1}$. At the critical points $A \in \Gamma$ of the norm functional, (recall $\Gamma = \{A \in \mathcal{A} | \partial_i A_i = 0\}$), $\mathrm{FP}_t(A)$ is an hermitian operator. Furthermore, $\mathrm{FP}_1(A)$ in that case coincides with the Faddeev-Popov operator $\mathrm{FP}(A)$ in eq. (3.2.5).

As an aside, note that the convexity of both the Gribov region and the fundamental domain follow directly from the property

$$\mathrm{FP}_t(sA + (1-s)B) = s\,\mathrm{FP}_t(A) + (1-s)\,\mathrm{FP}_t(B). \tag{3.3.4}$$

In eq. (3.3.1) $\mathrm{FP}_{1/2}(A)$ is defined as an hermitian operator acting on the vector space $\mathcal{L}$ of functions g over S^3 with values in the space of the quaternions $\mathbb{H} = \{q_\mu \sigma_\mu | q_\mu \in \mathbb{R}\}$. To be precise, we should require $g \in W_2^1(S^3, \mathbb{H})$, with $W_2^1(M, V)$ the Sobolev space of functions on M with values in the vector space V, whose first derivative is continuous and square integrable. We use the standard isomorphism between the complex spinors ψ (on which $\vec{T}_{1/2}$ acts in the standard way) and the quaternions, by combining ψ and $\bar{\sigma}_2 \psi^*$. To be specific, if $\psi_1 = q_0 + iq_3$ and $\psi_2 = iq_1 - q_2$, then $g = (\psi, \bar{\sigma}_2 \psi^*) = q \cdot \sigma$ is a quaternion (on which $\vec{T}_{1/2}$ now acts by matrix multiplication). Charge conjugation symmetry, $\mathcal{C}\psi = \bar{\sigma}_2 \psi^*$, implies that $[\mathrm{FP}_{1/2}(A), \mathcal{C}] = 0$ and guarantees that the operator preserves this isomorphism. Also note that this symmetry implies that all eigenvalues are two-fold degenerate. The gauge group $\mathcal{G}$ is contained in $\mathcal{L}$ by restricting to the unit quaternions: $\mathcal{G} = \{g \in \mathcal{L} | g = g_\mu \sigma_\mu, g_\mu \in \mathbb{R}, g_\mu g_\mu = 1\}$.

We can define Λ in terms of the absolute minima (apart from the boundary identifications) over $g \in \mathcal{G}$ of $\langle g, \mathrm{FP}_{1/2}(A)\, g\rangle$

$$\Lambda = \{A \in \Gamma | \min_{g \in \mathcal{G}} \left\langle g, \mathrm{FP}_{\frac{1}{2}}(A)\, g\right\rangle = 0\}. \tag{3.3.5}$$

When minimizing the same functional over the larger space $\mathcal{L}$ one obviously should find a smaller result, i.e.

$$\mathcal{G} \subset \mathcal{L} \Rightarrow \min_{g \in \mathcal{G}} \left\langle g, \mathrm{FP}_{\frac{1}{2}}(A)\, g\right\rangle \geq \min_{g \in \mathcal{L}} \left\langle g, \mathrm{FP}_{\frac{1}{2}}(A)\, g\right\rangle. \tag{3.3.6}$$

Writing

$$\bar{\Lambda} = \{A \in \Gamma | \min_{g \in \vec{\mathcal{L}}} \left\langle g, \mathrm{FP}_{\frac{1}{2}}(A)\, g \right\rangle = 0\}, \tag{3.3.7}$$

it follows directly from eq. (3.3.6) that $\bar{\Lambda} \subset \Lambda$. Since $\bar{\Lambda}$ is related to the minimum of a functional on a *linear* space, it will be easier to analyse $\bar{\Lambda}$ than Λ. We were inspired by appendix A of ref. [16] for this consideration. Remarkably, we will be able to prove that the boundary $\partial\bar{\Lambda}$ will touch the Gribov horizon $\partial\Omega$. This establishes the existence of singular points on the boundary of the fundamental domain due to the inclusion $\bar{\Lambda} \subset \Lambda \subset \Omega$.

In the (u, v) plane one easily finds that

$$\mathrm{FP}_l(A(u,v)) = 4\vec{L}_1^2 + \frac{2}{l}u\vec{L}_1 \cdot \vec{T}_l + \frac{2}{l}v\vec{L}_2 \cdot \vec{T}_l. \tag{3.3.8}$$

For fixed angular momentum $l \neq 0$ (where $\vec{L}_1^2 = \vec{L}_2^2 = l(l+1)$), the eigenvalues of $\vec{L}_a \cdot \vec{T}_{1/2}$ (which is a kind of spin-orbit coupling) are $-\frac{l+1}{2}$ and $\frac{l}{2}$. This is easily seen to imply that for g with $\vec{L}^2 g = l(l+1)g \quad (l \neq 0)$

$$-\frac{l+1}{2}\|g\|^2 \leq \left\langle g, \vec{L}_a \cdot \vec{T}_{\frac{1}{2}}\, g \right\rangle \leq \frac{l}{2}\|g\|^2, \tag{3.3.9}$$

and hence

$$\left\langle g, \mathrm{FP}_{\frac{1}{2}}(A(u,v))\, g \right\rangle \geq \|g\|^2 \left[4l(l+1) - (2l+1)(|u|+|v|) - u - v\right], \tag{3.3.10}$$

whereas of course for $l = 0$ we have $\langle g, \mathrm{FP}_{1/2}(A)\, g\rangle = 0$. Now let $\bar{\Lambda}_l$ be the region in the (u, v) plane where the right hand side of eq. (3.3.10) is positive:

$$\bar{\Lambda}_l = \{(u,v) | \left[4l(l+1) - (2l+1)(|u|+|v|) - u - v\right] \geq 0\}, \tag{3.3.11}$$

then one easily verifies that $\bar{\Lambda}_l \subset \bar{\Lambda}_{l+1/2}$ for $l \neq 0$. For illustration we have drawn the boundaries of $\bar{\Lambda}_{1/2}$ and $\bar{\Lambda}_1$ in fig. 3-2 (the two nested trapeziums). Consequently, restricted to the (u, v) plane $\bar{\Lambda}_{1/2}$, the trapezium spanned by the four points $(1, 0)$, $(0, 1)$, $(-3, 0)$ and $(0, -3)$, is contained in $\bar{\Lambda}$. As one easily checks, the vector potentials belonging to the sphalerons at $(1, 0)$ and $(0, 1)$ have the same norm. Since they are related by a gauge transformation (as was proved earlier) and lie on the boundary of $\bar{\Lambda}_{1/2}$, these sphalerons have to be on the boundary of the fundamental domain $\partial\Lambda$. Hence, $\bar{\Lambda}_{1/2}$ is seen to provide already quite a strong bound.

Before constructing $\bar{\Lambda}$ in the (u, v) plane, it is instructive to consider first the Gribov horizon, which is given by the zeros of the Faddeev-Popov determinant $\det(\mathrm{FP}_1(A))$. The operator $\mathrm{FP}_l(A(u,v))$ as given by eq. (3.3.8) not only commutes with $\vec{L}^2$, but also with $\vec{J}_l$, where

$$\vec{J}_l = \vec{L}_1 + \vec{L}_2 + \vec{T}_l. \tag{3.3.12}$$

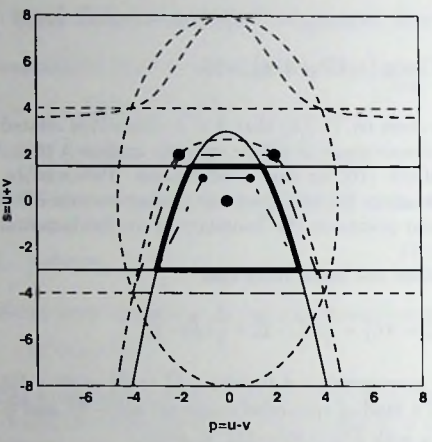

Figure 3-2. Location, for the (u, v) plane of the classical vacua (large dots), sphalerons (smaller dots), bounds on the Faddeev-Popov operator for $l = \frac{1}{2}$ and $l = 1$ (short-long dashed curves), zeros of the adjoint determinant (solid lines for $l = \frac{1}{2}$, dashed lines for $l = 1$) and the Gribov horizon (fat sections).

Note that this $\vec{J}_t$ differs from the operators $\vec{J}$ defined in chapter 2. Using the quantum numbers (l, j_t, j_t^z) one can easily diagonalize $\mathrm{FP}_t(A(u,v))$ for low values of l. Note that the eigenvalues are independent of j_t^z. Defining the scalar and pseudoscalar helicity combinations

$$s = u + v, \qquad p = u - v, \tag{3.3.13}$$

we take from ref. [25] the results

$$\det\left(\mathrm{FP}_1(A(u,v))|_{l=\frac{1}{2}}\right) = (3-2s)\,(9-3s-2p^2)^3\,(3+s)^5, \tag{3.3.14}$$

$$\det\left(\mathrm{FP}_1(A(u,v))|_{l=1}\right) = 512\,(8-2s)\,((8-2s)^2-s^2+p^2(2s-7))^3 \times (64-s^2-3p^2)^5\,(8+2s)^7, \tag{3.3.15}$$

the zeros of which are also exhibited in fig. 3-2 (solid lines for $l = \frac{1}{2}$, dashed lines for $l = 1$). The Gribov horizon in the (u, v) plane is indicated by the fat lines and is completely determined by the $l = \frac{1}{2}$ sector, a fact that we will now prove. Note that the set of infinitesimal gauge transformations $L_g = \{X : \mathrm{S}^3 \to \mathrm{su}(2)\}$ is contained in $\mathcal{L}$. Here su(2) is the Lie algebra for SU(2) (i.e. the traceless quaternions). It is easy to verify that for $X \in L_g$, we have for all vector potentials A

$$\langle X, \mathrm{FP}_1(A)\,X\rangle = \left\langle X, \mathrm{FP}_{\frac{1}{2}}(A)\,X\right\rangle. \tag{3.3.16}$$

This fact will enable us to use the same bounds for FP_1 and $\mathrm{FP}_{1/2}$ (cf. eq. (3.3.6)):

$$L_g \subset \mathcal{L} \Rightarrow \min_{X \in L_g} \langle X, \mathrm{FP}_1(A)\, X \rangle \geq \min_{g \in \mathcal{L}} \left\langle g, \mathrm{FP}_{\frac{1}{2}}(A)\, g \right\rangle . \tag{3.3.17}$$

Hence all zeros of the Faddeev-Popov determinant with $l \geq 1$ lie outside the trapezium $\bar{\Lambda}_1$, spanned by the four points $(2,0)$, $(0,2)$, $(-4,0)$, $(0,-4)$.

This then proves that $\mathrm{FP}_1(A) \geq 0$ within the region bounded by the zeros of eq. (3.3.14). We see from fig. 3-2 that along the line $s = u + v = -3$, for $|p| = |u - v| \leq 3$, the Gribov horizon coincides with $\partial\Lambda$ and consequently these are singular boundary points. Note that therefore it is necessary that the term third order in X in eq. (3.2.4) has to vanish if $\mathrm{FP}(A)\, X = 0$. As on the Gribov horizon any non-trivial zero-mode has $l = \frac{1}{2}$, whereas $A(u,v)$ has $l = 0$ or $l = 1$, this third order term vanishes along the whole Gribov horizon in the (u,v) plane (all its points are therefore bifurcation points [23]). It can, however, also be shown that these singular boundary points are *not* associated with non-contractable spheres (see app. A).

Next we will construct $\bar{\Lambda}$ in the (u,v) plane to get an even sharper bound on Λ. It is by now obvious that this will follow from finding $\det(\mathrm{FP}_{1/2}(A(u,v)))$ in the $l = \frac{1}{2}$ sector. A straightforward computation yields:

$$\det\left(\mathrm{FP}_{\frac{1}{2}}(u,v)|_{l=\frac{1}{2}}\right) = 9\,(3+s)^4\,(3-2\,s-p^2)^2, \tag{3.3.18}$$

where the multiplicity of 4 comes from the $j = \frac{3}{2}$ state and the multiplicity 2 from the two $j = \frac{1}{2}$ states in the decomposition $\frac{1}{2} \otimes \frac{1}{2} \otimes \frac{1}{2} = \frac{1}{2} \oplus \frac{1}{2} \oplus \frac{3}{2}$. In fig. 3-3 the bordering parabola going through the points $(0,-3)$, $(1,0)$, $(\frac{3}{4},\frac{3}{4})$, $(0,1)$ and $(-3,0)$, cut off by the line $s = -3$, forms the boundary of $\bar{\Lambda}$. As in the case of the Gribov horizon, $\bar{\Lambda}$ is completely determined by the $l = \frac{1}{2}$ sector, since also the zeros of $\det(\mathrm{FP}_{1/2}(A(u,v)))$ with $l \geq 1$ lie outside the trapezium $\bar{\Lambda}_1$. Notice that we have now also shown that $(u,v) = (\frac{3}{4},\frac{3}{4})$ is a singular boundary point.

We recall that in [25], part of $\partial\Lambda$ in the (u,v) plane was constructed by expanding around the sphalerons, which are known to be on $\partial\Lambda$. One solves for fixed (u,v) near $(0,1)$ for the extremum of $\langle g, \mathrm{FP}_{1/2}(A(u,v))\, g \rangle$ with respect to $g = n \cdot \bar{\sigma} \exp(X)$, where it can be shown that $X = -\vec{n} \cdot \vec{\sigma} f(n_0)$. This leads to a second order differential equation, solved by

$$f(x) = x \sum_{j=1} \sum_{k=0}^{j-1} a_{j,k}(v) u^j x^{2k}, \tag{3.3.19}$$

with

$$a_{1,0}(v) = \frac{2}{2+v}, \tag{3.3.20}$$

$$a_{2,0} = \frac{-2(v^2+6v-16)}{(2+v)^3(10+v)}, \tag{3.3.21}$$

$$a_{2,1}(v) = \frac{4(6+v)}{(v+2)^2(v+10)}, \quad \cdots \tag{3.3.22}$$

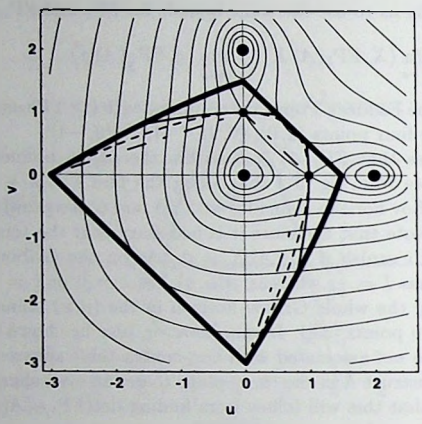

Figure 3-3. Location of the classical vacua (large dots), sphalerons (smaller dots), bounds on the Faddeev-Popov operator for $l = \frac{1}{2}$ (short-long dashed lines), the Gribov horizon (fat sections), zeros of the fundamental determinant in the sector $l = \frac{1}{2}$ (dashed curves) and part of the boundary of the fundamental domain (full curves). Also indicated are the lines of equal potential in units of 2^n times the sphaleron energy.

Substituting this now back in eq. (3.3.1) and demanding equality of norms yields $v(u)$:

$$\begin{aligned} v(u) &= 1 - \tfrac{1}{9}u^2 - \tfrac{2}{81}u^3 - \tfrac{25}{2673}u^4 - \tfrac{1238}{264627}u^5 - \tfrac{172442}{66950631}u^6 \\ &\quad - \tfrac{687429956}{457339760361}u^7 + \mathcal{O}\left(u^8\right), \end{aligned} \tag{3.3.23}$$

giving the part of $\partial\Lambda$ in the (u, v) plane going through the anti-sphaleron at $u = 0$. We have drawn the maximal extension to the Gribov horizon, but not all of it is expected to coincide with $\partial\Lambda$. Interchanging the two coordinates gives the part of $\partial\Lambda$ going through the sphaleron. Both parts are indicated by the curves in fig. 3-3. They are consistent with the inclusion $\bar{\Lambda} \subset \Lambda$. In this figure also lines of equal potential (eq. (2.2.27)) are drawn.

3.4 Gribov and fundamental regions for A(c,d)

We will now generalize our discussion to the 18-dimensional field space, parametrized by $A(c, d)$ in eq. (2.2.26). For this case one has

$$\mathrm{FP}_t(A(c,d)) = 4\vec{L}^2 - \frac{2}{t}c_i^a T_t^a L_1^i - \frac{2}{t}d_i^a T_t^a L_2^i. \tag{3.4.1}$$

This still commutes with $\vec{L}^2$, but for arbitrary (c,d) there are in general no other commuting operators (except for the charge conjugation operator $\mathcal{C}$ for $t = \frac{1}{2}$).

We first calculate the analogues of the regions $\bar{\Lambda}_l$, as defined in eq. (3.3.11). We decompose

$$c_i^a = \sum_{j=1}^{9} c_j \, (b_j)_i^a \,, \qquad d_i^a = \sum_{j=1}^{9} d_j \, (b_j)_i^a \,, \tag{3.4.2}$$

with c_j and d_j coefficients and the set $\{b_j\}$ a basis of $\mathbb{R}^{3,3}$, consisting of orthogonal matrices ($b_j^T = b_j^{-1}$) with unit determinant. We then have:

$$\begin{aligned} \mathrm{FP}_t(A(c,d)) &= 4\vec{L}^2 - \frac{2}{t} c_j T_t^a \, (b_j)_i^a \, L_1^i - \frac{2}{t} d_j T_t^a \, (b_j)_i^a \, L_2^i \\ &= 4\vec{L}^2 - \frac{2}{t} c_j \vec{T}_t \cdot \vec{L}_{1,j} - \frac{2}{t} d_j \vec{T}_t \cdot \vec{L}_{2,j}, \end{aligned} \tag{3.4.3}$$

with the proper angular momentum operators

$$L_{k,j}^a \equiv (b_j)_i^a L_k^i, \quad k = 1,2. \tag{3.4.4}$$

As in eq. (3.3.10), for g an eigenfunction of $\vec{L}^2$ with eigenvalue $l(l+1)$ $(l \neq 0)$, we find the bound

$$\begin{aligned} &\left\langle g, \mathrm{FP}_{\frac{1}{2}}(A(c,d))\, g \right\rangle \geq \\ &\qquad \|g\|^2 \left[4l(l+1) - (2l+1) \sum_{j=1}^{9} (|c_j| + |d_j|) + \sum_{j=1}^{9} (c_j + d_j) \right]. \end{aligned} \tag{3.4.5}$$

As before, we define $\bar{\Lambda}_l$ as the polyhedra where the right hand side of eq. (3.4.5) is positive. They are nested polyhedra, i.e. $\bar{\Lambda}_l \subset \bar{\Lambda}_{l+1/2}$. Hence we have the inclusion $\bar{\Lambda}_{1/2} \subset \bar{\Lambda} \subset \Lambda \subset \Omega$. If we restrict ourselves to the two-dimensional subspace where all but one of the c_j $(-u)$ and all but one of the d_j $(-v)$ are zero, we precisely recover the situation of the previous section. The bounds will, however, depend on the particular choice of the b_j matrices. The sharpest bound is obtained by forming the *union* of all $\bar{\Lambda}_l$ obtained by these various choices.

We now turn to the computation of the Faddeev-Popov determinants. In the sector $l = \frac{1}{2}$, which is $4(2t+1)$ dimensional, the problem of computing $\det(\mathrm{FP}_t(A(c,d)))$ is still manageable. A suitable basis is given by $|s_1, s_2, s_3\rangle$, with s_i the eigenvalues of the third component of the three angular momentum operators $\vec{L}_1$, $\vec{L}_2$ and $\vec{T}_t$. For $t = 1$ it is actually more convenient to consider $|s_1, s_2\rangle_a$, where a is the vector component. Using

$$\begin{aligned} L_1^{\pm}|s_1,s_2\rangle_a &= (\tfrac{1}{2} \mp s_1)|-s_1,s_2\rangle_a \,, \quad L_2^{\pm}|s_1,s_2\rangle_a = (\tfrac{1}{2} \mp s_2)|s_1,-s_2\rangle_a \,, \\ L_i^3|s_1,s_2\rangle_a &= s_i|s_1,s_2\rangle_a \,, \quad T_1^b|s_1,s_2\rangle_a = i\varepsilon_{bac}|s_1,s_2\rangle_c \,, \end{aligned} \tag{3.4.6}$$

where as usual $L_a^{\pm} = L_a^1 \pm iL_a^2$, one easily writes down the matrix for $M \equiv \mathrm{FP}_1(A(c,d))$ in this sector ($c_{\pm}^a \equiv c_1^a \mp ic_2^a$ and $d_{\pm}^a \equiv d_1^a \mp id_2^a$):

$$\begin{aligned} M|s_1,s_2\rangle_b &= -i\sum_{\alpha=\pm}\left\{(\tfrac{1}{2}-\alpha s_1)c_\alpha^a\varepsilon_{abc}|-s_1,s_2\rangle_c + (\tfrac{1}{2}-\alpha s_2)d_\alpha^a\varepsilon_{abc}|s_1,-s_2\rangle_c\right\} \\ &\quad + (3\delta_{bc} - 2i\varepsilon_{abc}(s_1c_3^a + s_2d_3^a))\,|s_1,s_2\rangle_c\ . \end{aligned} \tag{3.4.7}$$

In particular for the choice

$$c_i^a = x_i\delta_i^a\ , \qquad d_i^a = y_i\delta_i^a\ , \tag{3.4.8}$$

one can, with the help of MATHEMATICA [26], check that the following holds:

$$\begin{aligned} &\det\left(\mathrm{FP}_1(A(c,d))|_{t=\frac{1}{2}}\right) = \\ &\quad F(x_1+y_1,x_2+y_2,x_3+y_3)F(x_1-y_1,x_2-y_2,x_3+y_3)\times \\ &\quad F(x_1-y_1,x_2+y_2,x_3-y_3)F(x_1+y_1,x_2-y_2,x_3-y_3), \end{aligned} \tag{3.4.9}$$

with

$$F(\vec{z}) \equiv 2\prod_i z_i - 3\sum_i z_i^2 + 27. \tag{3.4.10}$$

To obtain the result for general (c,d) we first observe that we have invariance under rotations generated by $\vec{L}_1$ and $\vec{L}_2$ and under constant gauge transformations generated by $\vec{T}_t$, implying that $\det(\mathrm{FP}_t(A(c,d))|_{t=1/2})$ is invariant under

$$c_i^a \to (ScR_1)_i^a\ , \qquad d_i^a \to (SdR_2)_i^a\ , \tag{3.4.11}$$

with R_1, R_2 and S orthogonal matrices with unit determinant (note that the $\vec{L}_{kj}$, introduced in eq. (3.4.3), are nothing but the $\vec{L}_k$ generators, rotated by $R_1 = R_2 = b_j$). This also allows us to understand the large amount of symmetry in eq. (3.4.9), as a permutation of the x_i (y_i) and a simultaneous change of the sign of two of the x_i (y_i) is the remnant of this symmetry, when restricted to the diagonal configurations of eq. (3.4.8). The result for the generalization of eq. (3.4.9) to arbitrary (c,d) is presented in appendix B. Here we will treat the case $d = 0$. Using eq. (3.4.11) we first diagonalize c_i^a and then express $F(\vec{x})$ in terms of the complete set of rotational and gauge invariant parameters of c_i^a

$$\det c = \prod_i x_i,\ \ \mathrm{tr}(cc^T) = \sum_i x_i^2,\ \ \mathrm{tr}(cc^Tcc^T) = \sum_i x_i^4, \tag{3.4.12}$$

which implies $F(\vec{x}) = 2\det c - 3\,\mathrm{tr}(cc^T) + 27$ and

$$\det\left(\mathrm{FP}_1(A(c,0))|_{t=\frac{1}{2}}\right) = \left(2\det c - 3\,\mathrm{tr}(cc^T) + 27\right)^4. \tag{3.4.13}$$

This can also be easily derived by constructing the three-dimensional invariant subspace for ($c_i^a = x_i\delta_i^a$, $d = 0$), spanned by the 3 vectors $n_i\sigma_i$ (no sum over i), with respect to which the matrix for M takes the form

$$M(n_1\sigma_1, n_2\sigma_2, n_3\sigma_3) = \begin{pmatrix} 3 & x_3 & x_2 \\ x_3 & 3 & x_1 \\ x_2 & x_1 & 3 \end{pmatrix}\begin{pmatrix} n_1\sigma_1 \\ n_2\sigma_2 \\ n_3\sigma_3 \end{pmatrix}, \tag{3.4.14}$$

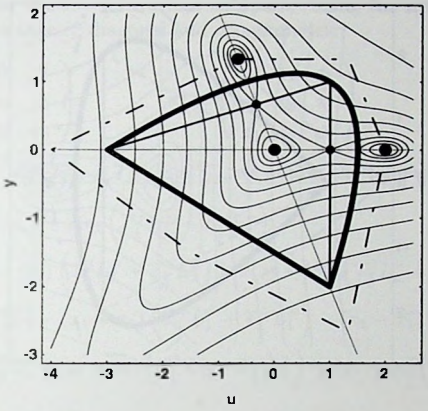

Figure 3-4 Location, for the (u, y) plane of the classical vacua (large dots), sphalerons (smaller dots), bounds on the Faddeev-Popov operator for $l = 1$ (short-long dashed curves), boundary of the fundamental domain (solid lines) and the Gribov horizon (fat curves), as well as the lines of equal potential.

whose determinant coincides with $F(\vec{x})$. It is not too difficult to construct the three other three-dimensional invariant subspaces with identical determinants.

Two special cases in this class were first considered by Cutkosky [27]:

$$\text{I} \;:\; c_i^a = \text{diag}(-u+y, -u+y, -u-2y), \tag{3.4.15}$$

$$\text{II} \;:\; c_i^a = \text{diag}(-u+x, -u-x, -u). \tag{3.4.16}$$

For F, which determines the Faddeev-Popov determinant at $l = \frac{1}{2}$, we find [27]

$$F_{\text{I}} = (u+2y+3)\,[(u+3)(3-2u) + 2(2u-3)y - 2y^2], \tag{3.4.17}$$

$$F_{\text{II}} = (u+3)^2\,(3-2u) + 2(u-3)x^2. \tag{3.4.18}$$

The associated zeros are drawn respectively in figs. 3-4 and 3-5. Note that the (u, y) plane admits a global gauge symmetry $(u, y) \to \frac{1}{3}(4y - u, y + 2u)$ generated by $S = \text{diag}(-1, -1, 1)$, which maps the vacuum at $(u, y) = (2, 0)$ to a vacuum at $(-\frac{2}{3}, \frac{4}{3})$. To conclude that these zeros coincide with the Gribov horizon, we have to show that the Faddeev-Popov operator for all $l \geq 1$ is positive within the region bounded by these zeros. Using eq. (3.3.17), it is sufficient to show that these zeros lie within $\bar{\Lambda}_1$, the region obtained from the bound on $\text{FP}_{1/2}(A)$ in eq. (3.4.5). Clearly we should try to construct this bound by taking for b_j the diagonal orthogonal matrices $\text{diag}(1,1,1)$, $\text{diag}(1,-1,-1)$, $\text{diag}(-1,-1,1)$ and $\text{diag}(-1,1,-1)$. It turns out to be sufficient to consider the union of the bounds obtained by applying eq. (3.4.5) for the

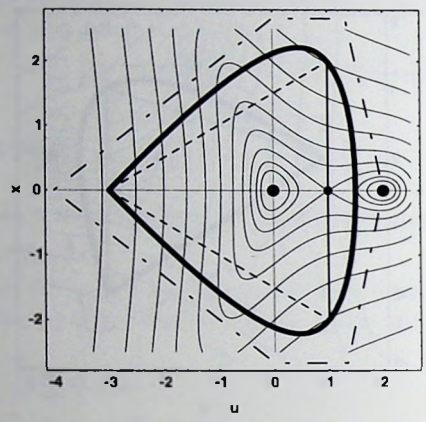

Figure 3-5. Location, for the (u, x) plane of the classical vacua (large dots), sphalerons (smaller dots), bounds on the Faddeev-Popov operator for $l = 1$ (short-long dashed curves), boundary of the fundamental domain (solid line), zeros of the fundamental determinant for $l = \frac{1}{2}$ (dashed lines) and the Gribov horizon (fat curves), as well as the lines of equal potential.

four triplets of possible choice of diagonal b_j. In terms of general x_i, this leads to the four bounds

$$\begin{aligned}
&4l(l+1) - \tfrac{1}{2}(2l+1)(|x_1+x_2| + |x_1+x_3| + |x_2+x_3|) - x_1 - x_2 - x_3 \geq 0,\\
&4l(l+1) - \tfrac{1}{2}(2l+1)(|x_1-x_2| + |x_1-x_3| + |x_2+x_3|) - x_1 + x_2 + x_3 \geq 0,\\
&4l(l+1) - \tfrac{1}{2}(2l+1)(|x_1+x_2| + |x_1-x_3| + |x_2-x_3|) + x_1 + x_2 - x_3 \geq 0,\\
&4l(l+1) - \tfrac{1}{2}(2l+1)(|x_1-x_2| + |x_1+x_3| + |x_2-x_3|) + x_1 - x_2 + x_3 \geq 0.
\end{aligned} \tag{3.4.19}$$

The union of these polyhedra respects the gauge and rotation symmetry and we take it as the definitions of $\tilde{\Lambda}_l$ for $d = 0$. They are again nested, such that it is sufficient to show that the convex regions bounded by the zeros of the Faddeev-Popov operator in the $l = \frac{1}{2}$ sector are contained within $\tilde{\Lambda}_1$. From figs. 3-4 and 3-5 we see that this is indeed the case, allowing the identification of $\partial\Omega$ (fat curves) and $\partial\tilde{\Lambda}$ (dashed or full lines) with the zeros of respectively $\det(\mathrm{FP}_1(A)|_{l=1/2})$ and $\det(\mathrm{FP}_{1/2}(A)|_{l=1/2})$.

We now turn to the calculation of $\det(\mathrm{FP}_{1/2}(A(c,d))|_{l=1/2})$ which will allow us to construct $\tilde{\Lambda}$ and to find possible further singular points on the boundary of the fundamental domain. In this case the basis $|s_1, s_2, s_3\rangle$, which was defined earlier, is

a convenient one for the $l = \frac{1}{2}$ invariant subspace. Using the invariance as given by eq. (3.4.11), we can take c_i^a diagonal and d_i^a symmetric:

$$c_i^a = \begin{pmatrix} x_1 & 0 & 0 \\ 0 & x_2 & 0 \\ 0 & 0 & x_3 \end{pmatrix}, \qquad d_i^a = \begin{pmatrix} y_1 & z_1 & z_2 \\ z_1 & y_2 & z_3 \\ z_2 & z_3 & y_3 \end{pmatrix}. \tag{3.4.20}$$

With $L_0^\pm$ as before and $T_{1/2}^\pm = T_{1/2}^1 \pm iT_{1/2}^2$, we obtain the following expression:

$$\begin{aligned} \mathrm{FP}_{\frac{1}{2}}(A(c,d)) &= 3 + 2iz_1\left(T_{\frac{1}{2}}^+ L_2^+ - T_{\frac{1}{2}}^- L_2^-\right) \\ &\quad - 2(z_2 - iz_3)\left(T_{\frac{1}{2}}^3 L_2^+ + T_{\frac{1}{2}}^+ L_2^3\right) - 2(z_2 + iz_3)\left(T_{\frac{1}{2}}^3 L_2^- + T_{\frac{1}{2}}^- L_2^3\right) \\ &\quad - 4x_3 T_{\frac{1}{2}}^3 L_1^3 - (x_1 + x_2)\left(T_{\frac{1}{2}}^+ L_1^- + T_{\frac{1}{2}}^- L_1^+\right) - (x_1 - x_2)\left(T_{\frac{1}{2}}^+ L_1^+ + T_{\frac{1}{2}}^- L_1^-\right) \\ &\quad - 4y_3 T_{\frac{1}{2}}^3 L_2^3 - (y_1 + y_2)\left(T_{\frac{1}{2}}^+ L_2^- + T_{\frac{1}{2}}^- L_2^+\right) - (y_1 - y_2)\left(T_{\frac{1}{2}}^+ L_2^+ + T_{\frac{1}{2}}^- L_2^-\right). \end{aligned} \tag{3.4.21}$$

In order to express the final result in invariants, we introduce the matrices X and Y via

$$X_b^a = (cc^T)_b^a, \quad Y_b^a = (dd^T)_b^a. \tag{3.4.22}$$

Using MATHEMATICA and expressing the result in terms of traces of products of X and Y, we obtain an expression which is manifestly invariant:

$$\det\left(\mathrm{FP}_{\frac{1}{2}}(A(c,d))|_{l=\frac{1}{2}}\right) = \mathcal{F}^2, \tag{3.4.23}$$

$$\begin{aligned} \mathcal{F} &= 81 - 18\,\mathrm{tr}(X+Y) + 24(\det c + \det d) \\ &\quad - \mathrm{tr}^2(X-Y) + 2\,\mathrm{tr}((X-Y)^2). \end{aligned} \tag{3.4.24}$$

With this, one easily reproduces the result of eq. (3.3.18) ($x_i = -u$, $y_i = -v$, $s = u + v$, $p = u - v$). Note the overall square, which is a consequence of the two-fold degeneration of the eigenvalues due to the fact that $\mathrm{FP}_{1/2}$ commutes with the charge conjugation operator C. Such a non-trivial commuting operator does not exist for FP_1, whose determinant does not factorize and was hence much more difficult to calculate (see app. B).

For $d = 0$ we find

$$\det\left(\mathrm{FP}_{\frac{1}{2}}(A(c,0))|_{l=\frac{1}{2}}\right) = \mathcal{F}^2, \tag{3.4.25}$$

$$\mathcal{F} = 81 - 18\,\mathrm{tr}\,X + 24\det c - \mathrm{tr}^2(X) + 2\,\mathrm{tr}(X^2). \tag{3.4.26}$$

In figs. 3-4 and 3-5 we have drawn $\partial\tilde{\Lambda}$ obtained from the zeros of eq. (3.4.25) for the two cases of eq. (3.4.15) and eq. (3.4.16):

$$\mathcal{F}_{\mathrm{I}} = 3(3 + u + 2y)^2(u-1)(4y - 3 - u), \tag{3.4.27}$$

$$\mathcal{F}_{\mathrm{II}} = 3(u+3)(u-1)[4x^2 - (3+u)^2], \tag{3.4.28}$$

which indeed provides further singular boundary points (since $\partial\bar{\Lambda}\cap\partial\Omega$ is not empty). Also the part of $\partial\Lambda$ that contains the sphaleron is easily derived from the fact that the gauge transformation with winding number -1, $g = n\cdot\sigma$, leads to

$$^{g}A(x_i,0) = (2+x_i)n\cdot\bar{\sigma}\frac{\sigma_i}{2}n\cdot\sigma, \tag{3.4.29}$$

for arbitrary diagonal configurations. Equality of norms implies the equation $\sum x_i + 3 = 0$. This means, since $\bar{\Lambda}\subset\Lambda$, that in fig. 3-4 the edges of $\bar{\Lambda}$ passing through the sphalerons coincide with $\partial\Lambda$, a fact that can also be concluded from the convexity of Λ. Hence, in fig. 3-4 $\bar{\Lambda}$ coincides with Λ and the line $u+2y=-3$ consists of singular boundary points. In fig. 3-5 it is not excluded that, at the dashed lines, $\partial\bar{\Lambda}$ does *not* coincide with $\partial\Lambda$, as was also the case for the (u,v) plane, see fig. 3-3. We can settle this issue by considering the embedding of the (u,x) plane within the three-dimensional space of the x_i.

All surfaces to be constructed have to respect the symmetries of the permutations and the double sign flips of the x_i coordinates. We first consider $\bar{\Lambda}_1$, see eq. (3.4.19), which can be seen as a tetrahedron spanned by the points $(4,4,4)$, $(-4,-4,4)$, $(4,-4,-4)$ and $(-4,4,-4)$, enlarged by adding to each face a symmetric pyramid, whose tips are given by the points $(-2,-2,-2)$, $(2,2,-2)$, $(-2,2,2)$ and $(2,-2,2)$ (corresponding to the copies of the classical vacuum at $\vec{x}=0$). For general l, $\bar{\Lambda}_l$ can be constructed from this twelve faced polygon by scaling the corners of the tetrahedron with $l+1$ and the tips of the pyramids with l, from which their nested nature is obvious. A special case arises for $l=\frac{1}{2}$, where the pyramids are of zero height, such that $\bar{\Lambda}_{1/2}$ is a tetrahedron. It is a remarkable fact that the fundamental Faddeev-Popov determinant in the sector $l=\frac{1}{2}$ (eq. (3.4.25)) vanishes on $\partial\bar{\Lambda}_{1/2}$. As this is enclosed by $\bar{\Lambda}_1$, where all eigenvalues of $\mathrm{FP}_{1/2}(A)$ with $l\geq 1$ are strictly positive, we conclude that $\bar{\Lambda}=\bar{\Lambda}_{1/2}$ (the tetrahedron spanned by $(3,3,3)$, $(-3,-3,3)$, $(3,-3,-3)$ and $(-3,3,-3)$). The convex region bounded by the zeros of the adjoint determinant (eq. (3.4.13)) can be shown to form a surface contained in $\bar{\Lambda}_1$ that can be visualized by stretching a rubber sheet around this tetrahedron, fixed at its edges and slightly inflated. This surface forms the Gribov horizon $\partial\Omega$, since also all eigenvalues of $\mathrm{FP}_1(A)$ with $l\geq 1$ are strictly positive inside $\bar{\Lambda}_1$. Because of the inclusion $\bar{\Lambda}\subset\Lambda\subset\Omega$, all points on the edges of the tetrahedron are singular boundary points. As all the faces of this tetrahedron contain a sphaleron, which we have proved earlier to be on the boundary of the fundamental domain (the edges of the tetrahedron are singular points on the same boundary), we conclude (using the convexity of Λ) that $\bar{\Lambda}=\Lambda$. This is consistent with eq. (3.4.29), where equality of norms gives the equation that describes the face of the tetrahedron through the sphaleron at $(-1,-1,-1)$, $\sum x_i + 3 = 0$. The other three faces follow from flipping the sign of two of the x_i, which is a symmetry. In fig. 3-6 we have drawn the fundamental modular domain for $d=0$ in $\vec{x}$ space and in fig. 3-7 we give the Gribov horizon and the edges of $\partial\bar{\Lambda}_1$ (dashed lines). This completes the construction of the fundamental domain for $d=0$.

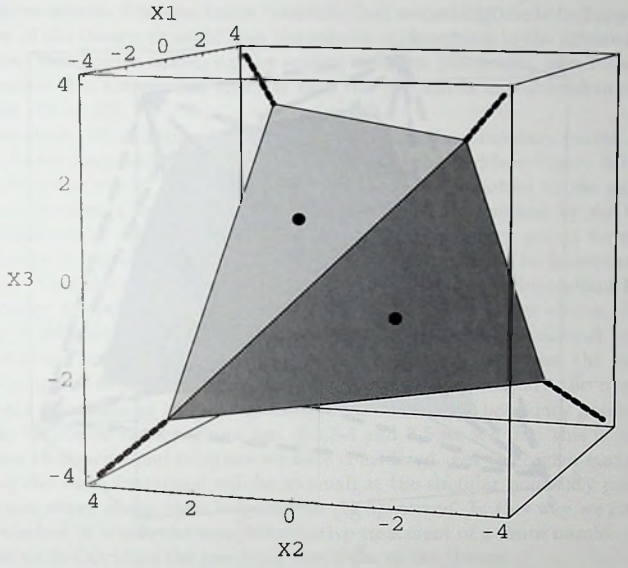

Figure 3-6. The fundamental modular domain for constant gauge fields on S^3, with respect to the "instanton" framing e^a_μ, in the diagonal representation $A_a = x_a\sigma_a/2$ (no sum over a). By the dots on the faces we indicate the sphalerons, whereas the dashed lines represent the symmetry axes of the tetrahedron.

3.5 Discussion

We have analysed in detail the boundary of the fundamental domain for SU(2) gauge theories on the three-sphere. We have constructed it completely for the gauge fields with $\vec{L}^2$=0 and have provided partial results for the 18-dimensional space of modes that are degenerate with these in energy to second order in the fields. Especially, the interesting point of explicitly demonstrating the presence of singular boundary points, i.e. points where the boundary of the fundamental domain coincides with the Gribov horizon, was addressed. In ref. [23] existence of singular boundary points was conjectured on the basis of the presence of non-contractable spheres [3] in the physical configuration space $\mathcal{A}/\mathcal{G}$. Not all singular boundary points are necessarily associated with such non-contractable spheres, which we demonstrated for the case at hand (see app. A). It is also important to note that it is necessary to divide $\mathcal{A}$ by the set of *all* gauge transformations, including those that are homotopically non-trivial, to get the physical configuration space. All the non-trivial topology is then retrieved by the

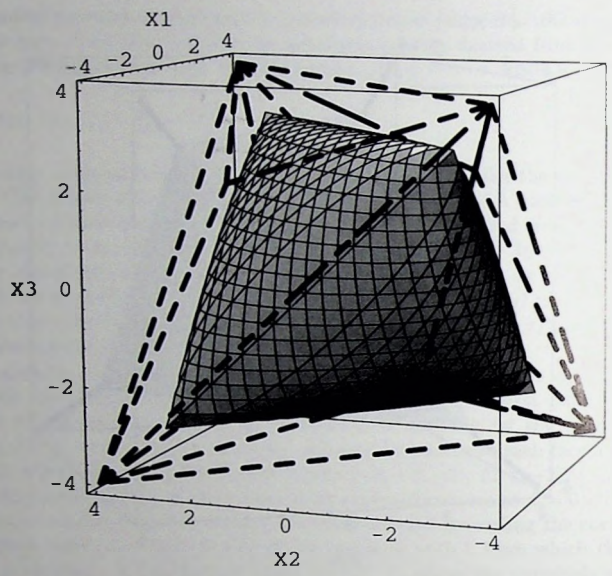

Figure 3-7. The Gribov horizon for constant gauge fields on S^3, with respect to the "instanton" framing e^a_μ, in the diagonal representation $A_a = x_a\sigma_a/2$ (no sum over a). The dashed lines represent the edges of $\tilde{\Lambda}_1$, which encloses the Gribov horizon, whereas the latter encloses the fundamental modular domain, coinciding with it at the singular boundary points along the edges of the tetrahedron of fig. 3-6.

identifications of points on the boundary of the fundamental domain. Zwanziger [28] (app. E) has constructed, for the case of $M = \mathrm{T}^3$, a gauge function parametrized by a two-sphere for which the norm functional is degenerate, but its vector potential lies outside the fundamental domain when also the anti-periodic gauge transformations are considered as part of $\mathcal{G}$ [23].

As we already mentioned in the introduction, the knowledge of the boundary identifications is important in the case that the wave functionals spread out in configuration space to such an extent that they become sensitive to these identifications. This happens at large volumes, whereas at very small volumes the wave functional is localized around $A = 0$ and one need not worry about these non-perturbative effects. That these effects can be dramatic, even at relatively small volumes (above a tenth of a fermi across), was demonstrated for the case of the torus [9, 21]. However, for that case the structure of the fundamental domain (restricted to the abelian zero-energy modes) is a hypercube [23] and deviates considerably from the fundamental domain

of the three-sphere. One can hence conclude that something needs to happen to the structure of the theory, to avoid that the infinite-volume limit in the infrared depends on the way this limit is taken, e.g. by scaling different geometries, like T^3 or S^3. One way to avoid this undesirable effect is that the vacuum is unstable against domain formation [12, 21, 23].

To conclude, let us return to the issue of the singular boundary points. Many of the coordinate singularities due to the vanishing of the Faddeev-Popov determinant (which plays the role of the jacobian for the change of variables to the gauge fixed degrees of freedom [4] in the hamiltonian formulation) are screened by the boundary of the fundamental domain. Although the singular boundary points form a set of zero measure in the configuration space, they can nevertheless be important for the dynamics. Near these points we have to choose different coordinates and formulate the necessary transition functions to move from one to the other choice. It is clear that this is difficult to formulate in all rigour in the infinite-dimensional field space. As the domain formation is anticipated to be due to the fact that the energies of the low-lying states flow over the sphaleron energy, we can study the dynamics of the domain formation as long as the energies of all singular boundary points are well above the sphaleron energy. From figs. 3-3,3-4 and 3-5 we see that this is indeed the case in the 18-dimensional subspace we have considered. For the higher energy modes the tail of the wave functional will be so small at the singular boundary points, that we need not worry about their influence on the spectrum. In this way we have a well defined window in which the non-perturbative treatment of a finite number of modes will allow us to calculate the low-lying spectrum of the theory.

Appendix A: Singular boundary points

In this appendix we shall demonstrate that the singular part of the boundary of the fundamental domain in the (u, v) plane does not contain points associated to non-contractable spheres. Such a non-contractable sphere implies at least a one parameter gauge function $g(t)$ along which the norm functional is degenerate and minimal. We will first show that this implies that the fourth order term in eq. (3.2.4) needs to be negative. After that we show that this is not the case for the singular boundary points under consideration. We write

$$g(t) = \exp(X(t)), \quad X(t) = tX_1 + t^2X_2 + t^3X_3 + t^4X_4 + \mathcal{O}\left(t^5\right). \tag{A.1}$$

For all t one should have that $\partial_i({}^{g(t)}A_i) = 0$. Using the fact that

$$\partial_i \frac{d}{dt}({}^{g(t)}A_i) = \partial_i D_i({}^{g(t)}A)\ (g^\dagger(t)\frac{d}{dt}g(t)), \tag{A.2}$$

one easily concludes that X_1 is a zero-mode for the Faddeev-Popov operator at $t = 0$, whereas the first order term in t gives the equation

$$\mathrm{FP}(A)X_2 = -\tfrac{1}{2}[\partial_a X_1, [X_1, A_a]]. \tag{A.3}$$

By considering the inner product of both sides of this equation with X_1, we conclude that it can only have a solution provided the third order term (for $X = X_1$) in eq. (3.2.4) vanishes, as should be obviously true since we are considering $A \in \Lambda$, i.e. the norm functional is at its absolute minimum. We now have sufficient information to compute $\|{}^{g(t)}A\|$ to fourth order in t (the explicit forms of X_3 and X_4 drop out of the expression for this order when we use respectively that $\mathrm{FP}(A)\,X_1 = 0$ and $\partial_a A_a = 0$):

$$\left\|{}^{g(t)}A\right\|^2 = \|A\|^2 + t^4\left\{3\left\langle X_2, \mathrm{FP}(A)\,X_2\right\rangle - \tfrac{1}{12}\left\langle [D_a X_1, X_1], [\partial_a X_1, X_1]\right\rangle\right\} + \mathcal{O}\left(t^5\right). \tag{A.4}$$

To obtain this result we used the Jacobi identity, partial integration, eq. (A.3) and the assumption that X_1 is an eigenfunction of $\bar{L}^2$. Since the first term is positive definite, the norm functional can only be degenerate if the second term is negative.

We now specialize to the case $A(u,v)$ and the singular boundary points that occur at $(u,v) = (\frac{3}{4},\frac{3}{4})$ and $u+v=-3$ for $|u-v| \leq 3$. The zero-modes for the Faddeev-Popov operator at these configurations are easily seen to be given by

$$X_1 = n_a Q^{ab}\sigma_b, \quad Q^{ab} = Q^{ba}, \tag{A.5}$$

where the trace part of the symmetric (real) tensor corresponds to the $j=0$ zero-mode (at $u+v=\frac{3}{2}$) and the traceless part to the $j=2$ zero-mode (at $u+v=-3$). It is now straightforward to substitute X_1 (eq. (A.5)) in eq. (A.4). After some algebra we find

$$-\left\langle [D_a X_1, X_1], [\partial_a X_1, X_1]\right\rangle/2\pi^2 = 2\,\mathrm{tr}(Q^4) - 2(\mathrm{tr}(Q^2))^2 + \tfrac{1}{3}(u+v)\left[(\mathrm{tr}\,Q)^2\,\mathrm{tr}(Q^2) + 2\,\mathrm{tr}\,Q\,\mathrm{tr}(Q^3) - (\mathrm{tr}(Q^2))^2 - 2\,\mathrm{tr}(Q^4)\right]. \tag{A.6}$$

With $Q^{ab} = \delta_{ab}$ and $u+v = \frac{3}{2}$ we find for the right hand side 3, which is positive. For a traceless Q we find $4\,\mathrm{tr}(Q^4) - (\mathrm{tr}(Q^2))^2$ at $u+v=-3$, which is likewise strictly positive. None of the singular boundary points can therefore be associated with a continuous degeneracy.

Appendix B: Gribov horizon for A(c,d)

In this appendix we will calculate $\det(\mathrm{FP}_1(A(c,d))|_{l=1/2})$ for general (c,d), thus extending the result in eq. (3.4.9). We will write the result in terms of the matrices X and Y defined in eq. (3.4.22). It is useful to introduce the following quantities:

$$\begin{aligned}
D_1 &\equiv \left(\varepsilon_{abc}c_i^a c_j^b d_k^c\right)^2 = \mathrm{tr}\,Y\left((\mathrm{tr}\,X)^2 - \mathrm{tr}(X^2)\right) + \mathrm{tr}(X^2Y) - 2\,\mathrm{tr}\,X\,\mathrm{tr}(XY),\\
D_2 &\equiv \left(\varepsilon_{abc}c_i^a d_j^b d_k^c\right)^2 = \mathrm{tr}\,X\left((\mathrm{tr}\,Y)^2 - \mathrm{tr}(Y^2)\right) + \mathrm{tr}(XY^2) - 2\,\mathrm{tr}\,Y\,\mathrm{tr}(XY),\\
D_3 &\equiv \left(\mathrm{tr}(X^2) - (\mathrm{tr}\,X)^2\right)\left(\mathrm{tr}(Y^2) - (\mathrm{tr}\,Y)^2\right) + 2\,\mathrm{tr}\left((XY)^2\right) - 2\left(\mathrm{tr}(XY)\right)^2,
\end{aligned}$$

$$
\begin{aligned}
F_0 &\equiv 27 + 2\det c + 2\det d - 3\,\mathrm{tr}\,X - 3\,\mathrm{tr}\,Y,\\
F_1 &\equiv 36\,\mathrm{tr}(XY) + 24(\mathrm{tr}\,X - \det c)(\mathrm{tr}\,Y - \det d) + 2D_1 + 2D_2,\\
F_2 &\equiv 6D_3 + 8\det c\det d\,(27 - \det c - \det d + 3\,\mathrm{tr}\,X + 3\,\mathrm{tr}\,Y)\\
&\quad +4\det c\left(9(\mathrm{tr}(Y^2) - (\mathrm{tr}\,Y)^2) - D_2\right)\\
&\quad +4\det d\left(9(\mathrm{tr}(X^2) - (\mathrm{tr}\,X)^2) - D_1\right),\\
F_3 &\equiv 48\,(\det c\det d)\,D_3 + 1296\,\mathrm{tr}\left((XY)^2\right)\\
&\quad +1728\left(\det c\det d\,\mathrm{tr}(XY) - \det c\,\mathrm{tr}(XY^2) - \det d\,\mathrm{tr}(X^2Y)\right)\\
&\quad +96(\det c)^2\left(9\,\mathrm{tr}(Y^2) - 6(\mathrm{tr}\,Y)^2 - 2\det d(\mathrm{tr}\,X + \mathrm{tr}\,Y)\right)\\
&\quad +96(\det d)^2\left(9\,\mathrm{tr}(X^2) - 6(\mathrm{tr}\,X)^2 - 2\det c(\mathrm{tr}\,X + \mathrm{tr}\,Y)\right)\\
&\quad +4\left(D_1 + 4\det c\det d - 2(\det d)^2 - 12\det c\,\mathrm{tr}\,Y\right)^2\\
&\quad +4\left(D_2 + 4\det c\det d - 2(\det c)^2 - 12\det d\,\mathrm{tr}\,X\right)^2\\
&\quad -16\,(\det c + \det d)^2\left((\det c)^2 - 6\det c\det d + (\det d)^2\right),\\
R &\equiv 576(\mathrm{tr}\,X + \mathrm{tr}\,Y)\left(\mathrm{tr}(X^2Y^2) - \mathrm{tr}\left((XY)^2\right)\right)\\
&\quad +576\left(\mathrm{tr}(X^2YXY) - \mathrm{tr}(X^3Y^2) + \mathrm{tr}(Y^2XYX) - \mathrm{tr}(Y^3X^2)\right).
\end{aligned}
$$

In terms of this list of invariants we have

$$
\det\left(\mathrm{FP}_1(A(c,d))|_{t=\frac{1}{2}}\right) = 2(F_0^4 + F_3) - (F_0^2 + F_1)^2 - 8F_0F_2 + R. \tag{B.1}
$$

The significance of this expansion becomes clear when we substitute the diagonal choices for c and d, eq. (3.4.8), for which

$$
F_0 = E_0,\ F_1 = \prod_{i=1}^{3} E_i,\ F_2 = \sum_{i=1}^{3} E_i^2,\ F_3 = \sum_{i=1}^{3} E_i^4, \tag{B.2}
$$

with

$$
\begin{aligned}
E_0 &= 27 + 2\textstyle\prod x_i + 2\prod y_i - 3\sum x_i^2 - 3\sum y_i^2,\\
E_1 &= 6x_1y_1 - 2y_1x_2x_3 - 2x_1y_2y_3,\\
E_2 &= 6x_2y_2 - 2y_2x_3x_1 - 2x_2y_3y_1,\\
E_3 &= 6x_3y_3 - 2y_3x_1x_2 - 2x_3y_1y_2.
\end{aligned}
$$

Most important is that R vanishes identically for eq. (3.4.8). Hence the way we came to eq. (B.1) was to first extend E_μ to invariant combinations, which is unique up to invariant polynomials that vanish identically for the diagonal configuration of eq. (3.4.8). The space of invariant polynomials with this property is 11 dimensional and by fitting the determinant with numerical values substituted for c and d, one can easily (with the help of MATHEMATICA) solve for the 11 coefficients. The final result of eq. (B.1) has then been checked for a large number of random choices of c and d.

4 The one-loop effective lagrangian

4.1 Introduction

In this chapter we will calculate the influence of the high-energy modes on the dynamics of the low-energy modes. This is achieved by integrating out the high-energy modes in the path integral, which gives us the one-loop effective lagrangian for the low-energy modes. Denoting the low-energy modes by $B(c,d)$, we will expand the one-loop effective lagrangian first up to the same order as the classical potential, i.e. up to fourth order in B and to second order in $\dot{B}$. This allows us to do the renormalization of the lagrangian properly.

Since we expect the physics to be sensitive to the details of the potential along the tunnelling path, we use an expansion of the effective potential around the sphaleron to construct a fit of the effective potential up to sixth order in the tunnelling parameter u. This allows us to write down the effective lagrangian including some fifth and sixth order terms in B as to reproduce the behaviour along the tunneling path.

It is our purpose to use the effective hamiltonian in a variational method to calculate the spectrum. Although it is possible to calculate the effective potential exactly along the tunnelling path, a polynomial approximation in B is much more useful, since this makes the analytic evaluation of the matrix elements feasible.

The one-loop effective lagrangian will be given in terms of a path integral over the high-energy modes and over ghost fields. Using Feynman diagrams to expand these path integrals is the standard method to proceed, but due to the fact that the theory is defined on S^3, the summation over the space components of a loop momentum looks rather different from the more familiar summation over the time component. To isolate the intricacies of the three-sphere, we will first assume B to be time independent. This allows us to perform the integrations over time components of loop momenta. Within this so-called adiabatic approximation the calculation of the effective potential in an expansion in B is then a purely algebraic problem.

After this we return to the use of Feynman diagrams to evaluate the one-loop contribution to the kinetic term. We will neglect higher order time derivatives of B and also terms of the form $B^n\dot{B}^2$. We choose a renormalization scheme that makes the renormalized kinetic part assume the form of the classical kinetic term, replacing the bare by the renormalized coupling constant. The result of this chapter is then a finite, renormalized effective potential.

4.2 Gauge fixing

For the low-energy modes, we fixed the gauge by restricting ourselves to a fundamental domain. We expect perturbative gauge fixing to be sufficient for the rest of

the modes. We will impose the background field gauge condition on these quantum modes through the usual Faddeev-Popov trick in the path integral. After this we will express the partition function in terms of functional determinants.

4.2.1 Split up of the gauge field

Consider a general gauge field on S^3:

$$A_\mu = (A_0, A_i), \tag{4.2.1}$$

where A_0 is the time component of the gauge field and A_i are the space components with respect to the framing e^i_μ. We will now project out the background field $B(c,d)$. Introduce a scalar projector P_S by

$$P_S\psi = P_0^L\psi = \frac{1}{2\pi^2}\int_{S^3}\psi, \tag{4.2.2}$$

and introduce vector projectors P_c and P_d by

$$(P_cA)_i = \left(P_0^LA\right)_i = \frac{1}{2\pi^2}\int_{S^3}A_i, \tag{4.2.3}$$

$$(P_dA)_i = \left(P_0^KA\right)_i = \left(\frac{1}{2\pi^2}\int_{S^3}A_kV_k^i\right)V_i^i. \tag{4.2.4}$$

With $P_V = P_c + P_d$ the projector on the (c,d) space, we define the background field B and the quantum field Q by respectively

$$B_\mu = (PA)_\mu = (P_SA_0, (P_VA)_i), \tag{4.2.5}$$

$$Q_\mu = A_\mu - B_\mu. \tag{4.2.6}$$

4.2.2 Faddeev-Popov trick

The euclidean partition function is given by the path integral

$$Z = \int DA_\mu \exp(-S_E[A]), \tag{4.2.7}$$

where S_E is the euclidean action. We define the gauge fixing function χ by

$$\chi = (1 - P_S)\,D_\mu(PA)A_\mu + P_SA_0. \tag{4.2.8}$$

The condition $\chi = 0$ imposes the background gauge condition:

$$\chi = 0 \Leftrightarrow \begin{cases} B_0 & = 0 \\ D_\mu(B)Q_\mu & = 0 \end{cases} \tag{4.2.9}$$

We now perform the standard manipulations with the partition function. With the help of the Faddeev-Popov determinant

$$\Delta[A] = \left(\int Dg\,\delta[\chi({}^gA)]\right)^{-1}, \tag{4.2.10}$$

we split off the infinite volume related to the integration over the gauge group and obtain

$$Z = \int DA_\mu \, \delta[\chi(A)] \, \Delta[A] \, \exp(-S_{\rm E}[A]). \tag{4.2.11}$$

The gauge condition $B_0 = 0$ is explicitly solved by restricting the integrations over A. The condition $D_\mu(B)Q_\mu = 0$ is replaced with $D_\mu(B)Q_\mu = f$ after which we average over all non-constant scalar modes f with a gaussian:

$$\begin{aligned} Z &= \int D'f \, DB_k \, D'Q_\mu \, \delta(D_\mu(B)Q_\mu - f) \, \Delta[A] \exp\left[-S_{\rm E}[A] + \frac{1}{\xi g_0^2}\int {\rm tr}(f^2)\right] \\ &= \int DB_k \, D'Q_\mu \, \Delta[A] \, \exp\left[\frac{1}{g_0^2}\int {\rm tr}\left(\tfrac{1}{2}F_{\mu\nu}^2(B+Q) + \frac{1}{\xi}(D_\mu(B)Q_\mu)^2\right)\right]. \end{aligned} \tag{4.2.12}$$

The primed integration means that we have excluded the $l = 0$ modes from the integration over the scalar fields f and Q_0 and the $l = 0$, $k = 1$ and $l = 1$, $k = 0$ modes (the (c,d) modes) from the integration over the vector field Q_k.

We now focus on the Faddeev-Popov determinant (4.2.10). Under an infinitesimal gauge transformation Λ the change in A_μ is given by $D_\mu(A)\Lambda$ and the change in the gauge fixing function by

$$\begin{aligned} \delta\chi &= \frac{\delta\chi}{\delta\Lambda}\Lambda \\ &= (1-P_S)\{D_\mu(PA)D_\mu(A)\Lambda + [(PD(A)\Lambda)_\mu, A_\mu]\} + P_S D_0(A)\Lambda \\ &= (1-P_S)\{D_\mu(B)D_\mu(A)\Lambda - [B_\mu, (PD(A)\Lambda)_\mu] \\ &\quad -[Q_\mu, (PD(A)\Lambda)_\mu]\} + P_S D_0(A)\Lambda \\ &= (1-P_S)\{D_\mu(B)(1-P)D_\mu(A)\Lambda + \partial_\mu(PD(A)\Lambda)_\mu \\ &\quad -[Q_\mu, (PD(A)\Lambda)_\mu]\} + P_S D_0(A)\Lambda \\ &= (1-P_S)\{D_\mu(B)(1-P)D_\mu(A)\Lambda - [Q_\mu, (PD(A)\Lambda)_\mu]\} \\ &\quad + P_S D_0(A)\Lambda. \end{aligned} \tag{4.2.13}$$

The Faddeev-Popov determinant is given by

$$\Delta[A] = \det\left(\frac{\delta\chi}{\delta\Lambda}\right). \tag{4.2.14}$$

Introducing ghost fields ψ and $\bar\psi$, this determinant can be written as a fermionic path integral. We will evaluate this path integral in the quadratic approximation, that is, we throw away terms of order three and higher in the quantum fields ψ and Q_μ. After this the integration over the $l = 0$ modes of ψ can be performed to give an irrelevant constant and we obtain

$$\begin{aligned} \Delta[A] &= \int D\psi \, D\bar\psi \exp\left[\beta\int {\rm tr}\left(\bar\psi\left((1-P_S)\{D_\mu(B)(1-P)D_\mu(B)\psi\} + P_S\partial_0\psi\right)\right)\right] \\ &\propto \int D'\psi \, D'\bar\psi \exp\left[\beta\int {\rm tr}\left(\bar\psi D_\mu(B)(1-P)D_\mu(B)\psi\right)\right]. \end{aligned} \tag{4.2.15}$$

Substituting this in the partition function with $\beta = -1/g_0^2$ we obtain

$$\begin{aligned} Z &= \int DB_k\, D'Q_\mu\, D'\psi\, D'\bar{\psi} \exp\left[\frac{1}{g_0^2}\int \mathrm{tr}\left(\bar{\psi}\left\{-D_\mu(B)(1-P)D_\mu(B)\right\}\psi\right.\right. \\ &\quad \left.\left. +\tfrac{1}{2}F_{\mu\nu}^2(B+Q) + \frac{1}{\xi}(D_\mu(B)Q_\mu)^2\right)\right]. \end{aligned} \tag{4.2.16}$$

4.2.3 The effective action

We now turn to the euclidean action $S_E = S_E[B+Q]$ which we will expand in the field Q_μ. After some manipulation one obtains

$$\begin{aligned} g_0^2 S_E &= g_0^2 \int_0^T d\tau\, (\mathcal{K}+\mathcal{V}) \\ &= -\int \mathrm{tr}\left(\tfrac{1}{2}F_{\mu\nu}^2(B+Q)\right) \\ &= \tfrac{1}{2}\langle F_{\mu\nu}(B), F_{\mu\nu}(B)\rangle - 2\langle (D_\mu F_{\mu\nu})(B), Q_\nu\rangle + \langle Q_\mu, \mathcal{M}_{\mu\nu}(B)Q_\nu\rangle \\ &\quad -2\langle D_\mu(B)[Q_\mu, Q_\nu], Q_\nu\rangle + \tfrac{1}{2}\langle [Q_\mu, Q_\nu], [Q_\mu, Q_\nu]\rangle, \end{aligned} \tag{4.2.17}$$

with

$$\mathcal{M}_{\mu\nu}(B) = W_{\mu\nu}(B) + D_\mu(B)D_\nu(B), \tag{4.2.18}$$

$$W_{\mu\nu}(B) = -2\,\mathrm{ad}\,(F_{\mu\nu}(B)) - (D_\rho^2(B))_{\mu\nu} + 2\delta_{\mu\nu}^{(3)}. \tag{4.2.19}$$

The last equation should be read as

$$\begin{cases} W_{00} &= -D_\rho^2(B) \\ W_{0i} &= -W_{i0} = -2\,\mathrm{ad}\,(\dot{B}_i) \\ W_{ij} &= -2\,\mathrm{ad}\,(F_{ij}(B)) - (D_\rho^2(B))_{ij} + 2\delta_{ij} \end{cases} \tag{4.2.20}$$

Remember that the covariant derivative $D_i(B)$ acting on vectors (or tensors) gives extra connection terms (due to S^3 being a curved manifold) e.g.

$$\begin{aligned} (D_i(B)C)_j &= \partial_i C_j + [B_i, C_j] - \varepsilon_{ijk}C_k \\ &= \left(-2iL_i + iB_i^a T^a - iS_i\right)_{jk} C_k. \end{aligned} \tag{4.2.21}$$

Note that

$$\begin{aligned} \mathcal{M}_{ij}(0) &= -\partial_0^2 + 2\delta_{ij} - (D_k^2(0))_{ij} + D_i(0)D_j(0) \\ &= -\partial_0^2 + 2\vec{L}^2\delta_{ij} + 2\vec{K}_{ij}^2 - 4Q_{ij}, \end{aligned} \tag{4.2.22}$$

thus regaining the quadratic fluctuation operator (2.2.24). Substituting the quadratic expansion for the action in the path integral and choosing the Feynman gauge $\xi = 1$

gives

$$\begin{aligned} Z &= \int DB_k \exp\left(-S_{\rm E}^{\rm eff}[B]\right) \\ &= \int DB_k\, D'Q_\mu\, D'\psi\, D'\bar\psi \exp\left[\frac{1}{g_0^2}\int \mathrm{tr}\left(\bar\psi\left\{-D_\mu(B)(1-P)D_\mu(B)\right\}\psi\right.\right. \\ &\quad \left.\left. + \tfrac{1}{2}F_{\mu\nu}^2(B) - 2(D_\mu F_{\mu\nu})(B)Q_\nu + Q_\mu W_{\mu\nu}(B)Q_\nu\right)\right]. \end{aligned} \tag{4.2.23}$$

The action contains a term $J_\nu Q_\nu$ with $J_\nu = (D_\mu F_{\mu\nu})(B)$. Since B need not satisfy the equations of motion, this term does not vanish. Upon expanding the path integral in Feynman diagrams, this term will give rise to extra diagrams, where J acts as a source. When we will treat this diagrammatic expansion, we will show that the presence of J will only contribute to terms in the effective lagrangian that we will consider to give only small corrections: they are at least of order c^2d^4 or c^4d^2.

Dropping for the time being the term linear in Q_μ, we are left with a gaussian integration over the fields ψ and Q_μ from which we extract the effective action

$$S_{\rm E}^{\rm eff}[B] = S_{\rm E}^{\rm cl}[B] - \ln\det\left(-D_\mu(B)(1-P)D_\mu(B)\right) + \tfrac{1}{2}\ln\det\left(W_{\mu\nu}\right). \tag{4.2.24}$$

Although we will not use the primed notation to denote it, the determinant does exclude the same modes that were not integrated over in the path integral.

4.3 The effective potential

For computing the effective potential, B is considered to be independent of time. The assumption $\dot B = 0$ directly implies $W_{0i} = 0$. This results in a factorization of the integral over Q_μ, and we obtain the one-loop contribution to the effective action

$$\begin{aligned} S_{\rm E}^{(1)}[B, \dot B = 0] &= -\ln\det\left(-D_\mu(B)(1-P)D_\mu(B)\right) \\ &\quad + \tfrac{1}{2}\ln\det\left(-D_\mu(B)D_\mu(B)\right) + \tfrac{1}{2}\ln\det\left(W_{ij}\right). \end{aligned} \tag{4.3.1}$$

The operators in this equation commute with ∂_0. It is this property that makes a reduction to an algebraic problem possible.

4.3.1 The operators

We start by expressing the various operators in terms of c and d. For the scalar operator $-D_\mu^2(B)$ we find

$$-D_\mu(B)D_\mu(B) = -\partial_0^2 - D_i(B)D_i(B). \tag{4.3.2}$$

As it acts on scalar functions, we have $D_i(B) = -2iL_i + iB_i^aT^a$ and we obtain

$$\begin{aligned} -D_i(B)D_i(B) &= 4\vec L^2 - 4B_i^aL_iT^a + B_i^aB_i^bT^aT^b \\ &= 4\vec L^2 - 4c_i^aL_{1i}T^a - 4d_i^aL_{2i}T^a \\ &\quad + \left(c_i^ac_i^b + d_i^ad_i^b + c_i^ad_m^bV_i^m + d_m^aV_i^mc_i^b\right)T^aT^b. \end{aligned} \tag{4.3.3}$$

The other scalar operator can also be written as

$$-D_\mu(B)(1-P)D_\mu(B) = -\partial_0^2 - D_i(B)(1-P_V)D_i(B), \tag{4.3.4}$$

where use was made of the fact that the operator does not act on constant functions. Let the new term $D_i(B)P_V D_i(B)$ act on a scalar mode $\Lambda = |(l_1 0)l_1\rangle$, where $|(ls)k\rangle$ for $s = 0, 1$ denotes respectively scalar and vector modes. We suppress here the quantum numbers m_R and m_k.

The resulting intermediate vector mode is given by

$$D_i(B)\Lambda = \partial_i\Lambda + [c_i, \Lambda] + [d \cdot V_i, \Lambda]. \tag{4.3.5}$$

The first term is longitudinal and has therefore $k = l = l_1$: it gets projected to zero by P_V. The second term will have $l = l_1$ and the third term will have $k = l_1$. The last claim can either be checked explicitly or be derived from the fact that the product $V_i\Lambda$ is essentially $|(11)0\rangle\,|(l_1 0)l_1\rangle$ and hence must have $k = l_1$.

The reasoning so far shows that only scalar modes with $l_1 = 1$ can result in vector modes that will not get necessarily projected to zero by P_V. By similar arguments one shows that matrix elements of $D_i(B)P_V D_i(B)$ between scalar states with $\vec{L}^2$ eigenvalues l_1 and l_2 can only be non-zero if $l_1 = l_2 = 1$. Explicitly, we find

$$\begin{aligned} D_i(B)P_V D_i(B) &= P_1^L D_i(B)(P_V)_{ij} D_j(B) P_1^L \\ &= -P_1^L \left(c_i^a (P_d)_{ij} c_j^b + d_m^a V_i^m (P_c) d_n^b V_i^n\right) T^a T^b P_1^L \\ &= -\tfrac{1}{3}\left\{\left(c_i^a c_i^b - c_i^a c_j^b L_{1j} L_{1i}\right) + \left(d_i^a d_i^b - d_i^a d_j^b L_{2j} L_{2i}\right)\right\} T^a T^b P_1^L. \end{aligned} \tag{4.3.6}$$

Since the intermediate vector mode can have only $k, l = 0, 1, 2$, we have used here the following expressions for the projectors:

$$P_c = P_0^L = \left(1 - \tfrac{1}{2}\vec{L}^2\right)\left(1 - \tfrac{1}{6}\vec{L}^2\right), \tag{4.3.7}$$

$$P_d = P_0^K P_1^L = \left(1 - \tfrac{1}{2}\vec{K}^2\right)\left(1 - \tfrac{1}{6}\vec{K}^2\right) P_1^L = -\tfrac{1}{3}\left(1 - (\vec{L}\cdot\vec{S})^2\right) P_1^L. \tag{4.3.8}$$

The vector operator W_{ij} is more complicated due to the extra connection terms. We write

$$W_{ij} = -\partial_0^2 \delta_{ij} + \bar{W}_{ij}, \tag{4.3.9}$$

with

$$\begin{aligned} \bar{W}_{ij} &= -2\,\mathrm{ad}\,(F_{ij}) + 2\delta_{ij} - (-2iL_k + iB_k^a T^a - iS_k)_{ij}^2 \\ &= 2\vec{L}^2\delta_{ij} + 2\vec{K}_{ij}^2 - 2iF_{ij}^a T^a + B_k^a B_k^b T^a T^b \delta_{ij} \\ &\quad -4B_k^a L_k T^a \delta_{ij} - 2B_k^a (S_k)_{ij} T^a. \end{aligned} \tag{4.3.10}$$

Using $F_{ij} = i(S_k)_{ij}\mathcal{B}_k$ with

$$\begin{aligned} \mathcal{B}_k &= \tfrac{1}{2}\epsilon_{klm} F_{lm} \\ &= -2c_k + 2d \cdot V_k + \varepsilon_{klm} c_l c_m - \varepsilon_{lmn} d_l d_m V_k^n + \varepsilon_{klm}[c_l, d \cdot V_m], \end{aligned} \tag{4.3.11}$$

we can suppress the spin-indices i, j and rewrite $\bar{W}_{ij}$ as

$$\begin{aligned}\bar{W}(B) &= 2\vec{L}^2 + 2\vec{K}^2 - 4c_k^a L_{1k} T^a - 4d_k^a L_{2k} T^a + (-6c_k^a + 2d_m^a V_k^m)\, S_k T^a \\ &+ \left(-\varepsilon_{ijk}\varepsilon_{abc} c_i^a c_j^b - 2\varepsilon_{ijk}\varepsilon_{abc} c_i^a d_m^b V_j^m + \varepsilon_{lmn}\varepsilon_{abc} d_l^a d_m^b V_k^n\right) S_k T^c \\ &+ \left(c_k^a c_k^b + d_k^a d_k^b + c_k^a d_m^b V_k^m + d_m^a V_k^m c_k^b\right) T^a T^b. \qquad (4.3.12)\end{aligned}$$

Note that putting $\vec{S} = 0$ transforms W into the scalar operator. Restricting to $d = 0$ gives the following operators:

$$\begin{aligned}-D_i(c)D_i(c) &= 4\vec{L}^2 - 4c_i^a L_i T^a + c_i^a c_i^b T^a T^b, \qquad (4.3.13)\\ -D_i(c)(1 - P_V)D_i(c) &= 4\vec{L}^2 - 4c_i^a L_i T^a + c_i^a c_i^b T^a T^b \\ &\quad -\tfrac{1}{3}\left(c_i^a c_i^b - c_i^a c_j^b L_j L_i\right) T^a T^b P_1^L, \qquad (4.3.14)\\ \bar{W}(c) &= 2\vec{L}^2 + 2\vec{K}^2 - 4c_k^a L_k T^a - 6c_k^a S_k T^a + c_k^a c_k^b T^a T^b \\ &\quad -\varepsilon_{ijk}\varepsilon_{abc} c_i^a c_j^b S_k T^c. \qquad (4.3.15)\end{aligned}$$

Restricting to the tunnelling path $c_i^a = -u\delta_i^a$ these operators reduce to

$$\begin{aligned}-D_i(u)D_i(u) &= 4\vec{L}^2 + 4u\vec{L}\cdot\vec{T} + 2u^2, \qquad (4.3.16)\\ -D_i(u)(1 - P_V)D_i(u) &= 4\vec{L}^2 + 4u\vec{L}\cdot\vec{T} + 2u^2 \\ &\quad -\tfrac{1}{3}u^2\left(2 - (\vec{L}\cdot\vec{T})^2 - \vec{L}\cdot\vec{T}\right) P_1^L, \qquad (4.3.17)\\ \bar{W}(u) &= 2\vec{L}^2 + 2\vec{K}^2 + 4u\vec{L}\cdot\vec{T} \\ &\quad +(6u - 2u^2)\vec{S}\cdot\vec{T} + 2u^2. \qquad (4.3.18)\end{aligned}$$

4.3.2 Reduction to spatial parts

As we have seen, the operators we are interested in are of the form

$$A(B) = -\partial_0^2 - \partial_\varepsilon^2 + \bar{A}(B), \qquad (4.3.19)$$

where we introduced a laplacian term for an ε-dimensional torus of size L that we attached to our space S^3 [29]. This allows us to neatly perform the dimensional regularization. The scale L should of course be chosen proportional to the radius R of the three-sphere. A precise choice of L would fix our regularization procedure completely, and different choices will be related through finite renormalizations fixing the relations between the associated Λ-parameters. We will comment on this in chapter 6.

Suppose that the spectrum of $\bar{A}$ is $\{\bar{\lambda}_i\}$. The spectrum of $-\partial_\varepsilon^2$ is $\{k_\varepsilon^2\}$ with $\vec{k}_\varepsilon = 2\pi\vec{n}/L$. If we also take the time periodic with period T, the spectrum of $-\partial_0^2$ is $\{k_0^2\}$ with $k_0 = 2\pi n/T$. Since $[\partial_0, \bar{A}(B)] = [\partial_\varepsilon, \bar{A}(B)] = 0$, the spectrum $\{\lambda_i\}$ of $A(B)$ follows trivially.

Consider the exponential integral

$$E_1(x) = \int_x^\infty \frac{ds}{s} e^{-s} = -\gamma - \ln(x) - \sum_{n=1}^{\infty} \frac{(-1)^n x^n}{n\, n!}. \qquad (4.3.20)$$

This implies

$$\int_\delta^\infty \frac{ds}{s} e^{-\lambda s} = -\ln(\lambda) - \ln(\delta) - \gamma + \mathcal{O}(\lambda\delta). \tag{4.3.21}$$

Taking the limit $\delta \downarrow 0$ in this integral, we can write, up to an irrelevant constant,

$$\begin{aligned}
\ln\det(A) &= \operatorname{tr}\ln(A) = \sum_i \ln(\lambda_i) \\
&= -\sum_{k_0}\sum_{k_\varepsilon}\sum_i \int_0^\infty \frac{ds}{s} e^{-s(k_0^2+k_\varepsilon^2+\tilde\lambda_i)} \\
&= -\frac{T}{2\pi}\left(\frac{L}{2\pi}\right)^\varepsilon \int_0^\infty \frac{ds}{s}\int dk_0\, d^\varepsilon k_\varepsilon\, e^{-s(k_0^2+k_\varepsilon^2)} \sum_i e^{-s\tilde\lambda_i} \\
&= -\frac{T}{2\sqrt{\pi}}\left(\frac{L}{2\sqrt{\pi}}\right)^\varepsilon \int_0^\infty ds\, s^{-\frac{3}{2}-\frac{\varepsilon}{2}} \sum_i e^{-s\tilde\lambda_i} \\
&= -\frac{T}{2\sqrt{\pi}}\left(\frac{L}{2\sqrt{\pi}}\right)^\varepsilon \Gamma(-\tfrac{1}{2}-\tfrac{\varepsilon}{2}) \sum_i \tilde\lambda_i^{\frac{1}{2}+\frac{\varepsilon}{2}} \\
&= -\frac{T}{2\sqrt{\pi}}\left(\frac{L}{2\sqrt{\pi}}\right)^\varepsilon \Gamma(-\tfrac{1}{2}-\tfrac{\varepsilon}{2}) \operatorname{tr}\left(\tilde A^{\frac{1}{2}+\frac{\varepsilon}{2}}\right).
\end{aligned} \tag{4.3.22}$$

For general B it will not be possible to find the spectrum $\{\tilde\lambda_i\}$ of $\tilde A$, so that we will have to use some expansion in B. We will shortly perform this expansion, which is essentially based on Bloch perturbation theory. First however, we focus on two configurations of the background field B where we can calculate the determinants exactly.

4.3.3 Exact determinants

The easiest case is of course given by the vacuum $B = 0$. For the scalar operator $-D_\mu(B)D_\mu(B)$ we have $\tilde A = -D_i(B)D_i(B) = 4\vec L^2$. To evaluate the trace, we use the basis $|l\, m_L\, m_R\rangle \otimes |1\, m_t\rangle$ and obtain

$$\begin{aligned}
\operatorname{tr}\left((4\vec L^2)^{-s}\right) &= 3\sum_{l=\frac{1}{2},1,\ldots}^\infty \frac{(2l+1)^2}{(4l(l+1))^s} \\
&= 3\sum_{k=2}^\infty \frac{k^2}{(k^2-1)^s} \\
&= 3\,\zeta(s-1,-1) + 3\,\zeta(s,-1).
\end{aligned} \tag{4.3.23}$$

Here we introduced the function $\zeta(s,a)$, which is defined by

$$\zeta(s,a) = \sum_{k=2}^\infty \frac{1}{(k^2+a)^s}, \quad \Re(s) > \tfrac{1}{2}. \tag{4.3.24}$$

After analytic continuation we have

$$\zeta(s,a) = \sum_{m=0}^\infty \frac{(s)_m}{m!}(-a)^m\,(\zeta_R(2s+2m)-1), \quad s \neq \tfrac{1}{2}, -\tfrac{1}{2}, \ldots, \tag{4.3.25}$$

where ζ_R denotes the Riemann ζ-function and $(s)_m$ is Pochhammer's symbol:

$$(s)_m = \frac{\Gamma(s+m)}{\Gamma(s)}. \tag{4.3.26}$$

Separating the divergent term in the expansion of eq. (4.3.25) we obtain

$$\begin{aligned}\zeta(n-\tfrac{1}{2}-\tfrac{\varepsilon}{2},a) &= \frac{(n-\frac{1}{2}-\frac{\varepsilon}{2})_{1-n}}{(1-n)!}(-a)^{1-n}(\zeta_R(1-\varepsilon)-1) \\ &\quad + \zeta_F(n-\tfrac{1}{2},a), \qquad n=1,0,-1,\ldots \end{aligned}\tag{4.3.27}$$

For the scalar operators the results are

$$\begin{aligned}&\ln\det(-D_\mu(B)D_\mu(B)) = \\ &\quad -\frac{T}{2\sqrt{\pi}}\left(\frac{L}{2\sqrt{\pi}}\right)^{\varepsilon}\Gamma(-\tfrac{1}{2}-\tfrac{\varepsilon}{2})\left\{3\,\zeta(-\tfrac{3}{2}-\tfrac{\varepsilon}{2},-1)+3\,\zeta(-\tfrac{1}{2}-\tfrac{\varepsilon}{2},-1)\right\},\end{aligned}\tag{4.3.28}$$

and

$$\ln\det(-D_\mu(B)(1-P)D_\mu(B)) = \ln\det(-D_\mu(B)D_\mu(B)). \tag{4.3.29}$$

For the vector operator we have $\bar{A} = 2\vec{L}^2 + 2\vec{K}^2$. With the help of the basis of vector modes $|l\,m_R; k\,m_k\rangle \otimes |1\,m_l\rangle$ we obtain

$$\mathrm{tr}\left((2\vec{L}^2+2\vec{K}^2)^{-s}\right) = 3\sum_{l,k}\frac{(2l+1)(2k+1)}{(2l(l+1)+2k(k+1))^s}. \tag{4.3.30}$$

The summation over (l,k) is as follows:

$$\sum_{l,k} = \sum_{m=\frac{1}{2},1,\ldots}^{\infty}(\delta_{lm}\delta_{km}+\delta_{l\,m+1}\delta_{km}+\delta_{lm}\delta_{k\,m+1}). \tag{4.3.31}$$

The summations can be expressed in terms of ζ-functions and of ζ_R-functions. The result is

$$\begin{aligned}\ln\det(W_{ij}) &= -\frac{T}{2\sqrt{\pi}}\left(\frac{L}{2\sqrt{\pi}}\right)^{\varepsilon}\Gamma(-\tfrac{1}{2}-\tfrac{\varepsilon}{2})\left\{3\,\zeta(-\tfrac{3}{2}-\tfrac{\varepsilon}{2},-1)+3\,\zeta(-\tfrac{1}{2}-\tfrac{\varepsilon}{2},-1)\right. \\ &\quad \left.+6\,(\zeta_R(-3-\varepsilon)-9)-6\,(\zeta_R(-1-\varepsilon)-3)\right\}.\end{aligned}\tag{4.3.32}$$

From eq. (4.3.1) we obtain the Casimir energy

$$\mathcal{V}^{(1)}(B=0) = -18+3\,\zeta_R(-3)-3\,\zeta_R(-1), \tag{4.3.33}$$

where we took the limit $\varepsilon \to 0$.

Another configuration for B where we can calculate the determinants exactly is the sphaleron. Here we have $-D_i(B)D_i(B) = 2\vec{L}^2 + 2\vec{J}^2 - 2$. Using the basis $|l\,m_R; j\,m_j\rangle$ we obtain

$$\mathrm{tr}\left((2\vec{L}^2+2\vec{J}^2-2)^{-s}\right) = \sum_{l,j}\frac{(2l+1)(2j+1)}{(2l(l+1)+2j(j+1)-2)^s}, \tag{4.3.34}$$

with

$$\sum_{l,j} = \sum_{m=\frac{1}{2},1,\ldots}^{\infty} (\delta_{lm}\delta_{jm} + \delta_{l\,m+1}\delta_{jm} + \delta_{lm}\delta_{j\,m+1}) + \delta_{l1}\delta_{j0}. \tag{4.3.35}$$

Thus we find

$$\begin{aligned}\ln\det(-D_\mu(B)D_\mu(B)) = \\ -\tfrac{T}{2\sqrt{\pi}}\left(\tfrac{L}{2\sqrt{\pi}}\right)^{\epsilon}\Gamma(-\tfrac{1}{2}-\tfrac{\epsilon}{2})\left\{\zeta(-\tfrac{3}{2}-\tfrac{\epsilon}{2},-3)+3\,\zeta(-\tfrac{1}{2}-\tfrac{\epsilon}{2},-3)\right. \\ \left.+2\,(\zeta(-\tfrac{3}{2}-\tfrac{\epsilon}{2},-2)-2\sqrt{2})+2\,(\zeta(-\tfrac{1}{2}-\tfrac{\epsilon}{2},-2)-\sqrt{2})+3\sqrt{2}\right\}.\end{aligned} \tag{4.3.36}$$

To evaluate the other scalar operator, note that at the sphaleron, eq. (4.3.17) implies that only the $l = j = 1$ eigenvalue changes from 6 to $\frac{16}{3}$. Hence we have

$$\begin{aligned}\ln\det(-D_\mu(B)(1-P)D_\mu(B)) = \\ \ln\det(-D_\mu(B)D_\mu(B)) + T\,(12\sqrt{3}-9\sqrt{6}).\end{aligned} \tag{4.3.37}$$

The vector operator at the sphaleron also assumes the form $\bar{W} = 2\vec{L}^2 + 2\vec{J}^2 - 2$, but it must be remembered that $\vec{J}$ in this case also contains a spin contribution. We use the basis $|(l1)k,j\rangle$ (where we suppress m_R and m_j) to evaluate the trace. The summation is given by

$$\begin{aligned}\sum_{l,j} \;=\; & \sum_{m=\frac{1}{2},1,\ldots}^{\infty} (\delta_{lm}\delta_{jm} + \delta_{l\,m+1}\delta_{jm} + \delta_{lm}\delta_{j\,m+1} + \delta_{l\,m+2}\delta_{jm} + \delta_{lm}\delta_{j\,m+2}) \\ & +\delta_{l1}\delta_{j0}\delta_{k1} + \delta_{l2}\delta_{j0}\delta_{k1} - \delta_{l1}\delta_{j1}\delta_{k0}.\end{aligned} \tag{4.3.38}$$

The last term corresponds to the exclusion of the d modes. For a state (l,j) the degeneracy is $(2l+1)(2j+1)$ multiplied by the number of possible k values. The latter is given by $(3-|j-l|)$, with the exception of $l = j = \frac{1}{2}$, where k can only assume the values $\frac{1}{2}$ and $\frac{3}{2}$. The result for the vector operator at the sphaleron is

$$\begin{aligned}\ln\det(W_{ij}) \;=\; & -\tfrac{T}{2\sqrt{\pi}}\left(\tfrac{L}{2\sqrt{\pi}}\right)^{\epsilon}\Gamma(-\tfrac{1}{2}-\tfrac{\epsilon}{2})\left\{-4+3\sqrt{2}-9\sqrt{6}+5\sqrt{10}\right. \\ & +3\,\zeta(-\tfrac{3}{2}-\tfrac{\epsilon}{2},-3)+9\,\zeta(-\tfrac{1}{2}-\tfrac{\epsilon}{2},-3) \\ & +4\,(\zeta(-\tfrac{3}{2}-\tfrac{\epsilon}{2},-2)-2\sqrt{2})+4\,(\zeta(-\tfrac{1}{2}-\tfrac{\epsilon}{2},-2)-\sqrt{2}) \\ & +2\,(\zeta(-\tfrac{3}{2}-\tfrac{\epsilon}{2},1)-5\sqrt{5}-10\sqrt{10}) \\ & \left.-10\,(\zeta(-\tfrac{1}{2}-\tfrac{\epsilon}{2},1)-\sqrt{5}-\sqrt{10})\right\}.\end{aligned} \tag{4.3.39}$$

Adding things up, we arrive at

$$\nu^{(1)}(\mathrm{Sph}) \;=\; \tfrac{1}{4\sqrt{\pi}}\left(\tfrac{L}{2\sqrt{\pi}}\right)^{\epsilon}\Gamma(-\tfrac{1}{2}-\tfrac{\epsilon}{2})\left\{4+6\sqrt{2}+24\sqrt{3}-9\sqrt{6}+5\sqrt{10}\right.$$

$$
\begin{aligned}
& -2\zeta(-\tfrac{3}{2}-\tfrac{\epsilon}{2},-3)-2\zeta(-\tfrac{3}{2}-\tfrac{\epsilon}{2},-2)-2\zeta(-\tfrac{3}{2}-\tfrac{\epsilon}{2},1) \\
& -6\zeta(-\tfrac{1}{2}-\tfrac{\epsilon}{2},-3)-2\zeta(-\tfrac{1}{2}-\tfrac{\epsilon}{2},-2)+10\zeta(-\tfrac{1}{2}-\tfrac{\epsilon}{2},1)\Big\} \\
= \; & -1-3\sqrt{2}-12\sqrt{3}+\tfrac{9}{2}\sqrt{6}-\tfrac{5}{2}\sqrt{10}+\tfrac{11}{4\epsilon}-\tfrac{11}{8}\gamma+\tfrac{11}{4}\log(2) \\
& +\tfrac{11}{4}\log\left(\tfrac{L}{2\sqrt{\pi}}\right)+\zeta_F(-\tfrac{3}{2},-3)+\zeta_F(-\tfrac{3}{2},-2)+\zeta_F(-\tfrac{3}{2},1) \\
& +3\zeta_F(-\tfrac{1}{2},-3)+\zeta_F(-\tfrac{1}{2},-2)-5\zeta_F(-\tfrac{1}{2},1). \qquad (4.3.40)
\end{aligned}
$$

The pole term $\frac{11}{4\epsilon}$ has to be absorbed through a renormalization of the coupling constant. Adding the classical potential at the sphaleron we get

$$
\mathcal{V}_{\rm eff}({\rm Sph}) = \frac{2\pi^2}{g_0^2}\frac{3}{2}+\frac{11}{4\epsilon}+\text{finite terms}. \qquad (4.3.41)
$$

So the infinite part of the renormalization is

$$
\frac{1}{g_R^2}=\frac{1}{g_0^2}+\frac{11}{12\pi^2\epsilon}. \qquad (4.3.42)
$$

This is the standard result for SU(2) gauge theory in $1+3$ dimensions as of course it should be: the renormalization is an ultra-violet effect and does not depend on the global properties of the space on which the theory is defined.

4.3.4 Along the tunnelling path

Consider a configuration along the tunnelling path: $c_i^a = -u\delta_i^a$. The spectra of the operators can still be calculated exactly, but the summations become tedious. Therefore we will expand the determinants around the two configurations studied above, that is, around $u=0$ and $u=1$. Using these expansions we construct a polynomial of sixth order in u that is a good fit to the effective potential along the tunnelling path.

We rewrite eq. (4.3.22) as follows

$$
\ln\det(A) = -\frac{T}{2\sqrt{\pi}}\left(\frac{L}{2\sqrt{\pi}}\right)^{\epsilon}\int_0^\infty ds\, s^{-\frac{3}{2}-\frac{\epsilon}{2}}\,\mathrm{tr}\left(e^{-s\tilde{A}}\right). \qquad (4.3.43)
$$

From eq. (4.3.16) it directly follows that the eigenfunctions of the scalar operator $\tilde{A}=-D_i(B)D_i(B)$ are the $|l\,m_R;j\,m_j\rangle$ with the eigenvalues $4l(l+1)+2u(j(j+1)-l(l+1)-2)+2u^2$. This allows us to write

$$
\mathrm{tr}\left(e^{-s\tilde{A}}\right) = \sum_{l=\frac{1}{2},1,\ldots}^{\infty}(2l+1)e^{-s4l(l+1)}\sum_{j=|l-1|}^{l+1}(2j+1)e^{-s(2u(j(j+1)-l(l+1)-2)+2u^2)}, \qquad (4.3.44)
$$

and to expand the second exponential in u. After performing the summation over j and the integration over s the l-summations can again be expressed in terms of ζ-functions. Most of the algebra was done using FORM [30]. The other scalar operator

can be treated similarly. The eigenvalues can be written down from eq. (4.3.17) as well: they differ from the ones above only for $l = 1$.

For the vector operator the situation is more complicated since the eigenvalues are not readily available. We write

$$\tilde{W}(u) = 2\vec{L}^2 + 2\vec{K}^2 + \hat{W}(u), \tag{4.3.45}$$

where the precise form of $\hat{W}(u)$ can be read off from eq. (4.3.18). Since $\hat{W}(0) = 0$ we can treat $\hat{W}(u)$ as a perturbation on the operator $2\vec{L}^2 + 2\vec{K}^2$. As $\tilde{W}$ commutes with the $\{\vec{L}^2, L_{2z}, \vec{J}^2, J_z\}$, the basis to use is $|(l1)k, j\rangle$. The dimension for the subspace in which we have to find the eigenvalues of $\tilde{W}$ is given by the number of possible k values. Since this dimension is maximally three, it is of course possible to obtain the eigenvalues of $\tilde{W}(u)$ exactly, but as explained earlier, it is more convenient to expand in u. The unperturbed eigenvalues within each sector are $2l(l+1) + 2k(k+1)$, so we need non-degenerate perturbation theory to obtain the expansion in u for the eigenvalues $\tilde{\lambda}(j,k,l)$. A method that implements this particularly nice is due to Bloch [31]

Using MATHEMATICA we computed the expansions for the eigenvalues. For this we needed the matrix elements of one of the operators $\vec{L}\cdot\vec{T}$ and $\vec{S}\cdot\vec{T}$; the matrix elements of the other then follow trivially. To calculate these matrix elements, we need the 6-j symbols [32]. For three angular momenta t, s and l we have

$$|t,(sl)k,j\rangle = \sum_q (-1)^{t+s+l+j}[(2q+1)(2k+1)]^{\frac{1}{2}} \left\{ \begin{array}{ccc} t & s & q \\ l & j & k \end{array} \right\} |(ts)q,l,j\rangle. \tag{4.3.46}$$

This gives

$$\begin{aligned} \langle t,(sl)k',j|\,\vec{S}\cdot\vec{T}\,|t,(sl)k,j\rangle &= -\tfrac{1}{2}(s(s+1)+t(t+1))\delta_{k'k} \\ &+\tfrac{1}{2}\sum_q q(q+1)(2q+1)[(2k+1)(2k'+1)]^{\frac{1}{2}} \left\{ \begin{array}{ccc} t & s & q \\ l & j & k' \end{array} \right\} \left\{ \begin{array}{ccc} t & s & q \\ l & j & k \end{array} \right\}. \end{aligned} \tag{4.3.47}$$

As in the case of the scalar operators, we expand the exponential in u and perform the s-integration. The summations over l can be expressed in ζ-functions. During the various stages of these calculations care has to be taken for low values of l, k and j: for certain values the Bloch result for the general eigenvalue $\tilde{\lambda}(j,k,l)$ will not be valid, since the subspace in which to perform the diagonalization may have less dimensions than the bulk value $3 - |l-j|$: some of the k values would be negative. Moreover, in the $l = 1$, $j = 1$ sector, which is a priori three dimensional, the $k = 0$ modes have to be thrown out explicitly, since they are the d modes. Exclusion of the c modes is simply achieved by starting the summation over l with $l = \frac{1}{2}$. The result for the effective potential up to fourth order in u is

$$\mathcal{V}^{(1)}(u) = -18 + 3\,\zeta_R(-3) - 3\,\zeta_R(-1)$$

$$
\begin{aligned}
&+V_{\rm cl}(u)\left(-\tfrac{1259}{1152}+\tfrac{11}{6\varepsilon}-\tfrac{11}{12}\gamma-\tfrac{11}{128}\sqrt{2}+\tfrac{11}{6}\log(2)+\tfrac{11}{6}\log\left(\tfrac{L}{2\sqrt{\pi}}\right)\right.\\
&\quad-\tfrac{23}{6}\zeta(\tfrac{3}{2},-1)-\tfrac{1}{6}\zeta(\tfrac{5}{2},-1)+\tfrac{53}{3}\zeta(\tfrac{7}{2},-1)+14\,\zeta(\tfrac{9}{2},-1)\\
&\quad\left.+\tfrac{16}{3}\zeta_R(3)-\tfrac{19}{6}\zeta_R(5)-\tfrac{1}{3}\zeta_R(7)\right)\\
&+u^2\left(\tfrac{179}{192}+\tfrac{33}{64}\sqrt{2}+13\,\zeta(\tfrac{3}{2},-1)-9\,\zeta(\tfrac{5}{2},-1)-106\,\zeta(\tfrac{7}{2},-1)\right.\\
&\quad\left.-84\,\zeta(\tfrac{9}{2},-1)+2\,\zeta_R(-1)-23\,\zeta_R(3)+19\,\zeta_R(5)+2\,\zeta_R(7)\right)\\
&+u^4\left(\tfrac{863}{768}+\tfrac{1475}{2048}\sqrt{2}-\tfrac{53}{4}\zeta(\tfrac{3}{2},-1)+\tfrac{17}{4}\zeta(\tfrac{5}{2},-1)+\tfrac{261}{2}\zeta(\tfrac{7}{2},-1)\right.\\
&\quad+47\,\zeta(\tfrac{9}{2},-1)-66\,\zeta(\tfrac{11}{2},-1)+\tfrac{63}{4}\zeta_R(3)-79\,\zeta_R(5)\\
&\quad\left.+\tfrac{227}{4}\zeta_R(7)+5\,\zeta_R(9)\right). \qquad (4.3.48)
\end{aligned}
$$

Here we eliminated the u^3 term in favour of the classical potential $V_{\rm cl}$ defined by

$$
\mathcal{V}_{\rm cl}=\frac{2\,\pi^2}{g_0^2}V_{\rm cl}, \qquad (4.3.49)
$$

so

$$
V_{\rm cl}(u)=\tfrac{3}{2}u^2(2-u)^2. \qquad (4.3.50)
$$

One checks that the pole term is absorbed by the coupling constant renormalization of eq. (4.3.42).

Results up to tenth order in u were calculated. As can be seen from fig. 4-1, the expansions do not converge to the exact result at $u=1$. This should come as no big surprise, since we have no reason to expect the radius of convergence of the expansion to be as large as one. Judging from the picture, one would estimate a radius of convergence of roughly 0.6.

To find the effective potential for larger u, we make a similar expansion of the effective potential around the sphaleron. Writing $u=1+a$, we have

$$
\begin{aligned}
-D_i(a)D_i(a) &= 2\vec{L}^2+2\vec{J}^2-2+4a(\vec{L}\cdot\vec{T}+1)+2a^2, && (4.3.51)\\
-D_i(a)(1-P_V)D_i(a) &= 2\vec{L}^2+2\vec{J}^2-2+4a(\vec{L}\cdot\vec{T}+1)+2a^2\\
&\quad-\tfrac{1}{3}(1+a)^2\left(2-(\vec{L}\cdot\vec{T})^2-\vec{L}\cdot\vec{T}\right)P_1^L, && (4.3.52)\\
\tilde{W}(a) &= 2\vec{L}^2+2\vec{J}^2-2+a(4+4\vec{L}\cdot\vec{T}+2\vec{S}\cdot\vec{T})\\
&\quad+a^2(2-2\vec{S}\cdot\vec{T}). && (4.3.53)
\end{aligned}
$$

The expansions of the determinants of the scalar operators can be obtained exactly as described above. The final l-summations can be expressed in terms of $\zeta(s,b)$ with $b=-3,-2,1$. For the vector operator, we could in principle again use the Bloch perturbation method to obtain the eigenvalues $\tilde{\lambda}(j,k,l)(a)$, although the $a=0$ level is now degenerate. There is however an easier way. Suppose we have $\hat{A}=F+\hat{A}$ with $F=\hat{A}(0)$ such that $[F,\hat{A}]=0$. This allows us to substitute in eq. (4.3.43)

$$
{\rm tr}\left(e^{-s\hat{A}}\right)={\rm tr}\left(e^{-sF}e^{-s\hat{A}}\right)=\sum_i e^{-sF_i}\sum_{n=0}^{\infty}\frac{(-s)^n}{n!}\,{\rm tr}_i\left(\hat{A}^n\right). \qquad (4.3.54)
$$

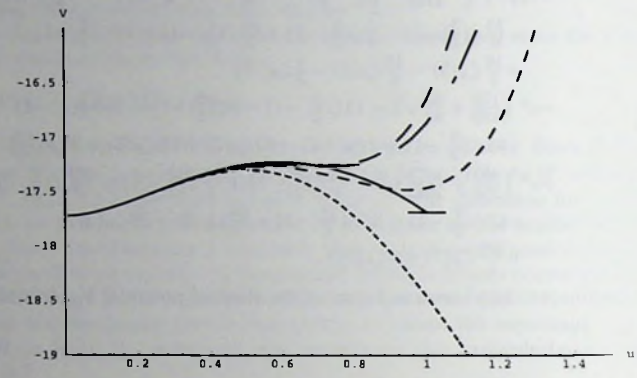

Figure 4-1. Expansion of $\mathcal{V}^{(1)}(u)$ in the tunnelling parameter u. We dropped the ε and $\log(L)$ dependent parts. We have drawn the expansion up to order u^4, u^6, u^8 and u^{10}. Longer dashes correspond to higher order expansions. The horizontal line at $u = 1$ denotes the exact potential at the sphaleron, the drawn curve is the sixth order fit to be explained in the text.

The sum over i is a sum over the eigenspaces of F, F_i is the corresponding eigenvalue and $\mathrm{tr}_i\,()$ denotes a trace within the eigenspace. For the operator W we indeed have that $F = \bar{W}(0) = 2\vec{L}^2 + 2\vec{J}^2 - 2$ commutes with $\bar{W}$ and we obtain

$$\ln\det(W) \;=\; -\frac{T}{2\sqrt{\pi}}\left(\frac{L}{2\sqrt{\pi}}\right)^{\epsilon}\sum_{l,j}(2l+1)(2j+1)\times$$
$$\int_0^\infty ds\, s^{-\frac{3}{2}-\frac{\epsilon}{2}} e^{-s(2l(l+1)+2j(j+1)-2)}\sum_{n=0}^{\infty}\frac{(-s)^n}{n!}\,\mathrm{tr}_{lj}\left(\hat{W}^n\right). \qquad (4.3.55)$$

The sum over l and j is essentially given by eq. (4.3.38). Note that the sum over different k values is now absorbed in the trace in the (l, j) space. When taking this trace one has to deal with the same subtleties connected with low values of l and j as described above. The resulting effective potential is plotted in fig. 4-2. The expansion seems to have a radius of convergence of roughly 0.4. Using the fourth order expansion in u and the first order expansion in a (i.e. the value and the slope of the potential at the sphaleron), we can construct a polynomial in u of degree six that is a good approximation to the effective potential.

Regarding the issue of the radius of convergence, one might think that also integrating out the (c, d) modes that are orthogonal to the u mode might result in better convergence. Also one expects the $u \to 2 - u$ symmetry to be restored in this case.

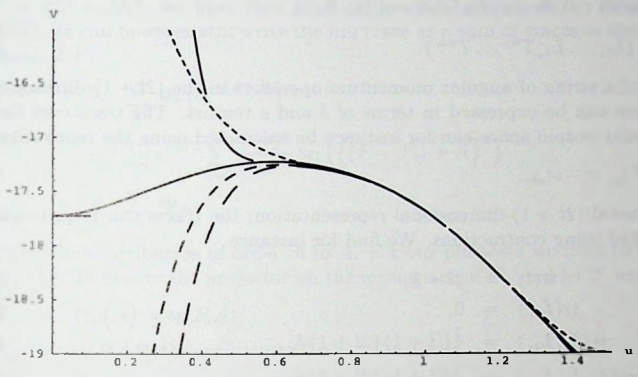

Figure 4-2. Expansion of $\mathcal{V}^{(1)}(u = 1+a)$ around the sphaleron. We dropped the ϵ and $\log(L)$ dependent parts. We have drawn the expansion up to order a^4, a^6, a^8 and a^{10}. Longer dashes correspond to higher order expansions. The horizontal line at $u = 0$ denotes the exact potential at the vacuum, the drawn curve is the sixth order fit.

With the techniques described above, performing this calculation is straightforward, provided one remembers to properly adjust the gauge fixing procedure. The new expansions in u and a have roughly the same convergence behaviour as before, so there is no improvement on this point. The symmetry is however manifestly restored: the expansion in a contains only even powers of a.

4.3.5 The c space

If we take a configuration $B(c, d)$ with $d = 0$, the operators no longer commute with $\vec{J}$. The eigenspace in which we have to diagonalize the operators will have a dimension that depends on l and we can no longer use Bloch perturbation to obtain the expansions of the eigenvalues for general l. The method of eq. (4.3.54) and a generalization thereof can however still be used. We will calculate the determinants up to fourth order in the field c. Starting with the scalar operator, we can write $-D_i(c)D_i(c) = F + \hat{A}(c)$, with (cf. eq. (4.3.13))

$$F = 4\vec{L}^2, \tag{4.3.56}$$

$$\hat{A}(c) = -4c_i^a L_i T^a + c_i^a c_i^b T^a T^b. \tag{4.3.57}$$

Since $[\vec{L}^2, \bar{A}(c)] = 0$, we can use eq. (4.3.54). The problem of calculating $\mathrm{tr}_l(\bar{A}^n(c))$ then reduces to calculating traces of the form

$$\mathrm{tr}_l\left(L_{i_1} \dots L_{i_n} T^{a_1} \dots T^{a_m}\right). \tag{4.3.58}$$

A trace of a string of angular momentum operators in the $(2l+1)$-dimensional representation can be expressed in terms of δ and ε tensors. The trace over the three-dimensional isospin space can for instance be calculated using the representation

$$(T^a)_{bc} = -i\varepsilon_{abc}. \tag{4.3.59}$$

For a general $(2l+1)$-dimensional representation, the traces can in principle all be constructed using contractions. We find for instance

$$\begin{aligned}
\mathrm{tr}(\mathbb{1}) &= 2l+1, && (4.3.60)\\
\mathrm{tr}(L_{i_1}) &= 0, && (4.3.61)\\
\mathrm{tr}(L_{i_1} L_{i_2}) &= \tfrac{1}{3} l(l+1)(2l+1)\,\delta_{i_1 i_2}, && (4.3.62)\\
\mathrm{tr}(L_{i_1} L_{i_2} L_{i_3}) &= \tfrac{i}{6} l(l+1)(2l+1)\,\varepsilon_{i_1 i_2 i_3}, && (4.3.63)\\
\mathrm{tr}(L_{i_1} L_{i_2} L_{i_3} L_{i_4}) &= \tfrac{1}{30} l(l+1)(2l(l+1)+1)(2l+1)\left(\delta_{i_1 i_2}\delta_{i_3 i_4} + \delta_{i_1 i_4}\delta_{i_2 i_3}\right)\\
&\quad + \tfrac{1}{30} l(l+1)(2l(l+1)-4)(2l+1)\,\delta_{i_1 i_3}\delta_{i_2 i_4}. && (4.3.64)
\end{aligned}$$

For our purposes, the $\vec{L}^2$ eigenspaces are $(2l+1)^2$ dimensional due to the extra quantum number m_R, so we have to multiply the results above by another factor $2l+1$.

There is another way of computing the traces. The $\vec{L}$ and $\vec{T}$ operators generate rotations and constant gauge transformations respectively. After contraction, the c dependence of the expression will only be through certain combinations that are invariant under these transformations. Explicitly, we will have invariance under

$$c_i^a \to (S c R_1)_i^a, \tag{4.3.65}$$

with S and R_1 orthogonal three by three matrices. Another way of dealing with $\mathrm{tr}_l(\bar{A}^n(c))$ is hence by replacing in each term the product of c matrices with the corresponding invariant times a projection operator. If we define $X = cc^T$, this means

$$\begin{aligned}
c_i^a &\to 0, && (4.3.66)\\
c_i^a c_j^b &\to \tfrac{1}{9}\,\mathrm{tr}(X)\,\delta^{ab}\delta_{ij}, && (4.3.67)\\
c_i^a c_j^b c_k^c &\to \tfrac{1}{6}\det(c)\,\varepsilon_{ijk}\varepsilon^{abc}. && (4.3.68)
\end{aligned}$$

The fourth order term gets replaced by a combination of the nine possible tensor structures, where the coefficients are linear combinations of the two invariants $\mathrm{tr}^2(X)$ and $\mathrm{tr}(X^2)$. After this projection, all the indices occurring under the traces are contracted. Using the su(2) commutation relations, the traces can now be evaluated easily. The remaining integration over s and the summation over l proceed as before.

For the vector operator we encounter a new problem. Writing $\hat{W}(c) = F + \hat{W}(c)$ with $F = 2\vec{L}^2 + 2\vec{K}^2$, we have that $[F, \hat{W}(c)] = 2[\vec{K}^2, \hat{W}(c)] \neq 0$. Returning to eq. (4.3.54), we can however still write the full trace as a sum of traces in the different eigenspaces of F:

$$\begin{aligned} \mathrm{tr}\left(e^{-s\hat{A}}\right) &= \sum_i \mathrm{tr}_i\left(e^{-s(F+\hat{A})}\right) \\ &= \sum_i e^{-sF_i} \sum_{n=0}^{\infty} \frac{(-s)^n}{n!} \mathrm{tr}_i\left(\left\{(F-F_i)+\hat{A}\right\}^n\right) \\ &= \sum_m \mathrm{sp}_m. \end{aligned} \tag{4.3.69}$$

Here sp_m is the contribution of order m in $\hat{A}$. For our purposes we need to calculate up to sp_4. Let P_i denote the projector on the eigenspace of F_i, and let $\mathcal{T}$ be given by

$$\mathcal{T}_i = \mathrm{tr}_i\left(\hat{A}\right) = \mathrm{tr}(P_i\hat{A}), \tag{4.3.70}$$

$$\mathcal{T}_{ij} = \mathrm{tr}(P_i\hat{A}P_j\hat{A}), \text{ etc.} \tag{4.3.71}$$

Writing $\Delta_{ji} = F_j - F_i$ we find

$$\mathrm{sp}_1 = \sum_i e^{-sF_i}(-s)\mathcal{T}_i, \tag{4.3.72}$$

$$\begin{aligned} \mathrm{sp}_2 &= \sum_i e^{-sF_i} \sum_{n=2}^{\infty} \frac{(-s)^n}{n!} \mathrm{tr}_i\left(\hat{A}(F-F_i)^{n-2}\hat{A}\right) \\ &= \sum_{ij} e^{-sF_i} \sum_{n=2}^{\infty} \frac{(-s)^n}{n!} \mathrm{tr}_i\left(\hat{A}P_j\hat{A}\right)\Delta_{ji}^{n-2} \\ &= \sum_i \mathcal{T}_{ii}e^{-sF_i}\frac{(-s)^2}{2} + \sum_{i\neq j}\mathcal{T}_{ij}e^{-sF_i}\frac{1}{\Delta_{ji}^2}\left(e^{-s\Delta_{ji}} - 1 + s\Delta_{ji}\right) \\ &= \sum_i \mathcal{T}_{ii}e^{-sF_i}\frac{s^2}{2} + \sum_{i\neq j}\mathcal{T}_{ij}e^{-sF_i}\frac{s}{\Delta_{ji}}, \end{aligned} \tag{4.3.73}$$

$$\mathrm{sp}_3 = \sum_{ijk}\mathcal{T}_{ijk}e^{-sF_i}\sum_{n=3}^{\infty}\frac{(-s)^n}{n!}\sum_{m_1=0}^{n-3}\Delta_{ji}^{m_1}\Delta_{ki}^{n-3-m_1}, \tag{4.3.74}$$

$$\mathrm{sp}_4 = \sum_{ijkl}\mathcal{T}_{ijkl}e^{-sF_i}\sum_{n=4}^{\infty}\frac{(-s)^n}{n!}\sum_{m_1=0}^{n-4}\sum_{m_2=0}^{n-4-m_1}\Delta_{ji}^{m_1}\Delta_{ki}^{m_2}\Delta_{li}^{n-4-m_1-m_2}. \tag{4.3.75}$$

We can rewrite sp_3 and sp_4 similarly to sp_2, but the resulting expressions are more difficult.

For the case of $\hat{A} = \hat{W}$, the eigenspaces i_m correspond to pairs (l_m, k_m). Starting with a pair (l_1, k_1), we can only reach states with $l = l_1$ ($\vec{L}^2$ commutes with $\hat{W}$) and with $k = |l_1 - 1|, \ldots l_1 + 1$. Extracting the overall summation over l turns the other summations into finite sums. For sp_2 for instance we have

$$\sum_{i_1 i_2} \to \sum_{l_1}\sum_{k_1=|l_1-1|}^{l_1+1}\sum_{k_2=|l_1-1|}^{l_1+1}. \tag{4.3.76}$$

Using FORM we perform these finite sums. The result is an l-dependent expression in which the $\mathcal{T}$ functions have the form

$$\mathcal{T}_{k_1 k_2 \ldots} = \mathrm{tr}_l \left(P^K_{k_1} \hat{W} P^K_{k_2} \hat{W} \cdots \right). \tag{4.3.77}$$

We will now describe the algorithm used to calculate the $\mathcal{T}$-functions. These functions are traces of products of S_i, L_i, T^a and projection operators $P^K_{k_i}$. First we perform the trace in isospin space. After this we expand the projectors $P^K_{k_i}$. Since the intermediate modes can only have $k = l-1, \ldots, l+1$, we can write

$$P^K_k = a_0(k) + a_1(k)\vec{K}^2 + a_2(k)(\vec{K}^2)^2, \tag{4.3.78}$$

for certain values of the coefficients. Simply expanding all the projectors in terms of $\vec{K}^2 = \vec{L}^2 + 2 + 2\vec{L}\cdot\vec{S}$ is a very inefficient method. We therefore start with expanding only the rightmost projector in terms of $\vec{K}^2$ and commute the $\vec{K}^2$ operators to the left, until they reach another projector. When this happens, $\vec{K}^2$ is replaced by the proper value $k(k+1)$ determined by the projector. In this way we get rid of all projectors, save the leftmost one. This last projector is then fully expanded and the remaining trace factorizes in a trace of L_i and one of S_i operators, both of which have been tabulated.

The last step is again to do the s-integration and the summation over l. This summation starts at $l = \frac{1}{2}$, which eliminates the possibility of intermediate states in the c space. Having the intermediate state in the d space corresponds to having one of the arguments k_i of $\mathcal{T}$ equal to zero, so these terms should be discarded, together with the terms where $k_i < 0$. The result for the effective potential is

$$\begin{aligned}
\mathcal{V}^{(1)}(c) = V_{\mathrm{cl}}(c) \Big(& -\tfrac{1259}{1152} + \tfrac{11}{6\varepsilon} - \tfrac{11}{12}\gamma - \tfrac{11}{128}\sqrt{2} + \tfrac{11}{6}\log(2) + \tfrac{11}{6}\log\left(\tfrac{L}{2\sqrt{\pi}}\right) \\
& - \tfrac{23}{6}\zeta(\tfrac{3}{2},-1) - \tfrac{1}{6}\zeta(\tfrac{5}{2},-1) + \tfrac{53}{3}\zeta(\tfrac{7}{2},-1) + 14\,\zeta(\tfrac{9}{2},-1) \\
& + \tfrac{16}{3}\zeta_R(3) - \tfrac{19}{6}\zeta_R(5) - \tfrac{1}{3}\zeta_R(7)\Big) \\
+ \mathrm{tr}(X) \Big(& \tfrac{11}{64}\sqrt{2} + \tfrac{179}{576} + \tfrac{13}{3}\zeta(\tfrac{3}{2},-1) - 3\,\zeta(\tfrac{5}{2},-1) - \tfrac{106}{3}\zeta(\tfrac{7}{2},-1) \\
& - 28\,\zeta(\tfrac{9}{2},-1) + \tfrac{2}{3}\zeta_R(-1) - \tfrac{23}{3}\zeta_R(3) + \tfrac{19}{3}\zeta_R(5) + \tfrac{2}{3}\zeta_R(7)\Big) \\
+ \mathrm{tr}^2(X) \Big(& \tfrac{1219}{12288}\sqrt{2} - \tfrac{6347}{46080} - \tfrac{53}{24}\zeta(\tfrac{3}{2},-1) + \tfrac{263}{40}\zeta(\tfrac{5}{2},-1) \\
& + \tfrac{2641}{60}\zeta(\tfrac{7}{2},-1) - \tfrac{1099}{30}\zeta(\tfrac{9}{2},-1) - \tfrac{2794}{15}\zeta(\tfrac{11}{2},-1) - \tfrac{572}{5}\zeta(\tfrac{13}{2},-1) \\
& + \tfrac{503}{120}\zeta_R(3) - \tfrac{1801}{120}\zeta_R(5) + \tfrac{122}{15}\zeta_R(7) + \tfrac{79}{30}\zeta_R(9)\Big) \\
+ \mathrm{tr}(X^2) \Big(& \tfrac{36301}{46080} - \tfrac{707}{12288}\sqrt{2} + \tfrac{53}{24}\zeta(\tfrac{3}{2},-1) - \tfrac{2197}{120}\zeta(\tfrac{5}{2},-1) \\
& - \tfrac{1771}{20}\zeta(\tfrac{7}{2},-1) + \tfrac{3767}{30}\zeta(\tfrac{9}{2},-1) + \tfrac{2684}{5}\zeta(\tfrac{11}{2},-1) + \tfrac{1716}{5}\zeta(\tfrac{13}{2},-1) \\
& - \tfrac{293}{40}\zeta_R(3) + \tfrac{2243}{120}\zeta_R(5) - \tfrac{329}{60}\zeta_R(7) - \tfrac{187}{30}\zeta_R(9)\Big).
\end{aligned} \tag{4.3.79}$$

It is easily checked that this reproduces eq. (4.3.48) when we substitute $c = -u\mathbb{1}$. Note that we have subtracted the $B = 0$ contribution.

4.3.6 The (c,d) space

In this section we treat the hardest part of the calculation: the (c, d) cross terms. For the scalar operators we calculate the determinants for a general $B(c, d)$ up to fourth order in the fields. For the vector operator, we will use the $c \leftrightarrow d$ symmetry to obtain the pure d-dependent term in the determinant. That leaves only the c^2d^2 terms to be evaluated.

Starting with the scalar operator, we can again write $-D_i(B)D_i(B) = F + \hat{A}(c, d)$, with $F = 4\vec{L}^2$. As can be seen from eq. (4.3.3), we now have $[\vec{L}^2, \hat{A}(c, d)] \neq 0$, due to the occurrence of V in $\hat{A}$. This means that we must use the method of eq. (4.3.69) where the intermediate levels in the $\mathcal{T}$-functions now are labelled with l_i to denote different eigenspaces of $\vec{L}^2$. Since V itself is an $l = 1$ mode, and a change in l_i can only be achieved through the multiplication with V, acting with the operator $\hat{A}$ can change l_i by maximally one unit.

We need the three functions $\mathcal{T}_{ll'}$ with $l' = l - 1, \ldots, l + 1$, but from the functions with three and four indices, we need only $\mathcal{T}_{lll}$ and $\mathcal{T}_{llll}$. This is a consequence of the fact that for instance $\mathcal{T}_{ll+1l}$ requires two of the three factors $\hat{A}$ to contribute the V term. The third factor $\hat{A}$ then makes the contribution to be a least of fifth order in the fields c and d. Conversely, up to the order we are interested in, we can replace these two $\mathcal{T}$-functions by respectively $\mathrm{tr}_l(\hat{A}^3)$ and $\mathrm{tr}_l(\hat{A}^4)$. This leaves only the projector $P^L_{l'}$ in $\mathcal{T}_{ll'}$ to be dealt with.

The evaluation of the $\mathcal{T}$-function now proceeds as follows. After taking the trace in isospin space, we replace all occurrences of c and d by the appropriate invariants and projectors. In particular, we make the substitution

$$\begin{aligned} c^a_i c^b_j d^l_k d^l_l \quad \rightarrow \quad & \tfrac{1}{270}(4\,\mathrm{tr}(X)\,\mathrm{tr}(Y) - 2\,\mathrm{tr}(XY))\,\delta_{ij}\,\delta_{kl}\,\delta^{ab}\,\delta^{cd} \\ & -\tfrac{1}{270}(\mathrm{tr}(X)\,\mathrm{tr}(Y) - 3\,\mathrm{tr}(XY))\,\delta_{ij}\,\delta_{kl}\,(\delta^{ac}\,\delta^{bd} + \delta^{ad}\,\delta^{bc}), \end{aligned} \tag{4.3.80}$$

with $Y = dd^T$. Next we commute the operators L_1 and L_2 to the right, expand the projector $P^L_{l'}$ in a polynomial of degree two in $\vec{L}^2$ and pull the operators V through this expansion. After this we eliminate V by either contracting them if there are two factors of V or by replacing the contraction $V^j_i L_{2j}$ by L_{1i}.

The remaining trace consists only of the operators L_{1i} and L_{2i}. Together with the rest of the manipulations, it can be dealt with as before. For the other scalar operator, $\hat{A}$ has some extra terms that are proportional to P^L_1. The evaluation of these extra terms poses no new problems.

For the vector operator, both the l and k value can get changed by the action of the operator $\hat{W}$. The summation over intermediate values in eq. (4.3.75) becomes hence more complicated, but can still be performed. The relevant traces are now $\mathcal{T}_{(k_1,l_1)(k_2,l_2)\ldots}$. One can show that not only l_i but also k_i changes by maximally one unit. Together with the condition $k_i = l_i - 1, \ldots, l_i + 1$, this reduces the number of $\mathcal{T}$-functions that have to be calculated.

The algorithm to evaluate these traces consists of first keeping only the c^2d^2 terms, projecting these on the invariants and taking the isospin trace. The operators P^K and

P^L are treated as described for the pure c case. Starting from the right, we expand them in respectively $\vec{K}^2$ and $\vec{L}^2$ and commute these operators to the left until they meet another projector. Since the range of intermediate k values is now bigger, the expansion of P^K is a fourth order polynomial in $\vec{K}^2$. In contrast with the previous case, the left most projectors are not expanded.

The next step is to eliminate L_2, which is particularly easy since it commutes with all other operators and occurs at most quadratically. After this we sweep all the S operators to the right, commute the V's to the left and get rid of these V's by contraction. We are left with a trace in a (k,l) subspace of only S_i and L_{1i} operators. These strings of contracted operators can be expressed in terms of $\vec{L}^2$ and $\vec{K}^2$, after which the evaluation of the trace becomes trivial.

The remaining steps proceed as before. In the summation the intermediate states with $l \leq 0$ or $k \leq 0$ should again be dropped. Since the precise form of the coefficients is not very illuminating, we postpone writing down the effective potential until we have performed the renormalization.

4.4 The effective kinetic term

In this section we will no longer assume $\dot{B} = 0$. The method of the previous section is replaced by the diagrammatic expansion of the path integral. The goal is to obtain the one-loop contribution to the operator $\dot{B}^2$. It is hence sufficient to restrict ourselves to the case $B = B(c)$.

4.4.1 The ghost sector

The fermionic path integral is given by

$$\begin{aligned} Z &= \int D\psi\, D\bar{\psi} \exp\left[\frac{1}{g_0^2}\int \mathrm{tr}\left(\bar{\psi}\left\{-D_\mu(B)(1-P)D_\mu(B)\right\}\psi\right)\right] \\ &= \int D\psi\, D\bar{\psi} \exp\left[\frac{1}{g_0^2}\int \mathrm{tr}\left(\bar{\psi}\left\{-\partial_0^2 - \partial_\epsilon^2 + 4\vec{L}^2\right\}\psi + \bar{\psi}\hat{A}\psi\right)\right]. \end{aligned} \tag{4.4.1}$$

The free propagator $S = -(-\partial_0^2 - \partial_\epsilon^2 + 4\vec{L}^2)^{-1}$ is given by

$$\begin{aligned} S(x,y) &= \int \frac{dk_0}{2\pi}\frac{d^\epsilon k_\epsilon}{(2\pi)^\epsilon} \sum_{l=\frac{1}{2},1,\ldots}^{\infty} \sum_{m_L=-l}^{l} \sum_{m_R=-l}^{l} \sum_{m_t=-1}^{1} e^{-ik_0(x_0-y_0)} e^{-ik_\epsilon\cdot(x_\epsilon-y_\epsilon)} \times \\ &\qquad \langle \vec{x}|l\, m_L\, m_R; m_t\rangle \frac{-1}{k_0^2 + k_\epsilon^2 + 4l(l+1)} \langle l\, m_L\, m_R; m_t|\vec{y}\rangle. \end{aligned} \tag{4.4.2}$$

Expanding the $\bar{\psi}\hat{A}\psi$ term gives $\ln Z$ as a sum of connected one-loop diagrams with insertions of $\hat{A}$: For the diagram with one insertion we find

$$= -\int \frac{dk_0}{2\pi} \frac{d^\varepsilon k_\varepsilon}{(2\pi)^\varepsilon} \sum_{l=\frac{1}{2},1,\ldots}^{\infty} \sum_{m_L=-l}^{l} \sum_{m_R=-l}^{l} \sum_{m_t=-1}^{1} \int dt\, d^\varepsilon x_\varepsilon \times$$

$$\langle l\, m_L\, m_R; m_t |\, \hat{A}(t)\, | l\, m_L\, m_R; m_t \rangle \frac{-1}{k_0^2 + k_\varepsilon^2 + 4l(l+1)}$$

$$= \frac{1}{2} \int dt \sum_{l=\frac{1}{2}}^{\infty} \mathrm{tr}_l \left(\hat{A}(t)\right) \frac{g_{\frac{1}{2}}(\varepsilon)}{(4l(l+1))^{\frac{1}{2}-\frac{\varepsilon}{2}}}. \tag{4.4.3}$$

The integral over $d^\varepsilon x_\varepsilon$ can be directly replaced by L^ε. We used the following integral

$$\begin{aligned} \int \frac{d^d k}{(2\pi)^d} \frac{1}{(C+k^2)^n} &= \frac{1}{(2\pi)^d C^{n-\frac{d}{2}}} \frac{2\pi^{\frac{d}{2}}}{\Gamma(\frac{d}{2})} \int_0^\infty dx \frac{x^{d-1}}{(1+x^2)^n} \\ &= \frac{1}{(2\pi)^d C^{n-\frac{d}{2}}} \frac{\pi^{\frac{d}{2}}}{\Gamma(\frac{d}{2})} B(\tfrac{d}{2}, n-\tfrac{d}{2}) \\ &= \frac{1}{C^{n-\frac{d}{2}}} \frac{\Gamma(n-\frac{d}{2})}{2^d \pi^{\frac{d}{2}} \Gamma(n)}. \end{aligned} \tag{4.4.4}$$

And we introduced

$$g_n(\varepsilon) = \int d^\varepsilon x_\varepsilon \int \frac{d^\varepsilon k_\varepsilon}{(2\pi)^\varepsilon} \frac{1}{(1+k_\varepsilon^2)^n} = \left(\frac{L}{2\sqrt{\pi}}\right)^\varepsilon \frac{\Gamma(n-\frac{\varepsilon}{2})}{\Gamma(n)}. \tag{4.4.5}$$

The result for this diagram is just the old effective potential result: taking $\hat{A}$ independent of t and inserting $g_{\frac{1}{2}}(\varepsilon)$, we get

$$= \frac{T}{2\sqrt{\pi}} \left(\frac{L}{2\sqrt{\pi}}\right)^\varepsilon \sum_{l=\frac{1}{2}}^{\infty} \mathrm{tr}_l \left(\hat{A}\right) \frac{\Gamma(\frac{1}{2}-\frac{\varepsilon}{2})}{(4l(l+1))^{\frac{1}{2}-\frac{\varepsilon}{2}}}. \tag{4.4.6}$$

This term corresponds to the term linear in s in eq. (4.3.54).

The diagram with two insertions of $\hat{A}$ gives new results. We will suppress the manipulations with the integrations over k_ε and x_ε. The dimensional regularization can be obtained by adding k_ε^2 to the denominators of all propagators and performing the integration

$$L^\varepsilon \int \frac{d^\varepsilon k_\varepsilon}{(2\pi)^\varepsilon}. \tag{4.4.7}$$

Note that a diagram with n insertions gets a symmetry factor $\frac{1}{n}$. Suppressing m_L, m_R and m_t, we find for the diagram with two insertions

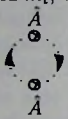

$$= -\tfrac{1}{2}\int \frac{dk_0}{2\pi}\frac{dk_0'}{2\pi}\sum_l\sum_{l'}\int dt\,dt'\frac{-1}{k_0^2+4l(l+1)}\langle l|\,\hat{A}(t')\,|l'\rangle\, e^{-ik_0(t-t')}\times$$

$$\frac{-1}{k_0'^2+4l'(l'+1)}\langle l'|\,\hat{A}(t)\,|l\rangle\, e^{-ik_0'(t'-t)}. \tag{4.4.8}$$

Noting that $[\vec{L}^2,\hat{A}(t)]=0$ and substituting $k_0=p$, $k_0'=p+q$ we write

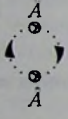

$$= -\tfrac{1}{2}\int \frac{dp}{2\pi}\frac{dq}{2\pi}\sum_l\int dt\,dt' e^{-iq(t-t')}\,\mathrm{tr}_l\left(\hat{A}(t)\hat{A}(t')\right)\times$$

$$\frac{1}{p^2+4l(l+1)}\,\frac{1}{(p+q)^2+4l(l+1)}. \tag{4.4.9}$$

Using contour integration, one proves

$$\int\frac{dp}{2\pi}\frac{1}{p^2+C}\,\frac{1}{(p+q)^2+C}=\frac{1}{\sqrt{C}\,(4C+q^2)}. \tag{4.4.10}$$

After performing the p integration and expanding in q^2 we obtain

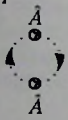

$$= -\tfrac{1}{2}\int \frac{dq}{2\pi}\sum_l\int dt\,dt' e^{-iq(t-t')}\,\mathrm{tr}_l\left(\hat{A}(t)\hat{A}(t')\right)\times$$

$$\frac{1}{4(4l(l+1))^{\frac{3}{2}}}\sum_{n=0}^{\infty}\frac{(-1)^n}{4^n}\frac{(q^2)^n}{(4l(l+1))^n}. \tag{4.4.11}$$

Next we substitute

$$q^2\to\frac{\partial^2}{\partial t\,\partial t'}, \tag{4.4.12}$$

and move these time derivatives to $\hat{A}$ by partial integration. The q and the t' integration thus become trivial, and we obtain

$$-\tfrac{1}{8}\int dt\sum_l\sum_{n=0}^{\infty}\frac{(-1)^n}{4^n}\frac{1}{(4l(l+1))^{n+\frac{3}{2}}}\,\mathrm{tr}_l\left(\hat{A}^{(n)}(t)\hat{A}^{(n)}(t)\right)\;\to$$

$$-\tfrac{1}{8}\int dt\sum_l\sum_{n=0}^{\infty}\frac{(-1)^n}{4^n}\frac{g_{n+\frac{3}{2}}(\varepsilon)}{(4l(l+1))^{n+\frac{3}{2}-\frac{\varepsilon}{2}}}\,\mathrm{tr}_l\left(\hat{A}^{(n)}(t)\hat{A}^{(n)}(t)\right). \tag{4.4.13}$$

The arrow indicates that we have performed the ε-dimensional integrations that were suppressed in the notation. The $n=0$ contribution can be related to the s^2 term in eq. (4.3.54), whereas the $n=1$ contribution gives us the $\dot{B}^2$ term that we were looking for:

$$\int dt\,\tfrac{1}{12}g_{\frac{5}{2}}(\varepsilon)\left(\zeta(\tfrac{1}{2}-\tfrac{\varepsilon}{2},-1)+\zeta(\tfrac{3}{2}-\tfrac{\varepsilon}{2},-1)\right)\dot{c}_i^a\dot{c}_i^a. \tag{4.4.14}$$

4.4.2 The field sector

The bosonic path integral is given by

$$\begin{aligned} Z &= \int D'Q_\mu \exp\left[\frac{1}{g_0^2}\int \mathrm{tr}\,(-2(D_\mu F_{\mu\nu})(B)Q_\nu + Q_\mu W_{\mu\nu}(B)Q_\nu)\right] \\ &= \int D'Q_0\, D'Q_i \exp\left[\frac{1}{g_0^2}\int \mathrm{tr}\,\Big(Q_0\left\{-\partial_0^2 - \vec{\partial}_\epsilon^2 + 4\vec{L}^2\right\}Q_0 \right. \\ &\quad + Q_i\left\{-\partial_0^2 - \vec{\partial}_\epsilon^2 + 2\vec{L}^2 + 2\vec{K}^2\right\}_{ij} Q_j + Q_0\hat{A}Q_0 + Q_i\hat{W}_{ij}Q_j \\ &\quad \left. -4Q_0\,\mathrm{ad}\,(\hat{B}_j)Q_j - 2J_0Q_0 - 2J_iQ_i\Big)\right]. \end{aligned} \tag{4.4.15}$$

with $J_\nu = (D_\mu F_{\mu\nu})(B)$. The propagator of the real Q_0 field is given by $\frac{1}{2}S(x,y)$, where S is given by eq. (4.4.2). The propagator of the vector field Q_i is $\frac{1}{2}S_{ij}(x,y)$, where S_{ij} is given by

$$\begin{aligned} S_{ij}(x,y) = \int \frac{dk_0}{2\pi}\frac{d^\epsilon k_\epsilon}{(2\pi)^\epsilon} \sum_{l,k} \sum_{m_R=-l}^{l} \sum_{m_k=-k}^{k} \sum_{m_l=-1}^{1} e^{-ik_0(x_0-y_0)} e^{-ik_\epsilon(x_\epsilon-y_\epsilon)} \times \\ {}_i\langle \vec{x}|l\,m_L;k\,m_k;m_l\rangle \frac{-1}{k_0^2+k_\epsilon^2+2l(l+1)+2k(k+1)} \langle l\,m_L;k\,m_k;m_l|\vec{y}\rangle_j. \end{aligned} \tag{4.4.16}$$

The loop diagrams with only Q_0

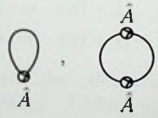

(4.4.17)

have the same structure as those of the ghost field. Apart from extra terms coming from the projector $1-P$ in the ghost case, the contribution is precisely $-\frac{1}{2}$ times the fermionic contribution. For the diagram with n insertions, we have n propagators and hence a relative factor of $\frac{1}{2^n}$. There is however an extra combinatorial factor of 2^{n-1} coming from the n vertices. The relative minus sign for the closed fermion loop is obvious.

We now turn to the loop diagrams with only Q_i. The diagram with one $\hat{W}$ insertion is given by

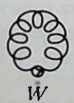

$$\begin{aligned} &= \int \frac{dk_0}{2\pi}\sum_{l,k}\int dt\ \mathrm{tr}_{lk}\left(\hat{W}(t)\right) \frac{-\frac{1}{2}}{k_0^2+2l(l+1)+2k(k+1)} \\ &\to -\frac{1}{4}\int dt \sum_{l,k} \mathrm{tr}_{lk}\left(\hat{W}(t)\right) \frac{g_{\frac{1}{2}}(\epsilon)}{(2l(l+1)+2k(k+1))^{\frac{1}{2}-\frac{\epsilon}{2}}}. \end{aligned} \tag{4.4.18}$$

This again corresponds to the effective potential term sp_1. For the diagram with $n = 2$ insertions the combinatorial $\frac{1}{n}$ drops out against the factor 2^{n-1} and we find:

$$
\begin{aligned}
&= \int \frac{dk_0}{2\pi}\frac{dk_0'}{2\pi}\sum_{l,k}\sum_{l',k'}\int dt\,dt' \frac{-\frac{1}{2}}{k_0^2+2l(l+1)+2k(k+1)} \times \\
&\quad \langle l,k|\,\hat{W}(t')\,|l',k'\rangle\, e^{-ik_0(t-t')} \frac{-\frac{1}{2}}{k_0'^2+2l'(l'+1)+2k'(k'+1)} \times \\
&\quad \langle l',k'|\,\hat{W}(t)\,|l,k\rangle\, e^{-ik_0'(t'-t)} \\
&= \tfrac{1}{4}\int \frac{dk_0}{2\pi}\frac{dk_0'}{2\pi}\sum_{l}\sum_{k=l-1}^{l+1}\sum_{k'=l-1}^{l+1}\int dt\,dt'\, e^{-ik_0(t-t')}e^{-ik_0'(t'-t)} \times \\
&\quad \frac{\langle l,k|\,\hat{W}(t')P_{k'}^{K}\hat{W}(t)|l,k\rangle}{(k_0^2+2l(l+1)+2k(k+1))\,(k_0'^2+2l(l+1)+2k'(k'+1))} \\
&= \tfrac{1}{4}\int \frac{dp}{2\pi}\frac{dq}{2\pi}\sum_{l}\sum_{k=l-1}^{l+1}\sum_{k'=l-1}^{l+1}\int dt\,dt' e^{-iq(t-t')} \times \\
&\quad \frac{1}{p^2+C}\,\frac{1}{(p+q)^2+D}\,\mathcal{T}_{kk'}(t,t'),
\end{aligned}
\tag{4.4.19}
$$

with

$$C = 2l(l+1)+2k(k+1), \tag{4.4.20}$$

$$D = 2l(l+1)+2k'(k'+1). \tag{4.4.21}$$

With the help of the following generalization of eq. (4.4.10)

$$\int \frac{dp}{2\pi}\,\frac{1}{p^2+C}\,\frac{1}{(p+q)^2+D} = \frac{\sqrt{C}+\sqrt{D}}{2\sqrt{CD}\left((\sqrt{C}+\sqrt{D})^2+q^2\right)}, \tag{4.4.22}$$

and following the same steps as in the scalar case, we obtain:

$$= \tfrac{1}{4}\int dt \sum_{l}\sum_{k=l-1}^{l+1}\sum_{k'=l-1}^{l+1}\sum_{n=0}^{\infty}\frac{(-1)^n\mathcal{T}_{kk'}^{(n)}(t)}{2\sqrt{CD}\,(\sqrt{C}+\sqrt{D})^{2n+1}}, \tag{4.4.23}$$

where $\mathcal{T}^{(n)}$ is just the old $\mathcal{T}$-function with $\hat{W}$ replaced by the n-th order time derivative of $\hat{W}$. In order to perform the k_ε integration, we want just a single denominator in the expression. If $k' = k$, we have that $C = D$ and this condition is met. If $k' \neq k$, we write

$$\frac{1}{2\sqrt{CD}(\sqrt{C}+\sqrt{D})^{2n+1}} = \frac{(\sqrt{C}-\sqrt{D})^{2n+1}}{2\sqrt{CD}\,(C-D)^{2n+1}}. \tag{4.4.24}$$

The rest of the calculation poses no new problems. The $n = 0$ term corresponds to the sp_2 contribution to the effective potential. The $\hat{B}^2$ part comes from the $n = 1$ contribution.

The $-4Q_0[\hat{B}_i, Q_i] \sim +4Q_i[\hat{B}_i, Q_0]$ term in the path integral gives rise to a loop diagram with one Q_0 and one Q_i propagator and two insertions of essentially $\hat{B}$. There is no extra combinatorial factor 2 in this diagram, and writing $\hat{A}(t)$ for the operator $-4\,\mathrm{ad}\,(\hat{B}(t))$, we have

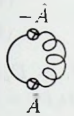

$$
\begin{aligned}
&= \tfrac{1}{2}\int \frac{dk_0}{2\pi}\frac{dk_0'}{2\pi}\sum_{l,k}\sum_{l'}\int dt\,dt'\,\frac{-\frac{1}{2}}{k_0^2+2l(l+1)+2k(k+1)}\times \\
&\quad \langle l,k|-\hat{A}(t')\,|l'\rangle\, e^{-ik_0(t-t')}\,\frac{-\frac{1}{2}}{k_0'^2+4l'(l'+1)}\,\langle l'|\,\hat{A}(t)\,|l,k\rangle\, e^{-ik_0'(t'-t)} \\
&= \tfrac{1}{8}\int \frac{dk_0}{2\pi}\frac{dk_0'}{2\pi}\sum_{l,k}\int dt\,dt' e^{-ik_0(t-t')}e^{-ik_0'(t'-t)}\times \\
&\quad \frac{\langle l,k|-\hat{A}(t')\hat{A}(t)|l,k\rangle}{(k_0^2+2l(l+1)+2k(k+1))\,(k_0'^2+4l(l+1))} \\
&= \tfrac{1}{8}\sum_{l,k}\int dt\sum_{n=0}^{\infty}\frac{(-1)^n\,\mathrm{tr}_{lk}\left(-\hat{A}^{(n)}(t)\hat{A}^{(n)}(t)\right)}{2\sqrt{C}D(\sqrt{C}+\sqrt{D})^{2n+1}},
\end{aligned}
\tag{4.4.25}
$$

with

$$C = 4l(l+1), \tag{4.4.26}$$

$$D = 2l(l+1)+2k(k+1). \tag{4.4.27}$$

The rest of the calculation is again straightforward. The $n = 0$ contribution gives us the $\hat{B}^2$ term. Adding up the different contributions, we obtain the one-loop contribution to the kinetic term in the lagrangian:

$$
\begin{aligned}
\mathcal{K}^{(1)}(c,d) &= \left(\dot{c}_i^a\dot{c}_i^a+\dot{d}_i^a\dot{d}_i^a\right)\left(\tfrac{1247}{1152}+\tfrac{5}{16}\sqrt{2}+\tfrac{11}{12\varepsilon}-\tfrac{11}{24}\gamma+\tfrac{11}{12}\log(2)\right. \\
&\quad +\tfrac{11}{12}\log(\tfrac{L}{2\sqrt{\pi}})+\tfrac{1}{6}\zeta(\tfrac{3}{2},-1)+11\,\zeta(\tfrac{5}{2},-1)+\tfrac{49}{6}\zeta(\tfrac{7}{2},-1) \\
&\quad \left.-\tfrac{4}{3}\zeta_R(3)-\tfrac{5}{12}\zeta_R(5)-\tfrac{8}{3}\zeta_F(\tfrac{1}{2},-1)\right).
\end{aligned}
\tag{4.4.28}
$$

The divergency will be absorbed by the same coupling constant renormalization of eq. (4.3.42) that also made the potential part finite.

4.4.3 The linear term in the path integral

In this section we will show that the term $J_\nu Q_\nu$ in eq. (4.4.15) does not make a contribution to the effective action up to the order we are interested in: the lowest order contribution from J to the effective potential will be of the form c^4d^2 and c^2d^4. We will study the precise form of J to show this.

The crucial remark is that in the path integral the constant modes are excluded from the integration over Q_0, and the (c,d) modes are excluded from the integration over Q_i. This means that one must remember to put projectors $(1-P)$ around operators like $W_{\mu\nu}$, and replace source currents like J_μ with $((1-P)J)_\mu$. We will show that after this projection J contains only terms that are cubic in B.

We have

$$F_{0i} = -F_{i0} = \dot{B}_i, \tag{4.4.29}$$

$$F_{ij} = -2\varepsilon_{ijk}(c_k - d\cdot V_k) + [B_i, B_j], \tag{4.4.30}$$

with $B_i = c_i + d\cdot V_i$. This implies $J_0 = D_\mu F_{\mu 0} = -[B_i, \dot{B}_i]$ and $J_j = D_\mu F_{\mu j} = \ddot{B}_j + D_i F_{ij}$. In our approximation we are only interested in the term $D_i F_{ij} = J_j^{(1)} + J_j^{(2)} + J_j^{(3)}$, where $J^{(n)}$ is of order n in the field B. From

$$D_i F_{ij} = \partial_i F_{ij} - \varepsilon_{ijk} F_{ik} + [A_i, F_{ij}], \tag{4.4.31}$$

we obtain

$$J_j^{(1)} = -4\, c_j, \tag{4.4.32}$$

$$J_j^{(2)} = -3\,\varepsilon_{ijk}[c_i, c_k] - 3\,\varepsilon_{mpn}[d_m, d_n]V_j^p, \tag{4.4.33}$$

$$\begin{aligned} J_j^{(3)} &= [B_i,[B_i,B_j]] \\ &= [c_i,[c_i,c_j]] + [d\cdot V_i,[d\cdot V_i,c_j]] \\ &\quad +[c_i,[c_i,d\cdot V_j]] + [d\cdot V_i,[d\cdot V_i,d\cdot V_j]] \\ &\quad +[d\cdot V_i,[c_i,c_j]] + [c_i,[d\cdot V_i,c_j]] \\ &\quad +[d\cdot V_i,[c_i,d\cdot V_j]] + [c_i,[d\cdot V_i,d\cdot V_j]] \end{aligned} \tag{4.4.34}$$

This directly implies that $(1-P_V)J^{(1)} = (1-P_V)J^{(2)} = 0$. The first four terms of $J^{(3)}$ do not contribute since they too are modes with $(l,k) = (0,1)$ or $(l,k) = (1,0)$. The last four terms of $J^{(3)}$ have components outside the (c,d) space. The fifth and sixth term are $l = 1$ terms, the last two terms have $k = 1$. To obtain the precise spectral decomposition of these terms we write them as follows:

$$A_{ij}^p V_i^p + B_i^{mn} V_i^m V_j^n, \tag{4.4.35}$$

with the su(2)-valued constants

$$A_{ij}^p = [d_p,[c_i,c_j]] + [c_i,[d_p,c_j]], \tag{4.4.36}$$

$$B_i^{mn} = [d_m,[c_i,d_n]] + [c_i,[d_m,d_n]]. \tag{4.4.37}$$

The matrices A^p and B_i can be decomposed in a trace part, an antisymmetric part and a symmetric traceless part. For the A^p terms, this is the decomposition into (l,k) is $(1,0)$, $(1,1)$ and $(1,2)$ respectively. For the B_i terms, it gives the split in the three possible l values. Projecting out the (c,d) modes from J_i, we obtain

$$((1-P_V)J)_j = \bar{A}_{ij}^p V_i^p + \bar{B}_i^{mn} V_i^m V_j^n, \tag{4.4.38}$$

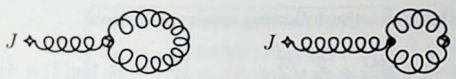

Figure 4-3. Feynman diagrams with one interaction with J.

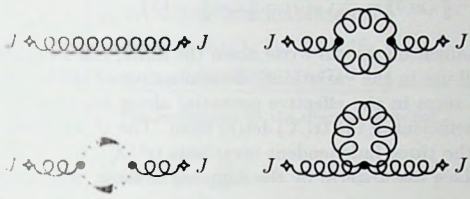

Figure 4-4. Feynman diagrams with two J's.

where $\bar{A}$ and $\bar{B}$ are obtained from the A and B of eq. (4.4.37) by projecting out the trace part.

Expanding the path integral of eq. (4.4.15) gives diagrams with interactions of the Q field with the external current $J(B)$. If we also take along the Q^3, BQ^3 and Q^4 terms in the action, diagrams with only one occurrence of J (fig. 4-3) can in principle give a contribution of the order c^2d^2. However, in order to obtain a c^2d^2 invariant, we must take the trace part of $\bar{A}$ and $\bar{B}$. Since these trace parts are zero, we see that even a single occurence of J can only give rise to higher order contributions.

The simplest diagram with two J's is the upper left one in fig. 4-4. Although it is of the order c^1d^2 and c^2d^1 we mention it for another reason: since it contains two vertices and only one propagator, it is of order $1/g_0^2$. This behaviour may seem dangerous, until one realizes that the Q^3 and Q^4 interactions, as well as the interactions of the ghosts with Q, will dress up the propagator. With the standard renormalization, we will be left with a finite contribution.

4.5 Renormalized results

In this section we will combine the results from the previous sections and write down the effective lagrangian that we will use as a starting point for the variational calculation. We will use a renormalization scheme such that the renormalized kinetic part looks just like the classical term:

$$\mathcal{K}_{\text{eff}} = \frac{2\pi^2}{2g_R^2}\left(\dot{c}_i^a\dot{c}_i^a + \dot{d}_i^a\dot{d}_i^a\right). \tag{4.5.1}$$

Using eq. (4.4.28) this gives the following renormalization:

$$\begin{aligned}\frac{1}{g_R^2} &= \frac{1}{g_0^2}+\frac{1}{\pi^2}\Big(\frac{1247}{1152}+\frac{5}{16}\sqrt{2}+\frac{11}{12\varepsilon}-\frac{11}{24}\gamma+\frac{11}{12}\log(2)+\frac{11}{12}\log\Big(\frac{L}{2\sqrt{\pi}}\Big)\\ &\quad+\tfrac{1}{6}\zeta(\tfrac{3}{2},-1)+11\,\zeta(\tfrac{5}{2},-1)+\tfrac{49}{6}\zeta(\tfrac{7}{2},-1)\\ &\quad-\tfrac{4}{3}\zeta_R(3)-\tfrac{5}{12}\zeta_R(5)-\tfrac{8}{3}\zeta_F(\tfrac{1}{2},-1)\Big).\end{aligned} \tag{4.5.2}$$

With this renormalization we can write down the finite, renormalized effective potential, which we will use in the variational determination of the spectrum in chapter 5. Note that the u^5 term in the effective potential along the tunnelling path uniquely determines the coefficient of the $\mathrm{tr}(X)\det(c)$ term. The u^6 term can be obtained from combinations of the three independent invariants $\mathrm{tr}^3(X)$, $\mathrm{tr}(X)\,\mathrm{tr}(X^2)$ and $\mathrm{tr}(X^3)$[1]. We choose to replace the u^6 term by the simplest of these, which is $\mathrm{tr}^3(X)$. We write

$$\mathcal{V}_{\mathrm{eff}}=\frac{2\pi^2}{g_R^2}V_{\mathrm{cl}}(c,d)+V_{\mathrm{eff}}^{(1)}(c,d), \tag{4.5.3}$$

with

$$\begin{aligned}V_{\mathrm{eff}}^{(1)}(c,d) &= V_{\mathrm{eff}}^{(1)}(c)+V_{\mathrm{eff}}^{(1)}(d)+\kappa_7\,\mathrm{tr}(X)\,\mathrm{tr}(Y)+\kappa_8\,\mathrm{tr}(XY),\\ V_{\mathrm{eff}}^{(1)}(c) &= \kappa_1\,\mathrm{tr}(X)+\kappa_2\det(c)+\kappa_3\,\mathrm{tr}^2(X)+\kappa_4\,\mathrm{tr}(X^2)\\ &\quad+\kappa_5\det(c)\,\mathrm{tr}(X)+\kappa_6\,\mathrm{tr}^3(X),\end{aligned} \tag{4.5.4}$$

The coeffients κ_i are given by

$$\begin{aligned}\kappa_1 &= -\tfrac{1787}{288}-\tfrac{5}{4}\sqrt{2}-4\,\zeta(\tfrac{3}{2},-1)-\tfrac{142}{3}\zeta(\tfrac{5}{2},-1)-\tfrac{98}{3}\zeta(\tfrac{7}{2},-1)\\ &\quad+\tfrac{2}{3}\zeta_R(-1)+\tfrac{25}{3}\zeta_R(3)+\tfrac{5}{3}\zeta_R(5)+\tfrac{32}{3}\zeta_F(\tfrac{1}{2},-1),\end{aligned} \tag{4.5.5}$$

$$\begin{aligned}\kappa_2 &= -\tfrac{1251}{64}-\tfrac{273}{64}\sqrt{2}-25\,\zeta(\tfrac{3}{2},-1)-133\,\zeta(\tfrac{5}{2},-1)+8\,\zeta(\tfrac{7}{2},-1)\\ &\quad+84\,\zeta(\tfrac{9}{2},-1)+48\,\zeta_R(3)-14\,\zeta_R(5)-2\,\zeta_R(7)+32\,\zeta_F(\tfrac{1}{2},-1),\end{aligned} \tag{4.5.6}$$

$$\begin{aligned}\kappa_3 &= -\tfrac{43877}{46080}-\tfrac{965}{12288}\sqrt{2}-\tfrac{13}{4}\zeta(\tfrac{3}{2},-1)+\tfrac{31}{30}\zeta(\tfrac{5}{2},-1)+\tfrac{887}{20}\zeta(\tfrac{7}{2},-1)\\ &\quad-\tfrac{497}{15}\zeta(\tfrac{9}{2},-1)-\tfrac{2794}{15}\zeta(\tfrac{11}{2},-1)-\tfrac{572}{5}\zeta(\tfrac{13}{2},-1)+\tfrac{743}{120}\zeta_R(3)\\ &\quad-\tfrac{1871}{120}\zeta_R(5)+\tfrac{161}{20}\zeta_R(7)+\tfrac{79}{30}\zeta_R(9)+\tfrac{4}{3}\zeta_F(\tfrac{1}{2},-1),\end{aligned} \tag{4.5.7}$$

$$\begin{aligned}\kappa_4 &= \tfrac{73831}{46080}+\tfrac{1477}{12288}\sqrt{2}+\tfrac{13}{4}\zeta(\tfrac{3}{2},-1)-\tfrac{383}{30}\zeta(\tfrac{5}{2},-1)-\tfrac{5333}{60}\zeta(\tfrac{7}{2},-1)\\ &\quad+\tfrac{1831}{15}\zeta(\tfrac{9}{2},-1)+\tfrac{2684}{5}\zeta(\tfrac{11}{2},-1)+\tfrac{1716}{5}\zeta(\tfrac{13}{2},-1)-\tfrac{373}{40}\zeta_R(3)\\ &\quad+\tfrac{771}{40}\zeta_R(5)-\tfrac{27}{5}\zeta_R(7)-\tfrac{187}{30}\zeta_R(9)-\tfrac{4}{3}\zeta_F(\tfrac{1}{2},-1),\end{aligned} \tag{4.5.8}$$

$$\begin{aligned}\kappa_5 &= -\tfrac{6775}{192}+\tfrac{21995}{3072}\sqrt{2}+\tfrac{49}{2}\sqrt{3}-\tfrac{19}{2}\sqrt{6}+\tfrac{19}{4}\sqrt{10}\\ &\quad-3\,\zeta(\tfrac{3}{2},-1)-\tfrac{29}{3}\zeta(\tfrac{5}{2},-1)-\tfrac{4}{3}\zeta(\tfrac{7}{2},-1)-\tfrac{116}{3}\zeta(\tfrac{9}{2},-1)-44\,\zeta(\tfrac{11}{2},-1)\end{aligned}$$

[1] The invariant $\det^2(c)$ can be expressed in these invariants.

$\kappa_1 =$	-0.2453459985179565
$\kappa_2 =$	3.66869179814223
$\kappa_3 =$	0.500703203096610
$\kappa_4 =$	-0.839359633413003
$\kappa_5 =$	-0.849965412245339
$\kappa_6 =$	-0.06550330854836428
$\kappa_7 =$	-0.3617122159967145
$\kappa_8 =$	-2.295356861354712

Table 4-1. The coefficients for the effective potential.

$$
\begin{aligned}
&+6\,\zeta_R(-3) - \tfrac{10}{3}\,\zeta_R(-1) - \tfrac{25}{6}\,\zeta_R(3) - \tfrac{221}{6}\,\zeta_R(5) + \tfrac{79}{2}\,\zeta_R(7) + \tfrac{10}{3}\,\zeta_R(9)\\
&-2\,\zeta_F(-\tfrac{3}{2},-3) - 2\,\zeta_F(-\tfrac{3}{2},-2) - 2\,\zeta_F(-\tfrac{3}{2},1) - 6\,\zeta_F(-\tfrac{1}{2},-3)\\
&-2\,\zeta_F(-\tfrac{1}{2},-2) + 10\,\zeta_F(-\tfrac{1}{2},1), \qquad (4.5.9)\\
\kappa_6 \;=\; &-\tfrac{17141}{5184} + \tfrac{35579}{55296}\sqrt{2} + \tfrac{41}{18}\sqrt{3} - \tfrac{8}{9}\sqrt{6} + \tfrac{47}{108}\sqrt{10}\\
&-\tfrac{1}{9}\,\zeta(\tfrac{3}{2},-1) - \tfrac{8}{9}\,\zeta(\tfrac{5}{2},-1) - \tfrac{55}{27}\,\zeta(\tfrac{7}{2},-1) - \tfrac{100}{27}\,\zeta(\tfrac{9}{2},-1) - \tfrac{22}{9}\,\zeta(\tfrac{11}{2},-1)\\
&+\tfrac{5}{9}\,\zeta_R(-3) - \tfrac{1}{3}\,\zeta_R(-1) - \tfrac{53}{108}\,\zeta_R(3) - \tfrac{61}{36}\,\zeta_R(5) + \tfrac{241}{108}\,\zeta_R(7) + \tfrac{5}{27}\,\zeta_R(9)\\
&-\tfrac{5}{27}\,\zeta_F(-\tfrac{3}{2},-3) - \tfrac{5}{27}\,\zeta_F(-\tfrac{3}{2},-2) - \tfrac{5}{27}\,\zeta_F(-\tfrac{3}{2},1) - \tfrac{5}{9}\,\zeta_F(-\tfrac{1}{2},-3)\\
&-\tfrac{5}{27}\,\zeta_F(-\tfrac{1}{2},-2) + \tfrac{25}{27}\,\zeta_F(-\tfrac{1}{2},1), \qquad (4.5.10)\\
\kappa_7 \;=\; &\tfrac{44725}{497664} - \tfrac{9439}{221184}\sqrt{2} - \tfrac{376}{6561}\sqrt{3} + \tfrac{1071707}{16796160}\sqrt{6} + \tfrac{115169}{3375000}\sqrt{15}\\
&+\tfrac{97}{9}\,\zeta(\tfrac{3}{2},-1) + \tfrac{61}{2}\,\zeta(\tfrac{5}{2},-1) - \tfrac{1493}{18}\,\zeta(\tfrac{7}{2},-1)\\
&-\tfrac{1970}{9}\,\zeta(\tfrac{9}{2},-1) - \tfrac{356}{3}\,\zeta(\tfrac{11}{2},-1) - \tfrac{14}{9}\,\zeta_F(\tfrac{1}{2},-1)\\
&-\tfrac{467}{72}\,\zeta_R(3) + \tfrac{8}{9}\,\zeta_R(5) + \tfrac{109}{18}\,\zeta_R(7) - \tfrac{10}{9}\,\zeta_R(9), \qquad (4.5.11)\\
\kappa_8 \;=\; &-\tfrac{319531}{497664} + \tfrac{89317}{221184}\sqrt{2} + \tfrac{40}{729}\sqrt{3} - \tfrac{950999}{5598720}\sqrt{6} - \tfrac{291601}{3375000}\sqrt{15}\\
&+\tfrac{67}{9}\,\zeta(\tfrac{3}{2},-1) - \tfrac{265}{18}\,\zeta(\tfrac{5}{2},-1) - \tfrac{979}{18}\,\zeta(\tfrac{7}{2},-1)\\
&+\tfrac{2}{3}\,\zeta(\tfrac{9}{2},-1) + \tfrac{272}{9}\,\zeta(\tfrac{11}{2},-1) - \tfrac{16}{9}\,\zeta_F(\tfrac{1}{2},-1)\\
&-\tfrac{11}{8}\,\zeta_R(3) - \tfrac{49}{6}\,\zeta_R(5) + 11\,\zeta_R(7) - \tfrac{20}{9}\,\zeta_R(9). \qquad (4.5.12)
\end{aligned}
$$

The numerical values for these coefficients can be found in table 4-1. Note that not all of these coefficients are small, which means that the one-loop correction to the spectrum, to be calculated in chapter 5, may be substantial.

5 Calculating the spectrum

5.1 Introduction

In this chapter we will approximate the spectrum of the effective hamiltonian by applying the Rayleigh-Ritz method [33]. This is a variational method that consists of truncating some suitably chosen basis of functions and calculating the matrix of the hamiltonian $\mathcal{H}$ with respect to this basis. A numerical diagonalization of this matrix will give upper bounds for the true eigenvalues. In order to get lower bounds, we use Temple's inequality [33, 34] which as input requires the expectation values of $\mathcal{H}^2$ for the variational eigenvectors. The obtained excitation energies correspond to the masses of the glueballs.

The hamiltonian itself need to be supplemented with suitable boundary conditions in field space to obtain a well-posed quantum mechanical problem. These conditions emerge when imposing gauge invariance through restricting our problem to the fundamental domain. We will use dynamical considerations to argue that we have enough freedom to choose tractable boundary conditions. After having defined the boundary conditions we will write down a basis of functions that respect these conditions. We arrive at these functions by studying the analytic solutions of the eigenvalue problem for the kinetic part of the hamiltonian, which is equivalent to studying the strong coupling limit.

Another interesting limit to study is the small coupling limit. Using ordinary quantum mechanical perturbation theory, we can compute expansions in the coupling constant for the energy levels. These results can be used as an extra check on the variational results.

The variational basis we defined is split up in a number of sectors corresponding to the symmetries of the hamiltonian. This will allow for an optimal block diagonalization of the hamiltonian. Moreover, it allows us to identify scalar and tensor glueballs. Using these symmetries, we can perform the computation of the matrix of $\mathcal{H}$ and $\mathcal{H}^2$ by calculating a limited set of reduced matrix elements.

The results of the numerical diagonalization are the energy levels in various sectors. Using these, we find the masses of the low-lying glueball states. We also estimate the window of validity of our effective model.

5.1.1 Temple's inequality

Consider a hamiltonian H whose spectrum $\sigma(H)$ is $\{\mu_1, \mu_2, \ldots\}$. The Rayleigh-Ritz method gives upper bounds $\tilde{\mu}_n \geq \mu_n$. We will use the generalized Temple inequality [33, 34] to arrive at lower bounds for the levels. Let ψ be a normalized trial wave

function and define

$$\gamma = \langle\psi|H|\psi\rangle, \tag{5.1.1}$$

$$\eta = \langle\psi|(H-\gamma)^2|\psi\rangle = \langle\psi|H^2|\psi\rangle - \gamma^2. \tag{5.1.2}$$

Note that $\eta \geq 0$ and that $\eta = 0$ implies that ψ is a true eigenfunction of H. With the help of the values of η we can derive lower bounds, but already the condition that $\eta \geq 0$ for *all* trial wave functions gives us a strong check on the calculations so far. Using this condition, we not only traced down a number of errors in the FORTRAN implementation of the Rayleigh-Ritz method, but we also discovered a subtle bug in the orthogonalization of the basis functions.

Suppose that $\sigma(H) \cap (a,b) = \emptyset$. Using the eigenfunction decomposition $\psi = \sum_n c_n\psi_n$, we have

$$\langle\psi|\left(H-\frac{a+b}{2}\right)^2|\psi\rangle = \sum_n |c_n|^2\left(\mu_n - \frac{a+b}{2}\right)^2 \geq \left(\frac{a-b}{2}\right)^2. \tag{5.1.3}$$

Expressing the left-hand side in terms of γ and η leads to $\eta \geq (\gamma-a)(b-\gamma)$. We conclude

$$\eta < (\gamma-a)(b-\gamma) \Rightarrow \sigma(H)\cap(a,b) \neq \emptyset. \tag{5.1.4}$$

Now assume that $\eta < (\gamma-a)(b-\gamma)$ and that the cross section of $\sigma(H)$ and (a,b) consists of a single point λ. Since $\eta \geq 0$, we know $a < \gamma < b$. The inequality for η can be rewritten in two ways

$$b > \gamma + \frac{\eta}{\gamma-a} \equiv b' \;\Leftrightarrow\; a < \gamma - \frac{\eta}{b-\gamma} \equiv a', \tag{5.1.5}$$

and we obtain $a < a' \leq \gamma \leq b' < b$. If we take $a < a'' < a'$, we have $\eta < (\gamma-a'')(b-\gamma)$ and thus we get $\sigma(H)\cap(a'',b) \neq \emptyset$. By repeating this argument for $b' < b'' < b$, we conclude

$$\sigma(H)\cap(a',b') \neq \emptyset, \tag{5.1.6}$$

and consequently.

$$\gamma - \frac{\eta}{b-\gamma} < \lambda < \gamma + \frac{\eta}{\gamma-a}. \tag{5.1.7}$$

Applying this general method to the n^{th} level μ_n of H, we have that $\gamma = \tilde{\mu}_n$. We assume our variational basis to be so accurate that

$$\mu_{n+1} > \frac{\tilde{\mu}_{n+1}+\tilde{\mu}_n}{2}. \tag{5.1.8}$$

Under this assumption we can take

$$a = \tilde{\mu}_{n-1}, \tag{5.1.9}$$

$$b = \frac{\tilde{\mu}_{n+1}+\tilde{\mu}_n}{2}. \tag{5.1.10}$$

For the ground state, $n = 1$, we can take $a = -\infty$. If the condition $\eta < (\gamma-a)(b-\gamma)$ is satisfied, we conclude

$$\tilde{\mu}_n - \frac{2\eta}{\tilde{\mu}_{n+1}-\tilde{\mu}_n} < \mu_n < \tilde{\mu}_n. \tag{5.1.11}$$

$$
\begin{aligned}
\lambda_1 &= \tfrac{2}{f} + \kappa_1 \\
\lambda_2 &= \tfrac{2}{f} + \tfrac{1}{3}\kappa_2 \\
\lambda_3 &= \kappa_3 + \kappa_4 \\
\lambda_4 &= \tfrac{2}{f} - 8\kappa_4 \\
\lambda_5 &= \tfrac{1}{3}\kappa_5 \\
\lambda_6 &= \kappa_6 \\
\lambda_7 &= \kappa_7 + \kappa_8 \\
\lambda_8 &= \tfrac{2}{f} - 6\kappa_8
\end{aligned}
$$

$$
\begin{aligned}
\mathrm{inv}_3(c) &= 3\det(c) \\
\mathrm{inv}_4(c) &= \tfrac{1}{8}\left(\mathrm{tr}^2(X) - \mathrm{tr}(X^2)\right) \\
\mathrm{inv}_2(c,d) &= \tfrac{1}{6}\left(\mathrm{tr}(X)\,\mathrm{tr}(Y) - \mathrm{tr}(XY)\right) \\
\mathrm{inv}_6(c) &= \mathrm{inv}_3^2(c) \\
\mathrm{inv}_7(c) &= \mathrm{inv}_3(c)\,\mathrm{inv}_4(c) \\
\mathrm{inv}_8(c) &= \mathrm{inv}_4^2(c)
\end{aligned}
$$

Table 5-1. The coefficients for the hamiltonian and the definition of several invariants.

5.2 Boundary conditions

In this section we will derive the boundary conditions for our model. We can treat the lowest order and the one-loop case on the same footing by writing

$$\mathcal{H} = -\frac{f}{2}\left(\frac{\partial^2}{\partial c_i^a \partial c_i^a} + \frac{\partial^2}{\partial d_i^a \partial d_i^a}\right) + \mathcal{V}(c,d), \quad f = \frac{g^2}{2\pi^2}, \tag{5.2.1}$$

$$\mathcal{V}(c,d) = \mathcal{V}(c) + \mathcal{V}(d) + \lambda_7 r_c^2 r_d^2 + \lambda_8\,\mathrm{inv}_2(c,d), \tag{5.2.2}$$

$$\mathcal{V}(c) = \lambda_1 r_c^2 + \lambda_2\,\mathrm{inv}_3(c) + \lambda_3 r_c^4 + \lambda_4\,\mathrm{inv}_4(c) + \lambda_5 r_c^2\,\mathrm{inv}_3(c) + \lambda_6 r_c^6. \tag{5.2.3}$$

The coefficients λ_i, as well as the definitions of the used invariants can be found in table 5-1. We have also given the definitions of the invariants that occur in $\mathcal{V}^2$. For the lowest order effective hamiltonian, we just set $\kappa_i = 0$, whereas for the one-loop effective hamiltonian we need to use the values for κ_i of table 4-1.

We have to provide boundary conditions at the boundary of the fundamental domain to obtain a well-defined quantum mechanical problem. Consider fig. 3-3. At weak coupling, the potential energy at the boundary of the fundamental domain is higher than the energy E of the wave function: the wave function is localized around the perturbative vacuum $c = d = 0$ and the boundary conditions are not felt.

Increasing the coupling results in the spreading of the wave function over the configuration space. We are interested in the regime where E is of the order of the sphaleron energy: we will have a substantial flow of the wave function over the instanton barrier, but at the rest of the boundary the potential is still much higher than E. This means that at most parts of the boundary, the wave function will have decayed exponentially before reaching it. As a consequence, the boundary conditions imposed there will not have a large effect on the spectrum. By the same token, the precise location of the boundary in these regions is not important either. This gives us the freedom to choose tractable boundary conditions.

At the sphalerons however, the boundary conditions are fixed. Since the gauge transformation connecting the two sphalerons has winding number one, we have to set

$$\Psi(A(\mathrm{Sph},0)) = e^{i\theta}\Psi(A(0,\mathrm{Sph})), \tag{5.2.4}$$

thus introducing the θ angle.

The variational basis we need must incorporate the boundary conditions. We define radial coordinates r_c and r_d by

$$r_c = [c_i^a c_i^a]^{\frac{1}{2}}, \quad r_d = [d_i^a d_i^a]^{\frac{1}{2}}. \tag{5.2.5}$$

The sphaleron has radial coordinates $(\sqrt{3}, 0)$ and angular coordinates $\bar{c}_i^a = -\delta_i^a$ (with $\bar{c}_i^a = c_i^a / r_c$). It will be connected with the anti-sphaleron at $(0, \sqrt{3})$. We will restrict the (r_c, r_d) plane by $r_c < \sqrt{3}$, $r_d < \sqrt{3}$ and impose boundary conditions at the edges. This means that we will be working towards basis functions of the form $\phi(r_c, r_d) Y(\bar{c}, \bar{d})$.

As argued above, for values of the coupling constant at which our approximation will be valid, only the effect of the boundary conditions at the sphaleron will be felt. By imposing boundary conditions in the (r_c, r_d) plane we pair up two submanifolds, of which only the sphaleron/anti-sphaleron need belong to the boundary of the fundamental domain.

Consider the following decomposition of the full wave function

$$\Psi = \frac{1}{r_c^4 r_d^4} \sum_{n=1}^{\infty} \psi^{(n)}(c,d) \chi^{(n)}_{[c,d]}(q), \tag{5.2.6}$$

where q denotes all the modes orthogonal to the c and d modes. This is just eq. (2.4.5) with an extra factor $r_c^4 r_d^4$ extracted for technical reasons (i.e. $\varphi^{(n)} \leftrightarrow \psi^{(n)} r_c^{-4} r_d^{-4}$). Under the adiabatic approximation, explained in chapter 2, we obtain a hamiltonian for $\psi = \psi^{(1)}$ given by

$$\mathcal{H} = -\frac{f}{2}\left(\frac{\partial^2}{\partial r_c^2} + \frac{\partial^2}{\partial r_d^2} - 12\left(\frac{1}{r_c^2} + \frac{1}{r_d^2}\right) + \frac{1}{r_c^2}\Delta_{\bar{c}} + \frac{1}{r_d^2}\Delta_{\bar{d}}\right) + \mathcal{V}(c,d), \tag{5.2.7}$$

with $\Delta_{\bar{c}}$ the laplacian in the angular coordinates. The extra term $V^{(1)}(c,d)$ that one might expect is contained within $\mathcal{V}(c,d)$.

The boundary condition on ψ follows directly from eq. (5.2.4), but care must be taken when imposing the condition on the normal derivative of ψ. Matching along the sphaleron path across the boundary of the fundamental domain, we need to compensate for the curvature with the appropriate jacobian factor. We will make this more precise.

Let us focus on the tunnelling path $c_i^a = -u\,\delta_i^a$. Note that this path is equivalent to all paths $c_i^a = -u\,S(\bar{\alpha})_i^a$, with S an orthogonal matrix, due to the residual gauge symmetry. We will first remove this gauge symmetry to obtain a genuine one-dimensional tunnelling parameter. Introduce the following decomposition for c:

$$c = S(\alpha_p) H(h_i), \quad S \in \mathrm{SO}(3),\ H^T = H. \tag{5.2.8}$$

If we write

$$H = \sum_{i=0}^{5} h_i H_i, \tag{5.2.9}$$

with $\mathrm{tr}(H_i H_j) = \delta_{ij}$ and with $H_0 \propto \mathbb{1}$, then h_0 will play the role of the gauge invariant tunnelling parameter. The sphaleron is located at $h_0 = \sqrt{3}$, $h_i = 0$, $(i = 1, \ldots, 5)$.

The isolation of the 18 (c, d) modes is appropriate close to the perturbative vacuum, because, as we have seen, they are the slow modes of the theory. Close to the sphaleron however, the only slow mode is the tunnelling mode $w = h_0/\sqrt{3}$. To derive the correct boundary conditions, we should reduce the dynamics around the sphaleron to a one-dimensional tunnelling problem, by integrating out all other modes. To this end, we consider the following decomposition of Ψ:

$$\Psi = \sum_n \varphi^{(n)}(w) \chi^{(n)}_{[w]}(q), \tag{5.2.10}$$

where q not only denotes the non-(c, d) modes, but also the d modes and the h_i modes with $i = 1, \ldots, 5$. Note that Ψ does not depend on the gauge degrees of freedom α_p. When imposing the boundary conditions, we want to relate the wave function at the sphaleron to the one at the anti-sphaleron. Consider the tranverse modes q within the (c, d) space at the sphaleron. The gauge transformation that maps the sphaleron to the anti-sphaleron will *not* map these modes on modes within the (c, d) space at the anti-sphaleron: transverse modes inside and outside the (c, d) space get mixed under the gauge transformation. The transverse wave function at the sphaleron restricted to the (c, d) modes does therefore not fit naturally to this transverse wave function at the anti-sphaleron. The full transverse wave functions do however map to each other. Another manifestation of this symmetry is the fact that the effective potential is symmetric around the sphaleron only when *all* transverse modes are integrated out.

Before going to the effective hamiltonian for $\varphi^{(1)}(w)$ we must remove the residual gauge freedom. The gauge invariant wave function Ψ is independent of the coordinates α_p. We will show that only after a suitable rescaling of the wave function, the laplacian takes its cartesian form with respect to the tunnelling parameter w. The boundary conditions at the sphaleron must be imposed on this rescaled wave function.

Consider the laplacian for the c modes. If we write $u_\mu = (h_0, \ldots, h_5, \alpha_1, \alpha_2, \alpha_3)$ the laplacian takes the form

$$\Delta\Psi = \frac{1}{J}\partial_\mu \left(J g^{\mu\nu} \partial_\nu \Psi \right). \tag{5.2.11}$$

Here $J = \det^{1/2}(g)$ and g is the metric which can be obtained from

$$d\sigma^2 = \mathrm{tr}(\dot{c}\dot{c}) = g_{\mu\nu} \dot{u}_\mu \dot{u}_\nu. \tag{5.2.12}$$

This leads to

$$g_{\mu\nu} = \begin{pmatrix} \mathbb{1}_6 & 0 \\ 0 & U \end{pmatrix} \begin{pmatrix} \mathbb{1}_6 & b \\ b^T & a \end{pmatrix} \begin{pmatrix} \mathbb{1}_6 & 0 \\ 0 & U^T \end{pmatrix} = \begin{pmatrix} \mathbb{1}_6 & bU^T \\ Ub^T & UaU^T \end{pmatrix}. \tag{5.2.13}$$

The matrix U is given by

$$S^{-1}\dot{S} = S^{-1}\partial_p S \dot{\alpha}_p = U_{pq}\varepsilon^q \dot{\alpha}_p, \tag{5.2.14}$$

with $(\varepsilon^q)_{rs} = \varepsilon_{qrs}$. The matrices a and b are given by

$$a_{pq} = -\operatorname{tr}(\varepsilon^p \varepsilon^q H^2), \tag{5.2.15}$$
$$b_{ip} = \operatorname{tr}(\varepsilon^p H H_i). \tag{5.2.16}$$

We have $\det(g) = |U|^2 \, |a - b^T b|$. Using

$$(a - b^T b)_{pr} = \tfrac{1}{2} \operatorname{tr}(\varepsilon^p \varepsilon^q H) \operatorname{tr}(\varepsilon^q \varepsilon^r H) = \tfrac{1}{2} \left(\operatorname{tr}(H)\mathbb{1} - H\right)^2_{pr}, \tag{5.2.17}$$

we arrive at

$$\det(g) = \tfrac{1}{8} |U|^2 \, |\operatorname{tr}(H)\mathbb{1} - H|^2. \tag{5.2.18}$$

The inverse of g is given by

$$\begin{aligned} g^{\mu\nu} &= \begin{pmatrix} \mathbb{1}_6 & 0 \\ 0 & (U^T)^{-1} \end{pmatrix} \begin{pmatrix} d & f \\ f^T & e \end{pmatrix} \begin{pmatrix} \mathbb{1}_6 & 0 \\ 0 & U^{-1} \end{pmatrix} \\ &= \begin{pmatrix} d & fU^{-1} \\ (U^T)^{-1} f^T & (U^T)^{-1} e U^{-1} \end{pmatrix}, \end{aligned} \tag{5.2.19}$$

with

$$e = (a - b^T b)^{-1}, \tag{5.2.20}$$
$$f = -be, \tag{5.2.21}$$
$$d = \mathbb{1} + beb^T. \tag{5.2.22}$$

For Ψ independent of $\vec{\alpha}$, eq. (5.2.11) reduces to

$$\Delta\Psi = \frac{1}{J} \frac{\partial}{\partial h_i} \left(J g^{ij} \frac{\partial}{\partial h_j} \Psi \right) + \frac{1}{J} \frac{\partial}{\partial \alpha_p} \left(J g^{pj} \right) \frac{\partial}{\partial h_j} \Psi. \tag{5.2.23}$$

The second term on the right-hand side is proportional to

$$f_{jq} \frac{\partial}{\partial \alpha_p} \left(|U| (U^{-1})_{qp} \right) = 0, \tag{5.2.24}$$

so we obtain

$$\Delta\Psi = \frac{1}{\tilde{J}} \partial_i \left(\tilde{J} d_{ij} \partial_j \Psi \right), \tag{5.2.25}$$

with $\tilde{J} = |\operatorname{tr}(H)\mathbb{1} - H|$. Writing $H = h_0 H_0 + \tilde{H}$, we can show that $d = \mathbb{1} + \mathcal{O}\left(\tilde{H}^2\right)$ and that $\tilde{J} = \frac{8}{9}\sqrt{3} h_0^3 + \mathcal{O}\left(\tilde{H}^2\right)$. Evaluating the laplacian at the sphaleron path gives us

$$\Delta\Psi = \frac{1}{h_0^3} \partial_i \left(h_0^3 \partial_i \Psi \right). \tag{5.2.26}$$

To obtain an ordinary one-dimensional tunnelling problem, we must rescale the wave function by $w^{3/2} \propto h_0^{3/2}$:

$$\varphi(w) = w^{-\frac{3}{2}}\bar{\varphi}(w). \tag{5.2.27}$$

The tunnelling problem then looks as

$$\left(-\frac{f}{2}\frac{\partial^2}{\partial w^2} + \bar{V}(w)\right)\bar{\varphi}(w) = E\bar{\varphi}(w). \tag{5.2.28}$$

We can derive a similar equation for a function $\bar{\varphi}'$ of the parameter w' corresponding to tunnelling through the anti-sphaleron. When matching these tunnelling paths through the relation $w' = 2 - w$, boundary conditions must be imposed on $\bar{\varphi}$ and on its normal derivative at the sphaleron $w = 1$. Combining the factors $w^{3/2}$ and r^{-4} leads to the following boundary conditions on ψ:

$$\psi(\mathrm{Sph}, 0) = e^{i\theta}\psi(0, \mathrm{Sph}), \tag{5.2.29}$$

$$\frac{\partial(r_c^{-\frac{5}{2}}\psi)}{\partial r_c}(\mathrm{Sph}, 0) = -e^{i\theta}\frac{\partial(r_d^{-\frac{5}{2}}\psi)}{\partial r_d}(0, \mathrm{Sph}). \tag{5.2.30}$$

5.3 The variational basis

We decided to use functions of the form $\phi(r_c, r_d)Y(\hat{c}, \hat{d})$ and to incorporate the boundary conditions in the (r_c, r_d) plane. Apart from the boundary conditions, we must also respect the symmetries of the hamiltonian as much as possible to obtain an optimal block diagonalization. Most of these symmetries, including the residual gauge symmetry, will be incorporated in the functions $Y(\hat{c}, \hat{d})$. After this, we will use the exact solution of the strong coupling limit of our hamiltonian problem as a guide to obtain a useful set of radial functions.

5.3.1 Symmetries

The hamiltonian $\mathcal{H}(c, d)$ is invariant under the transformation $c \to ScR_1$, $d \to SdR_2$ with $S, R_1, R_2 \in \mathrm{SO}(3)$ and under the interchange $c \leftrightarrow d$. The generators of left- and right multiplication are $\vec{L}_c^R$, $\vec{L}_c^S$, $\vec{L}_d^R$ and $\vec{L}_d^S$. These are su(2) angular momentum operators and we have for instance

$$\left(L_c^R\right)_i = -i\varepsilon_{ijk}c_j^a\frac{\partial}{\partial c_k^a}. \tag{5.3.1}$$

The operators $\vec{L}_c^R$ and $\vec{L}_d^R$ can be related to the symmetries of S^3. We rely on the material in appendix A of chapter 2 for the following considerations. The spatial symmetry of S^3 that corresponds to left multiplication on $SU(2) \cong \mathrm{S}^3$ is generated by $\vec{L}_1$. If we use Cutkosky's representation for the gauge field (here ψ is *not* a wave function)

$$\psi(n, n') = A_\mu(c, d)n'_\mu = c_j\eta^j_{\mu\nu}n_\nu n'_\mu + d_j\bar{\eta}^j_{\mu\nu}n_\nu n'_\mu, \tag{5.3.2}$$

the generator for the symmetry is $\vec{L}_1 + \vec{L}'_1$. We obtain

$$\delta_i\psi = (L_1 + L'_1)_i\psi = i\varepsilon_{ijk}c_j\eta^k_{\mu\nu}n_\nu n'_\mu \;\Rightarrow\; \delta_i c_k = i\varepsilon_{ijk}c_j. \tag{5.3.3}$$

The generator acting on functionals of the gauge field is thus

$$-\delta_i\psi\frac{\delta}{\delta\psi} = -i\varepsilon_{ijk}c_j\frac{\partial}{\partial c_k} \equiv \left(L^R_c\right)_i. \tag{5.3.4}$$

The following set of operators commutes:

$$\left\{\mathcal{H}, \vec{J}^S, \vec{J}^R, (\vec{L}^R_c)^2 + (\vec{L}^R_d)^2, \mathcal{P}\right\}. \tag{5.3.5}$$

$\mathcal{P}$ is defined by $\mathcal{P}f(c,d) \equiv f(d,c)$. On S^3 it corresponds to the parity $(n_0, \vec{n}) \leftrightarrow (n_0, -\vec{n})$ (cf. eq. (2.2.7)). The operator $\vec{J}^S \equiv \vec{L}^S_c + \vec{L}^S_d$ implements constant gauge transformations: we have to demand $(\vec{J}^S)^2 = 0$ for physical wave functions. The operator $\vec{J}^R \equiv \vec{L}^R_c + \vec{L}^R_d$ is the rotation operator. The spatial symmetry group is SO(4) and these symmetries cannot be simply divided in independent sets of translations and rotations. The operator on S^3 that corresponds to $\vec{J}^R$ is $\vec{L}_1 + \vec{L}_2$, and the corresponding symmetry on SU(2) is $g \to g_1^{-1}gg_1$. Writing $g = n\cdot\sigma$ and $g_1 = n'\cdot\sigma$ we have

$$n\cdot\sigma \;\to\; n_\mu(n'\cdot\bar{\sigma})\sigma_\mu(n'\cdot\sigma) = n_0\sigma_0 - n_iV^j_i(n')\sigma_j. \tag{5.3.6}$$

The symmetry on S^3 is thus seen to leave n_0 invariant and to perform an SO(3) rotation on $\vec{n}$. It is hence a rotation for points around the north and south pole of S^3. The operators $\vec{L}_1$ and $\vec{L}_2$ do not leave any point invariant and cannot be interpreted as rotation operators. Only their sum has this property and the different sectors ($j = 0, 1, \ldots$) under the symmetry $\vec{J}^R$ correspond to scalar glueballs, vector glueballs, etc.

To prepare the ground for the block diagonalization of the hamiltonian, we divide the function space in sectors characterized by the quantum numbers j, m, $l_1(l_1+1) + l_2(l_2+1)$ and p corresponding to the operators of eq. (5.3.5). Note that for low values of l_1 and l_2 there is a one-to-one correspondence between unordered pairs (l_1, l_2) and the numbers $l_1(l_1+1)+l_2(l_2+1)$. Since the spectrum of $\mathcal{H}$ is independent of the azimuthal quantum number m, we use the notation l_1l_2j-even and l_1l_2j-odd to denote the various sectors. We will interpret the lowest energy level in the scalar ($j = 0$) sector to be the vacuum. Energy differences with respect to this level will be the glueball masses. The lowest ground state in the various $j = 2$ sectors will for instance give rise to the mass of the tensor glueball.

5.3.2 The angular sector

We begin with constructing functions of $\hat{c}$ that are eigenfunctions of the following set of commuting operators

$$\left\{\Delta_{\hat{c}}, \vec{L}^R_c, \vec{L}^S_c\right\}. \tag{5.3.7}$$

Operator	$(\vec{L}_c^S)^2$	$(L_c^S)_3$	$(\vec{L}_c^R)^2$	$(L_c^R)_3$	$\Delta_{\hat{c}}$
Eigenvalue	$l_s(l_s+1)$	m_s	$l_r(l_r+1)$	m_r	$-L(L+7)$

Table 5-2. Behaviour of the functions $\langle\hat{c}|L;l_s,l_r,\tau;m_s,m_r\rangle$.

c_+^+	$= c_1^1 - c_2^2 + i(c_2^1 + c_1^2)$	$= \sqrt{2}r_1 e^{i\alpha_1}$
c_+^0	$= -\sqrt{2}\{c_1^3 + ic_2^3\}$	$= -\sqrt{2}r_3 e^{i\alpha_3}$
c_+^-	$= -\{c_1^1 + c_2^2 + i(c_2^1 - c_1^2)\}$	$= -\sqrt{2}r_2 e^{i\alpha_2}$
c_0^+	$= -\sqrt{2}\{c_3^1 + ic_3^2\}$	$= -\sqrt{2}r_4 e^{i\alpha_4}$
c_0^0	$= 2c_3^3$	
c_0^-	$= \sqrt{2}\{c_3^1 - ic_3^2\}$	$= \sqrt{2}r_4 e^{-i\alpha_4}$
c_-^+	$= -\{c_1^1 + c_2^2 - i(c_2^1 - c_1^2)\}$	$= -\sqrt{2}r_2 e^{-i\alpha_2}$
c_-^0	$= \sqrt{2}\{c_1^3 - ic_2^3\}$	$= \sqrt{2}r_3 e^{-i\alpha_3}$
c_-^-	$= c_1^1 - c_2^2 - i(c_2^1 + c_1^2)$	$= \sqrt{2}r_1 e^{-i\alpha_1}$

Table 5-3. Definition of the complex c variables.

Note that the space of the $\hat{c}$ makes up an S^8. From the appendix of chapter 2 we know that the eigenfunctions of the spherical laplacian $\Delta_{\hat{c}}$ will be the homogeneous harmonic polynomials in $\hat{c}$. If the degree of these polynomials is L, the eigenvalue of $\Delta_{\hat{c}}$ is $-L(L+7)$ and the degeneracy of this level is given by

$$\binom{L+8}{8} - \binom{L+6}{8}. \tag{5.3.8}$$

An orthonormal basis of functions of $\hat{c}$ is given by the set $\{\langle\hat{c}|L;l_s,l_r,\tau;m_s,m_r\rangle\}$. Each of these functions is a homogeneous harmonic polynomial of degree L in $\hat{c}$. Its eigenvalues under the various symmetries are collected in table 5-2. We used the operators $\vec{L}_c^R$ and $\vec{L}_c^S$ to further classify these functions, but for higher values of L we need the extra label τ for the remaining degeneracy. Explicitly, we have that $\langle\hat{c}|0;0,0,1;0,0\rangle$ is just the constant function. For $L=1$ we have the nine functions c_i^a. We define the raising- and lowering operators in the standard way:

$$L_\pm = L_1 \pm iL_2. \tag{5.3.9}$$

Introducing the operators $L_\pm^S$ and $L_\pm^R$ leads us to the complex combinations of table 5-3 and hence we arrive at the nine functions $\langle\hat{c}|1;1,1,1;m_s,m_r\rangle$. For $L=2$ we start with the function $c_+^+c_+^+$, which is, up to normalization, the function $\langle\hat{c}|2;2,2,1;2,2\rangle$. By applying the lowering operators we obtain the 25 functions $\langle\hat{c}|2;2,2,1;m_s,m_r\rangle$.

We use orthogonalization to obtain the other functions. Observe that the function $\langle\hat{c}|2;2,2,1;2,0\rangle$ is proportional to $c_+^+c_-^+ + c_0^+c_0^+$. From these two monomials, we

$l_r \backslash l_s$	2	1	0
2	$1^{(25)}$	0	$1^{(5)}$
1	0	$1^{(9)}$	0
0	$1^{(5)}$	0	0

Table 5-4. Degeneracy of representations (L, l_s, l_r) for $L = 2$. The index between parentheses gives the total degeneracy.

can construct one other combination that is orthogonal to this function. This is the combination $c_+^+ c_-^+ - \frac{1}{2} c_0^+ c_0^+$ which corresponds to the function $\langle \hat{c} | 2; 2, 0, 1; 2, 0 \rangle$. Applying the relevant lowering operator gives us the five functions $\langle \hat{c} | 2; 2, 0, 1; m_s, 0 \rangle$. In the same way, we can also construct the five functions $\langle \hat{c} | 2; 0, 2, 1; 0, m_r \rangle$, the nine functions $\langle \hat{c} | 2; 0, 1, 1; m_s, m_r \rangle$ and the singlet $\langle \hat{c} | 2; 0, 0, 1; 0, 0 \rangle$. The last function however, is just proportional to $\bar{c}_i^a \bar{c}_i^a$, i.e. to the constant function on S^8. Table 5-4 shows which representations $(2, l_s, l_r)$ occur. Note that we have obtained 44 functions, in agreement with the degeneration formula.

We will shortly give an algorithm which enables us to apply the method sketched above to the case of general L, but we first must comment on the way the inner product of functions of $\hat{c}$ is defined. We will integrate a monomial in the variables c_i^a over S^8. The purpose of this calculation is to arrive at a quick algorithm for evaluating such integrals.

With the definitions of the variables r_i and α_i of table 5-3 we find for the measure

$$\begin{aligned} \int_{S^8} d\hat{c} &= \int_{\mathbb{R}^9} d^9 c\, \delta\left([c_i^a c_i^a]^{\frac{1}{2}} - 1 \right) \\ &= \int_{-\infty}^{\infty} dc_3^3 \int_0^{\infty} dr_1\, r_1 \cdots \int_0^{\infty} dr_4\, r_4 \int_0^{2\pi} d\alpha_1 \cdots \int_0^{2\pi} d\alpha_4 \times \\ &\quad \delta\left(\left[r_1^2 + \cdots + r_4^2 + (c_3^3)^2 \right]^{\frac{1}{2}} - 1 \right). \end{aligned} \tag{5.3.10}$$

The result of the integrations over α_i and c_3^3 is that only terms will survive which are of the form

$$(r_1^2)^{n_1} \cdots (r_4^2)^{n_4} (c_3^3)^{2n_5}, \tag{5.3.11}$$

with n_i integers. This means that a factor $(c_+^+)^{n_1}$ in the monomial has to be balanced by a factor $(c_-^-)^{n_1}$. Performing the α_i integrations and introducing $q_i = r_i^2$ and $q_5 = (c_3^3)^2$ leaves us with the expression

$$\begin{aligned} &\frac{(2\pi)^4}{8} \int_0^{\infty} dq_1 \cdots dq_5\, q_1^{n_1} \cdots q_4^{n_4} q_5^{n_5 - \frac{1}{2}}\, \delta\left(1 - \sum_{i=1}^{5} q_i \right) = \\ &\quad \frac{(2\pi)^4}{8} \frac{1}{\Gamma\left(\sum_{i=1}^{5} n_i + \frac{9}{2} \right)} \Gamma(n_1 + 1) \cdots \Gamma(n_4 + 4) \Gamma(n_5 + \tfrac{1}{2}). \end{aligned} \tag{5.3.12}$$

$l_r \backslash l_s$	3	2	1	0
3	$1^{(49)}$	0	$1^{(21)}$	0
2	0	$1^{(25)}$	$1^{(15)}$	0
1	$1^{(21)}$	$1^{(15)}$	$1^{(9)}$	0
0	0	0	0	$1^{(1)}$

$l_r \backslash l_s$	4	3	2	1	0
4	$1^{(81)}$	0	$1^{(45)}$	0	$1^{(9)}$
3	0	$1^{(49)}$	$1^{(35)}$	$1^{(21)}$	0
2	$1^{(45)}$	$1^{(35)}$	$2^{(50)}$	$1^{(15)}$	$1^{(5)}$
1	0	$1^{(21)}$	$1^{(15)}$	$1^{(9)}$	0
0	$1^{(9)}$	0	$1^{(5)}$	0	$1^{(1)}$

Table 5-5. Degeneracy of representations (L, l_s, l_r) for $L = 3$ and $L = 4$. The index in parentheses gives the total degeneracy.

The algorithm that emerges from this calculation was implemented first in MATHEMATICA and later in FORM. Both these implementations give exact values for the integrals, and the implementation in FORM was fast enough for the calculations of the inner products needed for the orthogonalization for $L \leq 10$. However, when we needed to calculate matrix elements of operators between these functions, as described in the next section, the overall degree of the monomials can become as high as 28, and even FORM was not fast enough for our purposes. For the calculation of these integrals, we constructed a high-precision numerical implementation of the algorithm in C.

We return to the issue of constructing all representations (L, l_s, l_r, τ) for given (L, l_s, l_r). We start with the function

$$\left(c_+^\dagger\right)^L \propto \langle \tilde{c}|L; L, L, 1; L, L\rangle. \tag{5.3.13}$$

Note that for given L, we have that $l_s, l_r \leq L$. By applying the lowering operators, we can obtain the function $\langle \tilde{c}|L; L, L, 1; l_s, l_r\rangle$ which is a sum of monomials. The set of these monomials span the space $A_{l_r}^{l_s}$ which is the eigenspace of the operators L_3^S and L_3^R for the eigenvalue pair (l_s, l_r). Within this space of functions, but now regarded as functions of c in stead of $\tilde{c}$, we construct the intersection of the kernels of the operators $L_-^S L_+^S$, $L_-^R L_+^R$ and $(c_i^a c_i^a \Delta)$. The first two operators leave us with only those combinations of the monomials that have the prescribed $(\vec{L}^S)^2$ and $(\vec{L}^R)^2$ eigenvalues; the laplacian imposes the constraint that the polynomials must be harmonic: $\Delta = 0$.

If this intersection consists of more than one function, we use explicit Gram-Schmidt orthogonalization to arrive at the functions $\langle \tilde{c}|L; l_s, l_r, \tau; l_s, l_r\rangle$. With the lowering operators, we trivially construct the rest of the functions $\langle \tilde{c}|L; l_s, l_r, \tau; m_s, m_r\rangle$. Table 5-5 gives the results for $L = 3$ and $L = 4$. Note that for $(L, l_s, l_r) = (4, 2, 2)$ we need the index τ for the remaining degeneracy. The functions with $l_s = l_r = 0$ are invariant under the symmetry $c \to ScR$. Note that $\det(c) \propto r_c^3 \langle \tilde{c}|3; 0, 0, 1; 0, 0\rangle$ and that the harmonic combination of $\mathrm{tr}(X^2)$ and $\mathrm{tr}^2(X)$ is proportional to $r_c^4 \langle \tilde{c}|4; 0, 0, 1; 0, 0\rangle$.

The algorithm described above was implemented in MATHEMATICA. When the need for higher L functions developed, a few improvements were made. The construc-

Operator	$(\vec{L}_c^S)^2$	$(\vec{L}_d^S)^2$	$(\vec{J}^S)^2$	J_3^S	Δ_c
Eigenvalue	$l_s(l_s+1)$	$l_s(l_s+1)$	0	0	$-L_1(L_1+7)$

Operator	$(\vec{L}_c^R)^2$	$(\vec{L}_d^R)^2$	$(\vec{J}^R)^2$	J_3^R	$\Delta_{\bar{d}}$
Eigenvalue	$l_1(l_1+1)$	$l_2(l_2+1)$	$j(j+1)$	m	$-L_2(L_2+7)$

Table 5-6. Behaviour of the functions $\langle \hat{c}\hat{d}|j,m,l_s;L_1,l_1,\tau_1;L_2,l_2,\tau_2\rangle$.

tion of the space $A^{l_s}_{l_r}$ was improved, but the most important change was to use C to perform the construction of the intersection of the kernels of $L^S_- L^S_+$ and $L^R_- L^R_+$. This avoided the use of slow MATHEMATICA routines like 'NullSpace' by using explicit projectors on the required kernels. We used

$$P^S_{l_s} = \prod_{j=l_s+1}^{L} \left(1 - \frac{1}{j(j+1)-l_s(l_s+1)} L^S_- L^S_+\right), \tag{5.3.14}$$

and the analogous expression for $P^R_{l_r}$. Since all calculations had to be done exactly, we used arithmetic with (large) integers. In this way we explicitly constructed the representations (L,l_s,l_r,τ) for $L \leq 10$ and $l_r \leq 2$. As will be apparent from the sequel, we did not need higher values for l_r.

We construct functions of both $\hat{c}$ and $\hat{d}$ by using the familiar rules of adding angular momenta. Let i denote a representation $(L;l_s,l_r,\tau)$ and consider the functions $\langle \hat{c}|i_1;m_s,m_r\rangle$ and $\langle \hat{d}|i_2;m'_s,m'_r\rangle$. Using Clebsch-Gordan coefficients, we can define a function $Y^{i_1 i_2}(\hat{c},\hat{d})$ which is an eigenfunction of $\vec{J}^R$ and of $\vec{J}^S$. We will limit the construction to functions with $\vec{J}^S = 0$, as required by residual gauge symmetry. This implies that the functions of c and d need to have the same l_s, which restricts the possible combinations of i_1 and i_2. The resulting function $Y^{i_1 i_2}(\hat{c},\hat{d})$ is given by

$$\begin{aligned} Y &= \langle \hat{c}\hat{d}|j,m,l_s;L_1,l_1,\tau_1;L_2,l_2,\tau_2\rangle \\ &= \sum_{m_s=-l_s}^{l_s} \sum_{m_1=-l_1}^{l_1} \sum_{m_2=-l_2}^{l_2} (-1)^{l_1-l_2+m} \sqrt{2j+1} \begin{pmatrix} l_1 & l_2 & j \\ m_1 & m_2 & -m \end{pmatrix} \times \\ &\quad \frac{(-1)^{l_s-m_s}}{\sqrt{2l_s+1}} \langle \hat{c}|L_1;l_s,l_1,\tau_1;m_s,m_1\rangle \langle \hat{d}|L_2;l_s,l_2,\tau_2;-m_s,m_2\rangle. \end{aligned} \tag{5.3.15}$$

Its eigenvalues under the various symmetries are collected in table 5-6. Note the behaviour under parity:

$$\mathcal{P} Y^{i_1 i_2} = (-1)^{l_1+l_2+j} Y^{i_2 i_1}. \tag{5.3.16}$$

5.3.3 The radial sector

The strong coupling limit of our hamiltonian problem consists of the eigenvalue problem for the kinetic part of the hamiltonian of eq. (5.2.7). If we assume a solution $\varphi(r_c)\varphi(r_d)Y^{i_1 i_2}(\hat{c},\hat{d})$, the reduced one-dimensional eigenvalue problem becomes

$$\left(\frac{\partial^2}{\partial r^2} + \lambda - \frac{(12 + L(L+7))}{r^2}\right)\varphi(r) = 0, \tag{5.3.17}$$

whose regular solution is

$$\varphi_\gamma^{(L)}(r) = \gamma r j_{3+L}(\gamma r), \tag{5.3.18}$$

with $j_p(z)$ the spherical Bessel function of order p and $\lambda = \gamma^2$. The eigenfunctions of the kinetic part of the hamiltonian are thus given by

$$\varphi_{\gamma_1}^{(L_1)}(r_c)\varphi_{\gamma_2}^{(L_2)}(r_d)Y^{i_1 i_2}(\hat{c},\hat{d}), \tag{5.3.19}$$

with the energies given by

$$E = \frac{f}{2}\left(\gamma_1^2 + \gamma_2^2\right). \tag{5.3.20}$$

During the variational stage of the calculation, however, the use of spherical Bessel functions of different order will lead to a large number of integrals. Therefore we take the radial functions to be independent of L_1 and L_2 and define

$$\psi_{\gamma_1\gamma_2}^{i_1 i_2}(c,d) = \varphi_{\gamma_1}(r_c)\varphi_{\gamma_2}(r_d)Y^{i_1 i_2}(\hat{c},\hat{d}), \tag{5.3.21}$$

with $\varphi_\gamma(r) = \gamma r j_3(\gamma r)$. These functions are not eigenfunctions of the kinetic part of the hamiltonian and they will have discontinuities of the following kind. For $r \downarrow 0$, we have that $\varphi_\gamma(r) \sim r^4$. The wave function Ψ behaves as

$$\frac{1}{r^4}\varphi_\gamma(r)\langle\hat{c}|L; l_s, l_r, \tau; m_s, m_r\rangle, \tag{5.3.22}$$

and this function will be discontinuous at $r = 0$. The variational functions thus have discontinuities at $r_c = 0$ and $r_d = 0$. These form a set of measure zero, and a variational calculation will not feel them. Since the functions $\varphi_\gamma(r)$ are the eigenfunctions of the reduced one-dimensional problem with $L = 0$, they still constitute a complete set of functions.

The behaviour under parity can be obtained from eq. (5.3.16) and is given by

$$\mathcal{P}\psi_{\gamma_1\gamma_2}^{i_1 i_2} = (-1)^{l_1+l_2+j}\psi_{\gamma_2\gamma_1}^{i_2 i_1}. \tag{5.3.23}$$

Taking even and odd combinations gives

$$\psi_{\gamma_1\gamma_2}^{pi_1 i_2}(c,d) = \psi_{\gamma_1\gamma_2}^{i_1 i_2}(c,d) + p\,\psi_{\gamma_1\gamma_2}^{i_1 i_2}(d,c). \tag{5.3.24}$$

sector	$\|j, m, l_s; L_1, l_1, \tau_1; L_2, l_2, \tau_2\rangle$	γ_1	γ_2	E
000-even	$\|0,0,0;0,0,1;0,0,1\rangle$	1.9786	1.9786	$3.9149f$
000-even	$\|0,0,0;0,0,1;3,0,1\rangle$	4.1215	1.9786	$10.4508f$
000-odd	$\|0,0,0;0,0,1;0,0,1\rangle$	4.0345	6.0143	$26.2246f$
112-even	$\|2,m,1;1,1,1;1,1,1\rangle$	2.7406	2.7406	$7.5108f$
112-odd	$\|2,m,1;1,1,1;2,1,1\rangle$	4.7242	5.4016	$25.7476f$
022-even	$\|2,m,0;0,0,1;2,2,1\rangle$	1.9786	3.4456	$7.8936f$
022-odd	$\|2,m,0;0,0,1;2,2,1\rangle$	4.0345	5.4016	$22.7272f$

Table 5-7. Strong coupling limit: lowest energy levels in some sectors.

We implement the boundary conditions eq. (5.2.29) and (5.2.30) for $\theta = 0$ by imposing the following conditions on γ_1 and γ_2:

$$p = -1 \quad : \quad \varphi_{\gamma_1}(\sqrt{3}) = \varphi_{\gamma_2}(\sqrt{3}) = 0, \tag{5.3.25}$$

$$p = 1 \quad : \quad \frac{\partial(r^{-\frac{5}{2}}\varphi_{\gamma_1})}{\partial r}(\sqrt{3}) = \frac{\partial(r^{-\frac{5}{2}}\varphi_{\gamma_2})}{\partial r}(\sqrt{3}) = 0. \tag{5.3.26}$$

These conditions are expected to be accurate as long as the wave function transverse to the sphaleron path (near the sphalerons) is predominantly in its ground state. The case $\theta = \pi$ can be treated along the same lines as $\theta = 0$ by interchanging the boundary conditions for the cases $p = 1$ and $p = -1$.

The exact strong coupling results for the lowest levels in some sectors for $\theta = 0$ are collected in table 5-7. These values are obtained by imposing the boundary conditions above on the true eigenfunctions of eq. (5.3.19): the values of γ_1 and γ_2 are hence dependent on L_1 and L_2 respectively.

For general θ we multiply $\psi^{p;\tau_1\tau_2}_{\gamma_1\gamma_2}(c,d)$ with a phase factor $\exp(i\theta\alpha(r_c, r_d))$. The function α is a kind of Cherns-Simons functional that gives the correct behaviour to the wave function under large gauge transformations. The resulting functions no longer have well-defined parity, but they do obey the general boundary conditions for suitable α. Also the hermiticity of the hamiltonian for these functions can be checked explicitly. Sufficient conditions on α are: $\alpha(r_c, r_d) = -\alpha(r_d, r_c)$ and $\alpha(\sqrt{3}, 0) = \frac{1}{2}$. We choose

$$\alpha(r_c, r_d) = \frac{1}{2}\left(\left(\frac{r_c}{\sqrt{3}}\right)^\beta - \left(\frac{r_d}{\sqrt{3}}\right)^\beta\right). \tag{5.3.27}$$

For $\beta \to \infty$ we approach the situation that the phase factor over the entire edge is constant and equal to $e^{i\theta}$. But already for the choice $\beta = 2$, the boundary conditions at the sphalerons are taken into account properly.

5.3.4 Truncation of the basis

To construct a truncated basis, we use the following algorithm. We start by specifying a sector $l_1 l_2 j$ and, for $\theta = 0$, a parity $p_{\rm sec}$. Of course, l_1, l_2 and j must obey the triangular condition. Furthermore, we give the desired number of radial functions, $N_{\rm rad}$, as well as an upper bound $L_{\rm sum}$ on the sum $L_1 + L_2$. The method to restrict the number of angular functions is based on the fact the energy of the weak coupling functions grows as $L_1 + L_2$, as will be derived in the section on the weak coupling limit.

We construct all allowed angular functions $Y^{i_1 i_2}$: the two representations i_1 and i_2 must have the same l_s, their l_r values must match the prescribed unordered pair (l_1, l_2) and $L_1 + L_2 \leq L_{\rm sum}$. The number of functions thus obtained is called $N_{\rm ang}$. Next we consider the first $N_{\rm rad}$ radial functions $\varphi_{\gamma_1}(r_c)\varphi_{\gamma_2}(r_d)$ ordered according to the energy $\gamma_1^2 + \gamma_2^2$. To avoid double counting, we impose $\gamma_1 \leq \gamma_2$. These pairs (γ_1, γ_2) correspond to both $p = 1$ and $p = -1$.

The set $(\gamma_1, \gamma_2, i_1, i_2)$ corresponds to the function

$$\left(\psi^{i_1 i_2}_{\gamma_1 \gamma_2}(c,d) + p(-1)^{l_1+l_2+j}\psi^{i_2 i_1}_{\gamma_2 \gamma_1}(c,d)\right)\exp(i\theta\alpha(r_c, r_d)), \tag{5.3.28}$$

with $\psi^{i_1 i_2}_{\gamma_1 \gamma_2}(c,d)$ given by eq. (5.3.21). To obtain a normalized function $|n\rangle$, we must replace φ_γ by the normalized function $\hat{\varphi}_\gamma$ and we must multiply the function above with

$$\left(\frac{1}{\sqrt{2}}\right)^{1+\delta_{i_1 i_2}\delta_{\gamma_1 \gamma_2}}. \tag{5.3.29}$$

We take α from eq. (5.3.27) with $\beta = 2$:

$$\alpha(r_c, r_d) = \frac{1}{6}\left(r_c^2 - r_d^2\right). \tag{5.3.30}$$

We can now add $|n\rangle$ to the basis unless:

- the parity p of the pair (γ_1, γ_2) does not correspond to the prescribed parity $p_{\rm sec}$ (this cannot happen for $\theta \neq 0$).
- $\gamma_1 = \gamma_2$ and $i_1 > i_2$: this would result in double counting.
- $\gamma_1 = \gamma_2$, $i_1 = i_2$ and $p \neq (-1)^{l_1+l_2+j}$: the function would be null.

5.4 Matrix elements

In this section we will describe the calculation of the matrix elements of $\mathcal{H}$ and of $\mathcal{H}^2$. The hamiltonian $\mathcal{H} = \mathcal{K} + \mathcal{V}$ is given by eq. (5.2.7). Consider first the matrix element

$\langle n'|\mathcal{H}|n\rangle$. For the potential energy $\mathcal{V}$ the phase factor $\exp(i\theta\alpha(r_c,r_d))$ cancels against its complex conjugate. For the kinetic operator we obtain

$$\begin{aligned}
&\exp(-i\theta\alpha(r_c,r_d))\,\mathcal{K}\left(\psi^{i_1i_2}_{\gamma_1\gamma_2}(c,d)\exp(i\theta\alpha(r_c,r_d))\right) = \\
&\quad\frac{f}{2}\left(\gamma_1^2+\gamma_2^2+\frac{L_1(L_1+7)}{r_c^2}+\frac{L_2(L_2+7)}{r_d^2}\right)\psi^{i_1i_2}_{\gamma_1\gamma_2}(c,d) \\
&\quad+\frac{f}{2}\left(-i\theta\,\frac{2}{3}\left(r_c\frac{\partial\varphi_{\gamma_1}(r_c)}{\partial r_c}\varphi_{\gamma_2}(r_d)-\varphi_{\gamma_1}(r_c)r_d\frac{\partial\varphi_{\gamma_2}(r_d)}{\partial r_d}\right)\right)Y^{i_1i_2}(\hat{c},\hat{d}) \\
&\quad+\frac{f}{2}\left(\theta^2\,\frac{1}{9}(r_c^2+r_d^2)\varphi_{\gamma_1}(r_c)\varphi_{\gamma_2}(r_d)\right)Y^{i_1i_2}(\hat{c},\hat{d}).
\end{aligned} \tag{5.4.1}$$

To apply Temple's inequality, we need the matrix elements of $\mathcal{H}^2$. Using the hermiticity of $\mathcal{H}$ we write

$$\begin{aligned}
\langle n'|\mathcal{H}^2|n\rangle &= \langle(\mathcal{K}+\mathcal{V})n'|(\mathcal{K}+\mathcal{V})n\rangle \\
&= \tfrac{1}{2}\langle\mathcal{K}n'|\mathcal{K}n\rangle+\langle n'|\mathcal{V}\mathcal{K}|n\rangle+\tfrac{1}{2}\langle n'|\mathcal{V}^2|n\rangle \\
&\quad+\text{ hermitian conjugate.}
\end{aligned} \tag{5.4.2}$$

From these expressions we can read off which matrix elements we have to calculate.

5.4.1 Angular matrix elements

Since the potential $\mathcal{V}(c,d)$ is invariant under $\vec{L}_c^R$ and $\vec{L}_d^R$ as well as under $\vec{J}^S$, all the terms in $\mathcal{V}$ and $\mathcal{V}^2$ are of the form

$$\mathcal{A}=\langle\hat{c}\hat{d}|0,0,\bar{l}_s;\bar{L}_1,0,\bar{\tau}_1;\bar{L}_2,0,\bar{\tau}_2\rangle. \tag{5.4.3}$$

We will perform the reduction of the matrix elements of this operator to reduced matrix elements.

$$\begin{aligned}
&\langle j',m',i_1',i_2'|\mathcal{A}|j,m,i_1,i_2\rangle \\
&\quad=\langle j',m',l_s';L_1',l_1',\tau_1';L_2',l_2',\tau_2'| \\
&\qquad\left\{|0,0,\bar{l}_s;\bar{L}_1,0,\bar{\tau}_1;\bar{L}_2,0,\bar{\tau}_2\rangle|j,m,l_s;L_1,l_1,\tau_1;L_2,l_2,\tau_2\rangle\right\} \\
&\quad=\sum_{m_1',m_2'}(-1)^{l_1'-l_2'+m'}\sqrt{2j'+1}\begin{pmatrix}l_1' & l_2' & j'\\ m_1' & m_2' & -m'\end{pmatrix}\times \\
&\qquad\sum_{m_1,m_2}(-1)^{l_1-l_2+m}\sqrt{2j+1}\begin{pmatrix}l_1 & l_2 & j\\ m_1 & m_2 & -m\end{pmatrix}\times \\
&\qquad\sum_{m_s',\bar{m}_s,m_s}(-1)^{l_s'-m_s'}\frac{1}{\sqrt{2l_s'+1}}(-1)^{\bar{l}_s-\bar{m}_s}\frac{1}{\sqrt{2\bar{l}_s+1}}(-1)^{l_s-m_s}\frac{1}{\sqrt{2l_s+1}}\times \\
&\qquad\langle L_1';l_s',l_1',\tau_1';m_s',m_1'|\{|\bar{L}_1;\bar{l}_s,0,\bar{\tau}_1;\bar{m}_s,0\rangle|L_1;l_s,l_1,\tau_1;m_s,m_1\rangle\}\times \\
&\qquad\langle L_2';l_s',l_2',\tau_2';-m_s',m_2'|\{|\bar{L}_2;\bar{l}_s,0,\bar{\tau}_2;-\bar{m}_s,0\rangle|L_2;l_s,l_2,\tau_2;-m_s,m_2\rangle\}.
\end{aligned} \tag{5.4.4}$$

We introduce reduced matrix elements through

$$\langle L_1'; l_s', l_1', \tau_1'; m_s', m_1' | \{ | \tilde{L}_1; \tilde{l}_s, 0, \tilde{\tau}_1; \tilde{m}_s, 0 \rangle | L_1; l_s, l_1, \tau_1; m_s, m_1 \rangle \} =$$
$$(-1)^{m_s'+m_1'} \begin{pmatrix} l_s' & \tilde{l}_s & l_s \\ -m_s' & \tilde{m}_s & m_s \end{pmatrix} \begin{pmatrix} l_1' & 0 & l_1 \\ -m_1' & 0 & m_1 \end{pmatrix} \bar{F}(i_1', \tilde{\imath}_1, i_1). \tag{5.4.5}$$

Using

$$\begin{pmatrix} l_1' & 0 & l_1 \\ -m_1' & 0 & m_1 \end{pmatrix} = (-1)^{l_1 - m_1} \frac{1}{\sqrt{2l_1+1}} \delta_{l_1' l_1} \delta_{m_1' m_1}, \tag{5.4.6}$$

the summations over m_1' and m_2' become trivial and we obtain

$$\begin{aligned}
&\langle j', m', i_1', i_2' | \mathcal{A} | j, m, i_1, i_2 \rangle \\
&= \delta_{l_1' l_1} \delta_{l_2' l_2} (-1)^{m+m'} \sqrt{2j'+1} \sqrt{2j+1} \frac{1}{\left[(2l_s'+1)(2\tilde{l}_s+1)(2l_s+1)\right]^{\frac{1}{2}}} \times \\
&\quad (-1)^{l_1+l_2} \frac{1}{\sqrt{2l_1+1}} \frac{1}{\sqrt{2l_2+1}} \bar{F}(i_1', \tilde{\imath}_1, i_1) \bar{F}(i_2', \tilde{\imath}_2, i_2) \times \\
&\quad \left\{ \sum_{m_1, m_2} \begin{pmatrix} l_1 & l_2 & j' \\ m_1 & m_2 & -m' \end{pmatrix} \begin{pmatrix} l_1 & l_2 & j \\ m_1 & m_2 & -m \end{pmatrix} \right\} \times \\
&\quad \left\{ \sum_{m_s', \tilde{m}_s, m_s} (-1)^{l_s'+\tilde{l}_s+l_s} \begin{pmatrix} l_s' & \tilde{l}_s & l_s \\ -m_s' & \tilde{m}_s & m_s \end{pmatrix} \begin{pmatrix} l_s' & \tilde{l}_s & l_s \\ m_s' & -\tilde{m}_s & -m_s \end{pmatrix} \right\} \\
&= \delta_{l_1' l_1} \delta_{l_2' l_2} \delta_{j'j} \delta_{m'm} \delta(l_1, l_2, j) \delta(l_s', \tilde{l}_s, l_s) \frac{F(i_1', \tilde{\imath}_1, i_1) F(i_2', \tilde{\imath}_2, i_2)}{\left[(2l_s'+1)(2\tilde{l}_s+1)(2l_s+1)\right]^{\frac{1}{2}}}.
\end{aligned} \tag{5.4.7}$$

Here we used twice the completeness relation

$$\sum_{m_1 m_2} \begin{pmatrix} j_1 & j_2 & j_3 \\ m_1 & m_2 & m_3 \end{pmatrix} \begin{pmatrix} j_1 & j_2 & j_3' \\ m_1 & m_2 & m_3' \end{pmatrix} = \frac{1}{2j_3+1} \delta_{j_3' j_3} \delta_{m_3' m_3} \delta(j_1, j_2, j_3), \tag{5.4.8}$$

where $\delta(j_1, j_2, j_3) = 1$ if j_1, j_2 and j_3 satisfy the triangular condition, and is zero otherwise. We absorbed the factors $(-1)^{l_i}(2l_i+1)^{-1/2}$ for $i = 1, 2$ in the $\bar{F}$ functions. We can evaluate the F functions by setting in eq. (5.4.5)

$$m_1' = m_1 = l_1, \tag{5.4.9}$$
$$m_s = l_s, \tag{5.4.10}$$
$$m_s' = l_s', \tag{5.4.11}$$
$$\tilde{m}_s = l_s' - l_s. \tag{5.4.12}$$

Thus we find

$$F(i',\bar{\imath},i) = (-1)^{l'_s} \begin{pmatrix} l'_s & \bar{l}_s & l_s \\ -l'_s & l'_s - l_s & l_s \end{pmatrix}^{-1} \times$$
$$\langle L'; l'_s, l'_r, \tau'; l'_s, l'_r | \left\{ |\bar{L}; \bar{l}_s, 0, \bar{\tau}; l'_s - l_s, 0\rangle |L; l_s, l_r, \tau; l_s, l_r\rangle \right\}. \tag{5.4.13}$$

Note that the only dependence of the matrix elements on j is through the triangular condition on l_1, l_2 and j. Also note that the explicit δ functions

$$\delta_{l'_1 l_1}\, \delta_{l'_2 l_2}\, \delta(l'_s, \bar{l}_s, l_s) \tag{5.4.14}$$

are superfluous: they are also contained within the F functions. The $\delta(l_1, l_2, j)$ function can be deleted too: the corresponding triangular condition is satisfied from the beginning.

Specializing to the case where $\mathcal{A}$ only depends on c, we have $\bar{l}_s = 0$ and we can also absorb the factors $(-1)^{l_s}(2l_s+1)^{-1/2}$ in F. We have for instance

$$\langle j', m', i'_1, i'_2 | \operatorname{inv}_3(\bar{c}) | j, m, i_1, i_2\rangle = \delta_{j'j}\delta_{m'm} F_3(i'_1, i_1)\delta(i''_2, i_2), \tag{5.4.15}$$

with

$$F_3(i', i) = \langle L'; l'_s, l'_r, \tau'; l'_s, l'_r | \operatorname{inv}_3(\bar{c}) | L; l_s, l_r, \tau; l_s, l_r\rangle. \tag{5.4.16}$$

We similarly treat $\operatorname{inv}_4(\bar{c})$, $\operatorname{inv}_6(\bar{c})$, $\operatorname{inv}_7(\bar{c})$ and $\operatorname{inv}_8(\bar{c})$ which give rise to the reduced matrix elements F_4, F_6, F_7 and F_8 respectively. Operators that depend only on d and operators that are products of a function of c and of a function of d pose no problems either. We have for instance

$$\langle j', m', i'_1, i'_2 | \operatorname{inv}_3(\bar{d}) | j, m, i_1, i_2\rangle = \delta_{j'j}\delta_{m'm}\delta(i''_1, i_1) F_3(i'_2, i_2), \tag{5.4.17}$$

and

$$\langle j', m', i'_1, i'_2 | \operatorname{inv}_3(\bar{c}) \operatorname{inv}_3(\bar{d}) | j, m, i_1, i_2\rangle = \delta_{j'j}\delta_{m'm} F_3(i'_1, i_1) F_3(i'_2, i_2). \tag{5.4.18}$$

The operator $\operatorname{inv}_2(c, d)$ is treated with the general formulae eq. (5.4.7) and (5.4.13). One can show

$$\operatorname{inv}_2(\bar{c}, \bar{d}) = \tfrac{1}{9} - \tfrac{1}{99}\sqrt{5}\langle \bar{c}\bar{d} | 0, 0, 2; 2, 0, 1; 2, 0, 1\rangle. \tag{5.4.19}$$

Using eq. (5.4.13) we define

$$F_{22}(i', i) = (-1)^{l'_s} \begin{pmatrix} l'_s & 2 & l_s \\ -l'_s & l'_s - l_s & l_s \end{pmatrix}^{-1} \times$$
$$\langle L'; l'_s, l'_r, \tau'; l'_s, l'_r | \{ |2; 2, 0, 1; l'_s - l_s, 0\rangle |L; l_s, l_r, \tau; l_s, l_r\rangle \}, \tag{5.4.20}$$

and we obtain

$$\langle j', m', i''_1, i''_2 | \operatorname{inv}_2(\bar{c}, \bar{d}) | j, m, i_1, i_2\rangle =$$
$$\delta_{j'j}\delta_{m'm} \left\{ \tfrac{1}{9}\delta(i'_1, i_1)\delta(i'_2, i_2) - \tfrac{1}{99} \frac{F_{22}(i'_1, i_1) F_{22}(i'_2, i_2)}{[(2l'_s+1)(2l_s+1)]^{\frac{1}{2}}} \right\}. \tag{5.4.21}$$

For products like $\mathrm{inv}_3(c)\,\mathrm{inv}_2(c,d)$ we obtain

$$\langle j',m',i'_1,i'_2|\,\mathrm{inv}_3(\bar{c})\,\mathrm{inv}_2(\bar{c},\bar{d})|j,m,i_1,i_2\rangle = \delta_{j'j}\delta_{m'm}\left\{\tfrac{1}{9}F_3(i'_1,i_1)\delta(i'_2,i_2) - \frac{1}{99}\frac{F_{52}(i'_1,i_1)F_{22}(i'_2,i_2)}{[(2l'_s+1)(2l_s+1)]^{\frac{1}{2}}}\right\}, \tag{5.4.22}$$

with

$$F_{52}(i',i) = (-1)^{l'_s}\begin{pmatrix} l'_s & 2 & l_s \\ -l'_s & l'_s-l_s & l_s\end{pmatrix}^{-1}\times$$
$$\langle L';l'_s,l'_r,\tau';l'_s,l'_r|\,\{\mathrm{inv}_3(\bar{c})|2;2,0,1;l'_s-l_s,0\rangle|L;l_s,l_r,\tau;l_s,l_r\rangle\}\,. \tag{5.4.23}$$

Similarly the operator $\mathrm{inv}_3(c)\,\mathrm{inv}_2(c,d)$ leads to the reduced matrix element F_{62}.

The only operator in $\mathcal{V}^2$ that we have yet to deal with is $\mathrm{inv}_2^2(c,d)$. For this operator we need to construct the spectral decomposition. We write

$$\begin{aligned}\mathrm{inv}_2^2(\bar{c},\bar{d}) \;=\;& a\,|0,0,4;4,0,1;4,0,1\rangle + b\,|0,0,2;4,0,1;4,0,1\rangle\\ &+c\,|0,0,0;4,0,1;4,0,1\rangle + d\,|0,0,2;2,0,1;2,0,1\rangle\\ &+e\,(|0,0,2;4,0,1;2,0,1\rangle + |0,0,2;2,0,1;4,0,1\rangle)\\ &+f\,(|0,0,0;4,0,1;0,0,1\rangle + |0,0,0;0,0,1;4,0,1\rangle)\\ &+g\,|0,0,0;0,0,1;0,0,1\rangle.\end{aligned} \tag{5.4.24}$$

Using the explicit formulae for the corresponding polynomials, we solve for the coefficients $a,\ldots,g$. The new reduced matrix elements we need are F_{44}, F_{42} and F_{40} for the operators with $(\bar{L},\bar{l}_s,\bar{l}_r)$ respectively $(4,4,0)$, $(4,2,0)$ and $(4,0,0)$. The function F_{40} can be obtained from F_4 using the relation

$$\mathrm{inv}_4(\bar{c}) = \tfrac{1}{22} + \tfrac{1}{22}\sqrt{\tfrac{5}{39}}|4;0,0,1;0,0\rangle. \tag{5.4.25}$$

The result is

$$\langle j',m',i'_1,i'_2|\,\mathrm{inv}_2^2(\bar{c},\bar{d})|j,m,i_1,i_2\rangle = \delta_{j'j}\delta_{m'm}\left\{\frac{A}{[(2l'_s+1)(2l_s+1)]^{\frac{1}{2}}} + B\right\}, \tag{5.4.26}$$

with

$$\begin{aligned}A \;=\;& \tfrac{2}{11583}F_{44}(i'_1,i_1)F_{44}(i'_2,i_2)\\ &+\tfrac{4}{50193}F_{42}(i'_1,i_1)F_{42}(i'_2,i_2) - \tfrac{4}{1859}F_{22}(i'_1,i_1)F_{22}(i'_2,i_2)\\ &-\tfrac{1}{1859}\sqrt{\tfrac{56}{2187}}(F_{42}(i'_1,i_1)F_{22}(i'_2,i_2) + F_{22}(i'_1,i_1)F_{42}(i'_2,i_2)),\end{aligned} \tag{5.4.27}$$

$$\begin{aligned}B \;=\;& \tfrac{16}{45}F_4(i'_1,i_1)F_4(i'_2,i_2) - \tfrac{4}{135}(F_4(i'_1,i_1)\delta(i'_2,i_2) + \delta(i'_1,i_1)F_4(i'_2,i_2))\\ &+\tfrac{2}{135}\delta(i'_1,i_1)\delta(i'_2,i_2).\end{aligned} \tag{5.4.28}$$

5.4.2 Radial matrix elements

The radial integrals we need to compute are

$$J(n,\gamma',\gamma) = \int_0^{\sqrt{3}} dr\, r^n \hat{\varphi}_{\gamma'}(r)\bar{\varphi}_\gamma(r), \tag{5.4.29}$$

$$J_l(n,\gamma',\gamma) = \int_0^{\sqrt{3}} dr\, r^n \hat{\varphi}_{\gamma'}(r)\left(r\frac{\partial}{\partial r}\bar{\varphi}_\gamma(r)\right), \tag{5.4.30}$$

$$J_{ll}(n,\gamma',\gamma) = \int_0^{\sqrt{3}} dr\, r^n \left(r\frac{\partial}{\partial r}\hat{\varphi}_{\gamma'}(r)\right)\left(r\frac{\partial}{\partial r}\bar{\varphi}_\gamma(r)\right), \tag{5.4.31}$$

where $\bar{\varphi}_\gamma$ is normalized to one, and

$$\varphi_\gamma(r) = \gamma r j_3(\gamma r) = f(\gamma r), \tag{5.4.32}$$

$$f(z) = \left(1-\frac{15}{z^2}\right)\cos(z) + \left(-\frac{6}{z}+\frac{15}{z^3}\right)\sin(z). \tag{5.4.33}$$

Consider the integral for non-normalized φ functions and let $\alpha = \sqrt{3}\gamma$ and $\alpha' = \sqrt{3}\gamma'$. For an explicit value of n, but unspecified values of γ' and γ, we write

$$\begin{aligned}\bar{J}(n) &= \int_0^{\sqrt{3}} dr\, r^n \varphi_{\gamma'}(r)\varphi_\gamma(r) \\ &= (\sqrt{3})^{n+1}\int_0^1 dx\, x^n f(\alpha' x) f(\alpha x).\end{aligned} \tag{5.4.34}$$

We express products of sines and cosines of αx and $\alpha' x$ in sines and cosines of sx and vx with $s = \alpha' + \alpha$ and $v = \alpha' - \alpha$. The integrand as it stands is regular at $x = 0$, but individual terms need not be. We therefore introduce a cut-off ε, after which the integral is a sum of functions

$$\cos(m,a) = \int_\varepsilon^1 dx\, x^m \cos(ax), \tag{5.4.35}$$

$$\sin(m,a) = \int_\varepsilon^1 dx\, x^m \sin(ax). \tag{5.4.36}$$

Partial integration gives us the following recursion relations

$$\cos(m,a) = \begin{cases} \frac{1}{a}\left(\sin(a) - m\sin(m-1,a)\right) & m \geq 0 \\ \mathrm{Ci}(a) - \ln(a) - \gamma_E - \ln(\varepsilon) & m = -1 \\ \frac{1}{m+1}\left(\cos(a) - \varepsilon^{m+1}\cos(\varepsilon a) + a\sin(m+1,a)\right) & m < -1 \end{cases} \tag{5.4.37}$$

$$\sin(m,a) = \begin{cases} \frac{1}{a}\left(-\cos(a) + \delta_{m0} + m\cos(m-1,a)\right) & m \geq 0 \\ \mathrm{Si}(a) & m = -1 \\ \frac{1}{m+1}\left(\sin(a) - \varepsilon^{m+1}\sin(\varepsilon a) - a\cos(m+1,a)\right) & m < -1 \end{cases} \tag{5.4.38}$$

After eliminating the functions $\cos(m,a)$ and $\sin(m,a)$ and taking the limit $\varepsilon \downarrow 0$, the result is an expression in the functions sin, cos, Si, Ci and ln of the variables s and

v. By substituting values for s and v and performing the normalization we construct tables for $J(n, \gamma', \gamma)$. Note that we have to be careful for $\alpha' = \alpha$: we have to take the limit $v \to 0$ before substituting actual values.

The other integrals can be obtained as follows:

$$\begin{aligned}
\tilde{J}_l(n) &= \int_0^{\sqrt{3}} dr\, r^n \varphi_{\gamma'}(r) \left(r \frac{\partial}{\partial r} \varphi_\gamma(r) \right) \\
&= (\sqrt{3})^{n+1} \int_0^1 dx\, x^n f(\alpha' x) \left(x \frac{\partial}{\partial x} f(\alpha x) \right) \\
&= \alpha \frac{\partial}{\partial \alpha} \tilde{J}(n) \\
&= \frac{s-v}{2} \left(\frac{\partial}{\partial s} - \frac{\partial}{\partial v} \right) \tilde{J}(n). \qquad (5.4.39)
\end{aligned}$$

In a similar way we arrive at

$$\tilde{J}_{ll}(n) = \frac{s^2 - v^2}{4} \left(\frac{\partial^2}{\partial s^2} - \frac{\partial^2}{\partial v^2} \right) \tilde{J}(n). \qquad (5.4.40)$$

5.5 Weak coupling expansion

In this section we will perform the perturbative calculation of the energy levels of the hamiltonian. The results will serve as a check on the variational calculation in the regime of small coupling constant. Starting from the strong coupling basis, we could also develop a perturbation theory in $\frac{1}{f}$, but there are two reasons why this is less interesting. First, we are interested in the region where we just start to see the deviations from perturbative behaviour in f. Second, since our variational basis is in essence a strong coupling basis, the reproduction of the strong coupling limit does not give a strong check on the variational calculation.

For the weak coupling limit, we rescale $x_c = \sqrt{\frac{2}{f}} r_c$ and $x_d = \sqrt{\frac{2}{f}} r_d$ and we split the hamiltonian of eq. (5.2.7) in $\mathcal{H} = \mathcal{H}_0 + \mathcal{H}_1$, with

$$\mathcal{H}_0 = -\left(\frac{\partial^2}{\partial x_c^2} + \frac{\partial^2}{\partial x_d^2} - 12 \left(\frac{1}{x_c^2} + \frac{1}{x_d^2} \right) + \frac{1}{x_c^2} \Delta_{\hat{c}} + \frac{1}{x_d^2} \Delta_{\hat{d}} \right) + x_c^2 + x_d^2, \qquad (5.5.1)$$

$$\mathcal{H}_1(c,d) = \mathcal{H}_1(c) + \mathcal{H}_1(d) + \lambda_7 \left(\frac{f}{2} \right)^2 x_c^2 x_d^2 + \lambda_8 \left(\frac{f}{2} \right)^2 x_c^2 x_d^2 \, \mathrm{inv}_2(\hat{c}, \hat{d}), \qquad (5.5.2)$$

$$\begin{aligned}
\mathcal{H}_1(c) &= \left(\tfrac{f}{2} \lambda_1 - 1 \right) x_c^2 + \left(\frac{f}{2} \right)^{\frac{3}{2}} \lambda_2 x_c^3 \, \mathrm{inv}_3(\hat{c}) + \left(\frac{f}{2} \right)^2 \lambda_3 x_c^4 \\
&\quad + \left(\frac{f}{2} \right)^2 \lambda_4 x_c^4 \, \mathrm{inv}_4(\hat{c}) + \left(\frac{f}{2} \right)^{\frac{5}{2}} \lambda_5 x_c^5 \, \mathrm{inv}_3(\hat{c}) + \left(\frac{f}{2} \right)^3 \lambda_6 x_c^6. \qquad (5.5.3)
\end{aligned}$$

5.5.1 The unperturbed problem

The eigenvalue problem for $\mathcal{H}_0$ leads to the following one-dimensional eigenvalue problem:

$$\left(\frac{\partial^2}{\partial x^2} + \lambda - \frac{12 + L(L+7)}{x^2} - x^2\right)\varphi(x) = 0. \tag{5.5.4}$$

The regular solution of this equation is [35]

$$\varphi(x) = e^{-\frac{1}{2}x^2} x^{L+4} {}_1F_1(-\frac{\lambda - 2L - 9}{4}, L + \frac{9}{2}, x^2), \tag{5.5.5}$$

with ${}_1F_1$ the confluent hypergeometric function. As in the strong coupling case, we can use the boundary conditions at $x = \sqrt{\frac{6}{f}}$ to discretize the possible values for λ and hence the energy. This will give us an alternative to the strong coupling basis constructed above. Disadvantages of this basis are that the functions themselves depend on the coupling constant f. Also the matrix elements of operators between two confluent hypergeometric functions are hard to calculate. For the variational method, we will therefore use the strong coupling basis.

We can however use the weak coupling basis for perturbation purposes. For $f \downarrow 0$ the location where the boundary conditions have to be imposed moves away to infinity, which is equivalent to saying that the wave function, in the original coordinates, is strongly localized around $c = d = 0$. We can replace the boundary conditions at $x = \sqrt{\frac{6}{f}}$ by demanding normalizability of the functions $\varphi(x)$. This means that the ${}_1F_1$ function must reduce to a polynomial, which is the case if its first argument is $-n$ with $n = 0, 1, \ldots$. The ${}_1F_1$ function then reduces to a Laguerre polynomial

$${}_1F_1(-n, L + \tfrac{9}{2}, x^2) \propto L_n^{(L+\frac{7}{2})}(x^2), \tag{5.5.6}$$

and we obtain the discretization $\lambda = 9 + 2L + 4n$. The weak coupling eigenfunctions are thus

$$\psi^{i_1 i_2}_{n_1 n_2} = L_{n_1}^{(L_1+\frac{7}{2})}(x_c^2) L_{n_2}^{(L_2+\frac{7}{2})}(x_d^2) x_c^{(L_1+4)} x_d^{(L_2+4)} e^{-\frac{1}{2}x_c^2} e^{-\frac{1}{2}x_d^2} Y^{i_1 i_2}(\hat{c}, \hat{d}), \tag{5.5.7}$$

and the energies are given by

$$E = 18 + 2(L_1 + L_2) + 4(n_1 + n_2). \tag{5.5.8}$$

5.5.2 Weak coupling perturbation theory

Bloch perturbation theory [31] was used already in chapter 4 without much explanation. Since we need some details on the method here, we give a short sketch of the method. Suppose we have a hamiltonian $H = H_0 + H_1$, where we will treat H_1 as a perturbation. Let E_0 be some eigenvalue of H_0 and let P_0 be the projector on the corresponding eigenspace Ω_0. We define the operator $\mathcal{U}$ by

$$\mathcal{U} = \mathcal{U}^{(0)} + \mathcal{U}^{(1)} + \mathcal{U}^{(2)} + \ldots \tag{5.5.9}$$

where $\mathcal{U}^{(n)}$ is of order n in H_1 and is defined recursively by

$$\mathcal{U}^{(0)} = P_0, \tag{5.5.10}$$

$$\mathcal{U}^{(n)} = \frac{Q_0}{a}\left[H_1\mathcal{U}^{(n-1)} - \sum_{p=1}^{n-1}\mathcal{U}^{(p)}H_1\mathcal{U}^{(n-p-1)}\right]. \tag{5.5.11}$$

Here we set $Q_0 = \mathbb{1} - P_0$, and $a = H_0 - E_0$. Consider the operator $P_0H_1\mathcal{U}$. This operator is defined on Ω_0 and its eigenvalues are the corrections to the unperturbed eigenvalue E_0.

We now turn to the weak coupling expansion of our hamiltonian. For this we need the matrix elements of $\mathcal{H}_I$ w.r.t. the basis of eq. (5.5.7). The angular integrations have already been treated. The radial integrals take the form

$$\int_0^\infty dx\, x^n e^{-x^2} x^{L'+4} x^{L+4} L_{n'}^{(L'+\frac{7}{2})}(x^2) L_n^{(L+\frac{7}{2})}(x^2). \tag{5.5.12}$$

We calculate these integrals by substituting the explicit form of the Laguerre polynomials.

We will argue that the number of intermediate levels (the levels on which Q_0 projects) that we have to take into account is finite; moreover, for perturbation up to $\mathcal{O}(f^3)$, all the levels needed are contained in the truncated bases that we used. A similar restriction cannot be given when using the strong coupling basis: Bloch perturbation theory for this case would hence be more complicated.

First note that although we are constructing a perturbative expansion in $\sqrt{f}$, the result of the Bloch perturbation theory will be an expansion in f, as can be seen by parity arguments. Each factor of $\mathcal{H}_I$ contributes at least a factor $\sqrt{f}$, so for $\mathcal{O}(f^3)$ precision, we need therefore not go beyond $\mathcal{U}^{(3)}$, which corresponds to four factors of $\mathcal{H}_I$. Also note that the final contribution from the terms in $\mathcal{H}_I$ corresponding to λ_5 and λ_6 will be of $\mathcal{O}(f^3)$ and we can remove them from the effective perturbation.

Consider the matrix element

$$\mathcal{M} = \langle n_1', n_2', i_1', i_2'|\mathcal{H}_I|n_1, n_2, i_1, i_2\rangle, \tag{5.5.13}$$

with the functions $|n_1, n_2, i_1, i_2\rangle$ given by eq. (5.5.7), and their energies E and E' given by eq. (5.5.8). We will prove:

$$|L_1' - L_1| > 4 \;\Rightarrow\; \mathcal{M} = 0, \tag{5.5.14}$$

$$|L_2' - L_2| > 4 \;\Rightarrow\; \mathcal{M} = 0, \tag{5.5.15}$$

$$|E' - E| > 8 \;\Rightarrow\; \mathcal{M} = 0. \tag{5.5.16}$$

The angular functions in $\mathcal{H}_I$ have $L \leq 4$, so the first two claims are a direct consequence of the triangular condition. Consider a term in $\mathcal{H}_I$ with a $x_c^{\alpha_1}$ behaviour. A possible dependence on $\hat{c}$ of this term will be through a function with $\tilde{L}_1 \leq \alpha_1$ and with $\alpha_1 - \tilde{L}_1$ even.

Let us assume that $n_1 \geq n_1'$. The integration over $\hat{c}$ will imply that $L_1' + L_1 + \tilde{L}_1$ is even and the triangular condition will imply $|L_1' - L_1| \leq \tilde{L}_1 \leq \alpha_1$. Combining this

leads to $\beta = (L_1' - L_1 + \alpha_1)/2 \geq 0$ and β integer. The radial integral over x_c will be proportional to

$$\int_0^\infty dy\, e^{-y} y^{\frac{7}{2}+L_1} L_{n_1}^{\frac{7}{2}+L_1}(y) y^\beta L_{n_1'}^{\frac{7}{2}+L_1'}(y). \tag{5.5.17}$$

The product of the last two factors is a polynomial in y with the highest power of y being given by $\beta + n_1'$. From the orthogonality of the Laguerre polynomials, we conclude that the integral is zero if $n_1 > n_1' + \beta$, which is equivalent to $2(n_1 - n_1') + L_1 - L_1' > \alpha_1$. If we had assumed $n_1' \geq n_1$, the condition for the vanishing of the integral would have been $2(n_1' - n_1) + L_1' - L_1 > \alpha_1$. Combining these two cases leads to the condition $|\Delta E_1| > 2\alpha_1$.

For each term in the effective $\mathcal{H}_1$ (i.e. without the λ_5 and λ_6 terms), we have $\alpha_1 + \alpha_2 \leq 4$. The condition $|\Delta E| > 8$ then allows us to write

$$|\Delta E_1| + |\Delta E_2| \geq |\Delta E| > 8 \geq 2(\alpha_1 + \alpha_2), \tag{5.5.18}$$

hence we have

$$|\Delta E_1| > 2\alpha_1 \text{ or } |\Delta E_2| > 2\alpha_2, \tag{5.5.19}$$

and the matrix element vanishes.

The $E = 18$ eigenspace consists of only one function, which has $L_1 = L_2 = 0$. The only contribution, up to $\mathcal{O}(f^3)$, from $\mathcal{U}^{(3)}$ will be through terms in $\mathcal{H}_1$ that are proportional to $\sqrt{f}$. These interaction terms have $\alpha_1 + \alpha_2 \leq 3$ and the maximum possible change per step for E and L becomes respectively six and three. After taking four steps, i.e. after visiting three intermediate levels, we must return to the original level. The highest intermediate E and L values that can be reached are thus

$$E_{\max} = 18 + 6 + 6 = 30, \tag{5.5.20}$$
$$L_{\max} = 0 + 3 + 3 = 6. \tag{5.5.21}$$

One checks that the contributions from $\mathcal{U}^{(1)}$ and $\mathcal{U}^{(2)}$ cannot go beyond these limits. For the two-dimensional $E = 22$ eigenspace in the same sector (i.e. 000), we have

$$E_{\max} = 22 + 6 + 6 = 34, \tag{5.5.22}$$
$$L_{\max} = 0 + 3 + 3 = 6. \tag{5.5.23}$$

Note that we could use the parity symmetry to split this problem in two one-dimensional problems. The $E = 22$ level in the sector 112-even is one dimensional and consists of a function with $L_1 = L_2 = 1$. Hence we have

$$E_{\max} = 22 + 6 + 6 = 34, \tag{5.5.24}$$
$$L_{\max} = 1 + 3 + 3 = 7. \tag{5.5.25}$$

The reason to restrict us to these levels, is that they will turn out to correspond to the lowest glueball masses. For each of these levels we construct the finite matrix of $\mathcal{H}_1$ with respect to the functions that satisfy the limits on E and L. We then calculate

the Bloch matrix $P_0\mathcal{H}_1\mathcal{U}$ to obtain the perturbative expansion for the eigenvalue. We obtain the following results:

$$E^{(0)}_{000\text{-even}} = 18 + f\left(\frac{9}{8} + \frac{9}{2}\kappa_1\right) + f^2\left(\frac{63}{512} - \frac{9}{16}\kappa_1{}^2 - \frac{3}{8}\kappa_2 + \frac{99}{8}\kappa_3 + \frac{63}{8}\kappa_4 + \frac{81}{16}\kappa_7 + \frac{27}{16}\kappa_8\right) + \mathcal{O}\left(f^3\right), \quad (5.5.26)$$

$$E^{(1)}_{000\text{-even}} = 22 + f\left(-\frac{9}{8} + \frac{11}{2}\kappa_1\right) + f^2\left(\frac{903}{512} + 3\kappa_1 - \frac{11}{16}\kappa_1{}^2 - \frac{13}{8}\kappa_2 + \frac{165}{8}\kappa_3 + \frac{105}{8}\kappa_4 + \frac{135}{16}\kappa_7 + \frac{45}{16}\kappa_8\right) + \mathcal{O}\left(f^3\right), \quad (5.5.27)$$

$$E^{(0)}_{000\text{-odd}} = 22 + f\left(-\frac{13}{8} + \frac{11}{2}\kappa_1\right) + f^2\left(\frac{1063}{512} + \frac{13}{4}\kappa_1 - \frac{11}{16}\kappa_1{}^2 - \frac{13}{8}\kappa_2 + \frac{165}{8}\kappa_3 + \frac{165}{8}\kappa_4 + \frac{99}{16}\kappa_7 + \frac{33}{16}\kappa_8\right) + \mathcal{O}\left(f^3\right), \quad (5.5.28)$$

$$E^{(0)}_{112\text{-even}} = 22 + f\left(\frac{13}{24} + \frac{11}{2}\kappa_1\right) + f^2\left(\frac{3167}{4608} + \frac{25}{24}\kappa_1 - \frac{11}{16}\kappa_1{}^2 - \frac{7}{8}\kappa_2 + \frac{143}{8}\kappa_3 + \frac{91}{8}\kappa_4 + \frac{121}{16}\kappa_7 + \frac{47}{16}\kappa_8\right) + \mathcal{O}\left(f^3\right). \quad (5.5.29)$$

5.6 Results

With the results of the previous section, we are in a position to actually perform the variational calculation. We constructed a FORTRAN programme which as input requires the sector $l_1 l_2 j$, the parity $p_{\text{sec}} = \pm 1$ for the case $\theta = 0$, and the limits N_{rad} and L_{sum}. Using the last two numbers, the truncated basis is constructed. The reduced angular matrix elements F and the radial integrals J are read from files. Also the values for f and θ are read from input files and the hamiltonian is constructed. Note that the angular matrix elements are independent of the value of j. The construction of the basis only depends on j through the number $(-1)^{l_1+l_2+j}$. As a result, we have that for instance the scalar and tensor sectors 110 and 112 are completely degenerate.

For the case $\theta = 0$ the hamiltonian is real, and we performed the diagonalization using routines from the Nag-library. For $\theta \neq 0$ we used diagonalization routines from the Eispack library. The output consisted of the upper bounds $\tilde{\mu}_n$ for the lowest energy eigenvalues and of the corresponding values for η. These will be presented shortly.

We also produced graphical representations of the wave function. These can be used in verifying a posteriori whether the assumption is true that the boundary conditions are only felt at the sphalerons.

5.6.1 Lowest-order hamiltonian

We start by considering the lowest order results. An overview of the lowest energy levels for $\theta = 0$ in the various sectors is given in fig. 5-1. For clarity, we did not plot the lower bounds on the levels. From the spectrum, we see that the lowest glueball masses are to be found in the sectors 000-even, 000-odd and 112-even for respectively the scalar and the tensor glueballs. We reinstated the R dependence

J	000-even	
	γ	η
0.08	18.0908	0.00106
	21.9218	0.034
	24.0215	0.0465
0.1	18.1137	4.67e-05
	21.9047	0.00222
	24.0205	0.0191
0.125	18.1425	4.76e-05
	21.8860	0.00483
	24.0160	0.0411
0.15	18.1715	8.96e-05
	21.8694	0.00978
	24.0057	0.0857
0.175	18.2006	0.000159
	21.8546	0.0185
	23.9840	0.195
0.2	18.2299	0.000269
	21.8396	0.0364
	23.9172	0.548
0.225	18.2592	0.000448
	21.8165	0.076
	23.7221	1.21
0.25	18.2884	0.000521
	21.7642	0.125
	23.4259	1.26
0.3	18.3438	0.00129
	21.4943	0.238
	23.1291	0.618
0.35	18.3819	0.00274
	21.1036	0.173
	23.2513	0.281
0.4	18.3715	0.0048
	20.7847	0.0954
	23.3721	0.176
0.45	18.2713	0.00746
	20.5807	0.0559
	22.9356	0.157
0.5	18.0569	0.0107
	20.4505	0.0398
	22.5930	0.0901
0.6	17.3489	0.0175
	20.2528	0.0281
	22.6566	0.0381
0.7	16.5009	0.0224
	20.2249	0.0223
	22.2227	0.0399
0.8	15.7101	0.0245
	20.4066	0.0188
	21.9580	0.0346

J	000-odd	
	γ	η
0.08	21.8859	0.0411
	24.0612	0.352
0.1	21.8572	0.00139
	24.0176	0.0153
0.15	21.7998	0.0067
	24.0009	0.074
0.2	21.7528	0.0173
	23.9805	0.164
0.225	21.7377	0.0214
	24.0032	0.168
0.25	21.7351	0.021
	24.0669	0.137
0.275	21.7521	0.0183
	24.1689	0.103
0.3	21.7948	0.0148
	24.2978	0.0866
0.325	21.8669	0.00958
	24.4418	0.0506
0.35	21.9704	0.00711
	24.5970	0.0331
0.4	22.2709	0.00504
	24.9399	0.0166
0.45	22.6891	0.00461
	25.3409	0.00983
0.5	23.2123	0.00477
	25.8136	0.00701

J	112-even	
	γ	η
0.1	22.0620	0.0232
	24.0740	0.0972
0.15	22.0990	0.0287
	24.1204	0.198
0.2	22.1406	0.0572
	24.1737	0.344
0.25	22.1845	0.108
	24.2245	0.6
0.3	22.1959	0.103
	24.0590	0.456
0.35	22.1247	0.095
	23.8186	0.497
0.4	21.8983	0.115
	23.5788	0.433
0.45	21.5210	0.126
	23.2763	0.385
0.5	21.0556	0.113
	22.8994	0.291
0.55	20.5711	0.0928
	22.4949	0.23
0.6	20.1129	0.0748
	22.0971	0.148
0.65	19.7017	0.0642
	21.7446	0.115
0.7	19.3443	0.0582
	21.4502	0.0928
0.75	19.0407	0.0546
	21.2167	0.0778
0.8	18.7884	0.0519
	21.0412	0.0698
0.9	18.4232	0.047
	20.8443	0.0636
1	18.2184	0.042
	20.8190	0.0588
1.2	18.1831	0.0323
	21.1591	0.0671
1.4	18.5134	0.0239
	21.8762	0.0764
1.6	19.0985	0.0174
	22.8567	0.0431
1.8	19.8661	0.0125
	24.0288	0.0715
2	20.7681	0.00903
	25.3401	0.0312

Table 5-8. Raw data for the lowest levels in the sectors 000-even, 000-odd and 112-even.

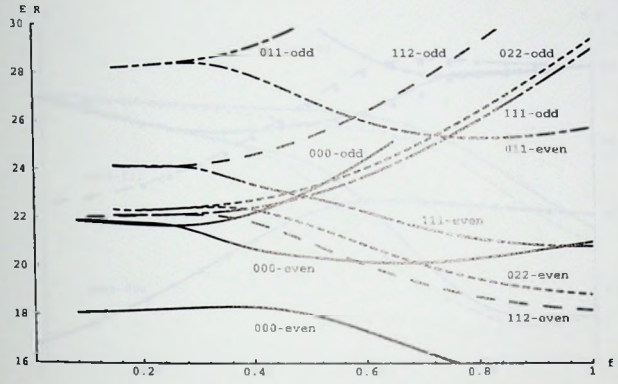

Figure 5-1. Lowest energy levels in various sectors. Going up at $f = 0.6$ we have:
Drawn curves: 000-even, 000-even, 000-odd.
Dashed curves: 112-even, 022-even, 022-odd, 112-odd.
Long-short dashed curves: 111-even, 111-odd, 011-even, 011-odd.

using dimensional arguments. Note that the crossing of levels only happens for levels that are in different sectors. States within the same sector would exhibit avoided level crossing due to level repulsion.

The raw data for these sectors is given in table 5-8. The corresponding levels, including the lower bounds and the perturbative expansions, are plotted in fig. 5-2. For small coupling, the deviations of the wave function from the perturbative one will be small. To reproduce the energy eigenvalues correctly, we can suffice with a relatively low number of angular functions, but to be able to accommodate the strong localization around $c = d = 0$, we need a large number of radial functions. For larger values of f we can reduce the number of radial functions, but we must increase the number of angular functions. The data in table 5-8 was obtained by combining different runs with various choices for the truncated basis as controlled by the parameters N_{rad} and L_{sum}.

In the 000-even sector we maximally used $N_{\mathrm{rad}} = 150$ and $L_{\mathrm{sum}} = 10$ for small f, and $N_{\mathrm{rad}} = 50$ and $L_{\mathrm{sum}} = 14$ for larger values of f. These values correspond to bases consisting of over 3000 vectors. Increasing the number of basis vectors becomes quickly limited by the amount of free memory available in the computer. A 3000 by 3000 matrix of double precision reals takes up roughly 72 Mbytes. For the case $\theta \neq 0$, the hamiltonian is complex and we need a factor of two more memory. In the

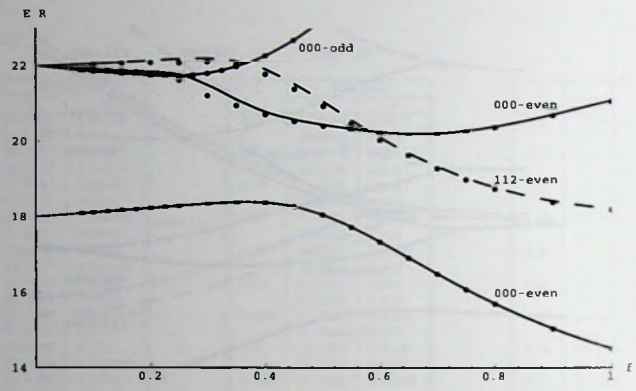

Figure 5-2. Lowest energy levels for $\theta = 0$. Drawn curves correspond to levels in the $(0,0,0)$ sector. The dashed curve denotes the ground level in the $(1,1,2)$-even sector. The short-dashed curves are the perturbative expansions, and the individual dots are lower bounds on the levels as obtained by Temple's inequality.

112-even sector, the same number for $L_{\rm sum}$ resulted in higher numbers of angular functions. Here we went up to $N_{\rm rad} = 150$ and $L_{\rm sum} = 8$ for small f, and $N_{\rm rad} = 30$ and $L_{\rm sum} = 12$ for larger values of f.

We did most of the calculations on Sun workstations. For some values of f we wanted more accurate results and used computer time on a Cray YMP. We also developed a pruning technique: after diagonalization, we examine the variational wave function obtained for, say, the ground state. We replace those basis vectors (roughly ten to twenty percent) that have a small coefficient in this wave function by new basis vectors and repeat the diagonalization. Repeating this procedure allows us to sample a larger variational basis, but we do not have the guarantee that the results will improve in this way: it is possible that the true wave function has substantial overlap with very many vectors in our basis.

Returning to our calculation, the lowest-lying scalar ($j = 0$) and tensor ($j = 2$) levels are found in respectively the sectors 000 and 112. For $\theta = 0$, the vacuum corresponds to the ground state of the 000-even sector. The scalar glueball 0^+ can be identified with the first excited state in the 000-even sector, the tensor glueball 2^+ with the ground state in the 112-even sector. Note that at $f = 0.6$ these levels cross, thus making the scalar glueball heavier than the tensor. We do however not expect our model to be valid anymore for these values of the coupling constant.

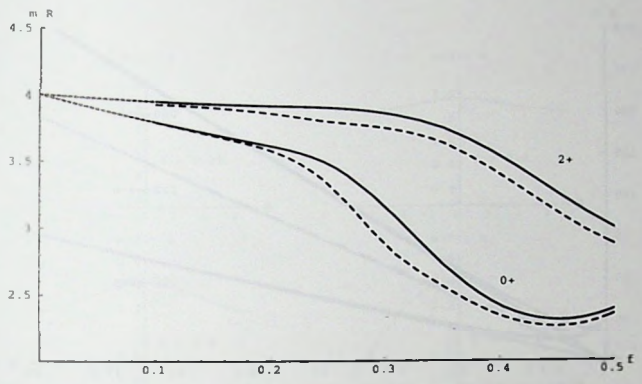

Figure 5-3. Glueball masses for $\theta = 0$ as a function of the coupling constant. The lower and upper drawn curves are the masses of resp. the first scalar (0^+) and tensor (2^+) glueball. The dashed lines denote the lower bounds, the dotted lines the perturbative results.

Taking differences of the energy levels with respect to the ground state in the 000-even sector gives us the masses of the low-lying glueball states (fig. 5-3). To check on the strong coupling results, we also performed variational calculations for large values of f. The comparison with the results of table 5-7 can be seen in fig. 5-4.

For small f, there is virtually no dependence of the masses on θ, whereas for larger f the θ dependence becomes bigger. This is shown in fig. 5-5. For $\theta = \pi$ we can impose the boundary conditions exactly, that is, without using the trick with the Cherns-Simons like operator, but with the same method that we imposed the $\theta = 0$ conditions. The variational results obtained in this way are also plotted in fig. 5-5. Remember that a θ dependence is a sign that the boundary in the (r_c, r_d) plane is felt. Our model is valid for values of the coupling constant at which only the boundary conditions at and near the sphalerons are felt. Checking this a posteriori with the help of plots of the wave function (fig. 5-6) indicates that f should not be larger than roughly 0.5. These plots were obtained as follows. Consider the function

$$|\psi(r_c, r_d)|^2 = \int d\hat{c}\, d\hat{d}\, |\psi(c, d)|^2, \tag{5.6.1}$$

which is a measure of the probability distribution in the (r_c, r_d) plane (see fig. 5-7). Dividing this $|\psi(r_c, r_d)|$ by $r_c^4 r_d^4$, we obtain a function with the expected behaviour of the true wave function: it is localized at the sphalerons and decays exponentially in the transverse directions (see fig. 5-6). Note that the characteristic width grows

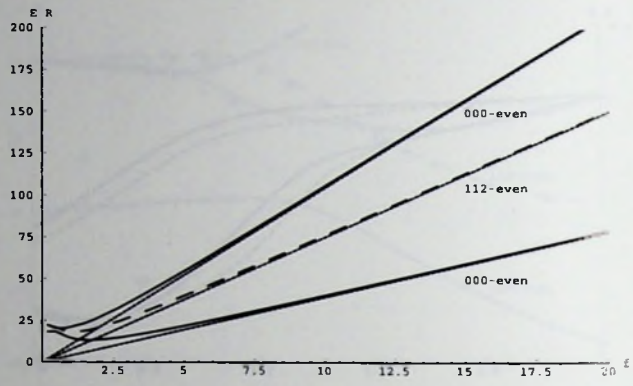

Figure 5-4. Strong coupling limit, $\theta = 0$: the drawn and dashed lines are the variational results for the lowest levels in the sectors 000-even and 112-even respectively. The dotted lines represent the analytic strong coupling limit.

with increasing f. Although the lowest barrier is the sphaleron, the measure factor $r_c^4 r_d^4$ causes the configurations that are close to the sphaleron but have a somewhat higher energy to make the dominant contribution to the tunnelling. The relevant parameter here is the characteristic decay length of the wave function, which in turn is determined by the rise of the potential in the transverse directions.

Although we are primarily interested in the case $\theta = 0$, an appreciable dependence on θ for a certain value of f shows that the non-perturbative influence of the boundary has become important. To explain the fact that the spectrum is not exactly periodic in θ, note that our implementation of the θ dependence (eq. (5.3.27)) only has this periodicity in the limit $\beta \to \infty$. The volume effect described above implies that the relevant distribution $|\psi(r_c, r_d)|$ samples a piece of the boundary over which the phase difference already starts to depart from $e^{i\theta}$. This also implies that the results using the exact implementation of the boundary conditions for the case $\theta = \pi$ can be expected to differ from those using the method of eq. (5.3.27). Increasing β would improve the periodicity properties, but would not result in a better effective model: although it would be less apparent, the wave function would still be spread out over the boundary.

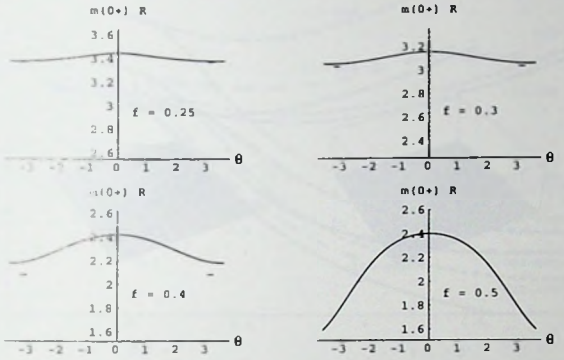

Figure 5-5. Scalar glueball mass at $f = 0.25$, $f = 0.3$, $f = 0.4$ and $f = 0.5$ as a function of θ. The dashes at $\theta = \pm\pi$ denote the variational result with exact implementation of the boundary conditions. Note that the vertical range in these four plots is the same.

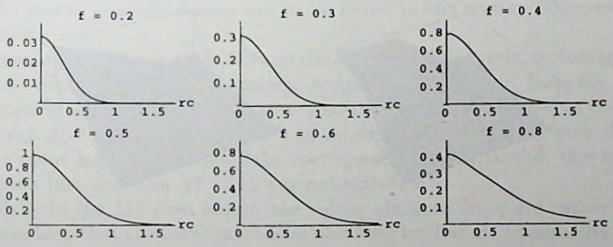

Figure 5-6. The wave function $\Psi \propto |\psi(r_c, r_d)|/(r_c^4 r_d^4)$ plotted at $r_d = \sqrt{3}$ for the ground state in the sector 000-even.

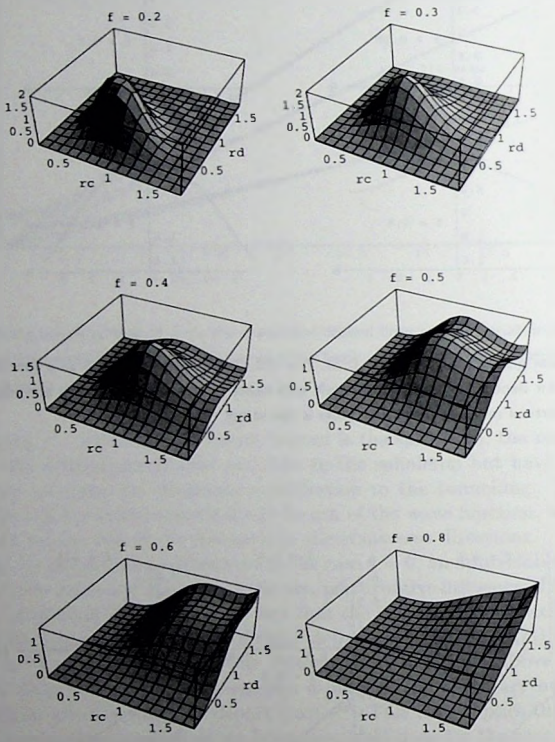

Figure 5-7. The distribution $|\psi(r_c, r_d)|$ for the ground state in the sector 000-even.

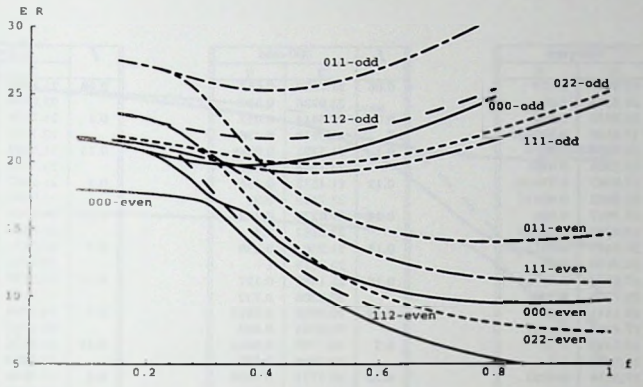

Figure 5-8. One-loop results. Lowest energy levels in various sectors. Going up at $f = 0.6$ we have:
Drawn curves: 000-even, 000-even, 000-odd.
Dashed curves: 112-even, 022-even, 022-odd, 112-odd.
Long-short dashed curves: 111-even, 011-even, 111-odd, 011-odd.

5.6.2 One-loop hamiltonian

We present basically the same plots for the one-loop hamiltonian as for the lowest order hamiltonian. Thus fig. 5-8 gives an overview of the lowest energy levels. As before, the lowest glueball masses are to be found in the sectors 000-even, 000-odd and 112-even.

The raw data is given in table 5-9 and the corresponding levels, including the lower bounds and the perturbative expansions, are plotted in fig. 5-9. Note the avoidance of level crossing between the ground state and the first excited stated in the 000-even sector, which give rise (cf. eq. (5.1.11)) to relative large errors for even the ground state. If a point is plotted without the corresponding lower bound, this means that the condition just above eq. (5.1.11) was not satisfied.

Especially in the 112-even sector, the values obtained for η are rather large. We like to stress here that the lower bounds as obtained by Temple's inequality are rather conservative and that the actual error is often much smaller. This insight is gained in studying toy models, but the effect can also be observed in the case at hand. Going from $L_{\text{sum}} = 12$ to $L_{\text{sum}} = 14$ in the 112-even sector, the upper bounds shifted very little, whereas a reduction of the η value by a factor of two was achieved.

It is to be expected that for the one-loop hamiltonian a larger number of basis vectors is required, since the potential has a more complicated structure in this case

f	000-even	
	γ	η
0.06	17.9777	0.153
	21.8578	1.95
	23.9076	0.926
0.08	17.9527	0.000894
	21.7006	0.0272
	23.7995	0.0481
0.1	17.9247	6.57e-05
	21.5903	0.00417
	23.7017	0.035
0.15	17.8232	0.00029
	21.2421	0.0313
	23.3190	0.33
0.2	17.6702	0.00255
	20.7239	0.296
	22.1441	3.41
0.25	17.4464	0.0107
	19.5425	1.15
	21.0058	1.6
0.275	17.2818	0.0323
	18.6999	1.21
	19.6693	2.36
0.3	16.9944	0.208
	17.6871	1.23
	18.7510	1.2
0.325	16.2095	0.824
	17.0077	0.452
	18.2462	0.65
0.35	15.1460	0.77
	16.5987	0.292
	17.3844	1.99
0.375	14.1275	0.743
	16.1017	1.23
	16.2342	0.717
0.4	13.1731	0.589
	15.0631	1.25
	15.8264	0.391
0.425	12.2963	0.613
	14.1701	1.04
	15.4917	0.862
0.45	11.4773	0.419
	13.4143	0.874
	15.1224	0.364
0.5	10.0548	0.306
	12.2216	0.641
	14.5172	0.39
0.55	8.9018	0.771
	11.4215	1.97
	14.0219	1.2
0.6	7.9189	0.555
	10.7487	1.51
	13.5224	1.24

f	000-odd	
	γ	η
0.06	21.7950	0.667
	23.9236	0.889
0.08	21.6814	0.052
	23.8519	0.436
0.1	21.5751	0.0888
	23.7888	0.661
0.12	21.4573	0.155
	23.7120	0.98
0.14	21.3272	0.249
	23.6182	1.4
0.15	21.2361	0.259
	23.3619	1
0.16	21.1486	0.127
	23.2368	0.732
0.18	20.9686	0.0672
	22.9994	0.593
0.2	20.7745	0.0814
	22.7928	0.583
0.22	20.5721	0.0986
	22.6409	0.53
0.24	20.3742	0.103
	22.5473	0.554
0.25	20.2808	0.0888
	22.5101	0.436
0.26	20.1936	0.0786
	22.4813	0.352
0.28	20.0406	0.0632
	22.4344	0.252
0.3	19.9197	0.051
	22.3841	0.2
0.35	19.7661	0.0297
	22.2169	0.144
0.4	19.8148	0.0183
	22.1005	0.106
0.45	20.0405	0.0122
	22.1388	0.073
0.5	20.4158	0.00884
	22.3490	0.0486
0.55	20.9163	0.00699
	22.7130	0.0331
0.6	21.5211	0.00603
	23.2062	0.0238
0.65	22.2131	0.0056
	23.8057	0.0183
0.7	22.9783	0.0055
	24.4925	0.0153
0.75	23.8052	0.00561
	25.2516	0.0135

f	112-even	
	γ	η
0.08	21.8509	0.0619
	23.8422	0.111
0.1	21.7836	0.0272
	23.7701	0.136
0.15	21.5604	0.0641
	23.5225	0.378
0.2	21.2267	0.102
	23.0188	0.61
0.25	20.6308	0.693
	21.6456	4.09
0.3	18.2875	3.83
	19.7954	2.74
0.35	16.0137	2.29
	17.2296	3.12
0.4	14.0859	1.38
	15.0787	2.73
0.45	12.4516	1.08
	13.5250	2.25
0.5	11.0848	0.893
	12.3763	1.42
0.55	10.0241	1.4
	11.5789	1.41
0.6	9.1387	1.13
	10.9561	1.04

Table 5-9. One-loop results. Raw data for the lowest levels in the sectors 000-even, 000-odd and 112-even.

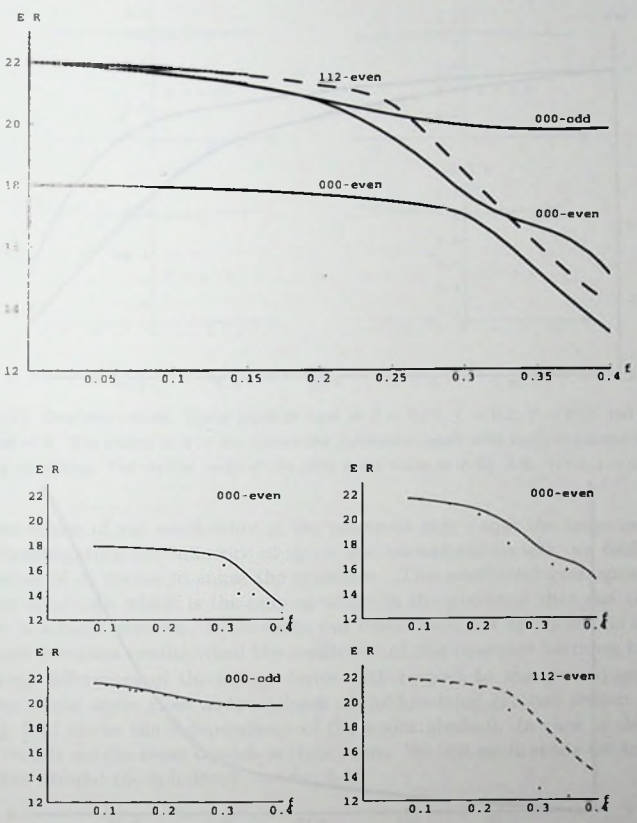

Figure 5-9. One-loop results. Lowest energy levels for $\theta = 0$. Drawn curves correspond to levels in the $(0,0,0)$ sector. The dashed curve denotes the ground level in the $(1,1,2)$-even sector, the short-dashed curves are the perturbative expansions. The four small plots also show the lower bounds (individual dots) as obtained by Temple's inequality.

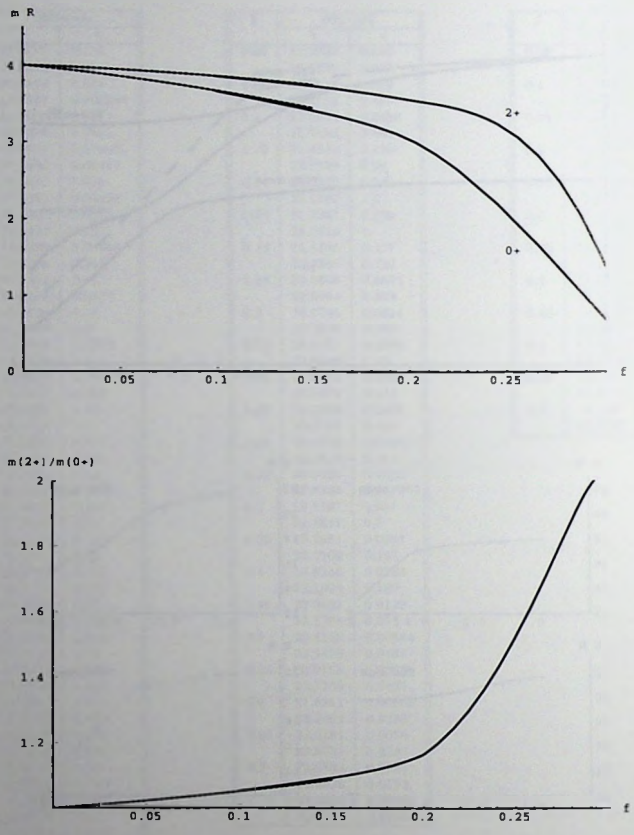

Figure 5-10. One-loop results. Glueball masses for $\theta = 0$ as a function of the coupling constant. In the upper plot, the lower and upper drawn curves are the masses of resp. the first scalar (0^+) and tensor (2^+) glueball. The dotted lines denote the perturbative results. The lower plot shows the tensor to scalar mass ratio.

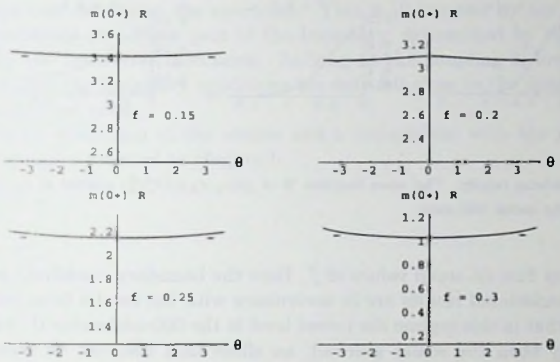

Figure 5-11. One-loop results. Scalar glueball mass at $f = 0.15$, $f = 0.2$, $f = 0.25$ and $f = 0.3$ as a function of θ. The dashes at $\theta = \pm\pi$ denote the variational result with exact implementation of the boundary conditions. The vertical range of the plots is the same as in fig. 5-5.

Also the values of the coefficients in the potential may cause the large values of η. When investigating the influence of λ_i on the variational results, we find that the large value of λ_8 seems to cause the problems. This coefficient corresponds to the operator $\mathrm{inv}_2(c,d)$, which is the only operator in the potential that can change the l_3 value of a basis function. Apparently, our basis could not be chosen so large as to yield high-precision results when the coefficient of this operator becomes large.

Taking differences of the energy levels with respect to the ground state in the 000-even sector again gives us the masses of the low-lying glueball states: see fig. 5-10. Fig. 5-11 shows the θ dependence of the scalar glueball. In view of the remarks above, we left out the lower bounds in these cases. We can again study the localization properties around the sphaleron: see fig. 5-12.

5.6.3 Discussion

Using the Rayleigh-Ritz method we can determine the spectrum of the effective hamiltonians. The use of Temple's inequality gives us confidence that our results are accurate, especially since experience tells us that the actual error is usually much smaller than the conservative estimates based on the values of η. The results are also consistent with the strong coupling limit and with a weak coupling perturbative expansion that was done up to $\mathcal{O}(f^3)$.

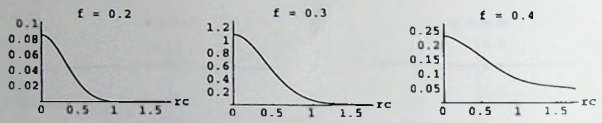

Figure 5-12. One-loop results. The wave function $\Psi \propto |\psi(r_c, r_d)|/(r_c^4 r_d^4)$ plotted at $r_d = \sqrt{3}$ for the ground state in the sector 000-even.

Let us focus first on small values of f. Here the boundary conditions are not felt yet, and the variational results are in accordance with the results from perturbation theory. Note that in this regime the lowest level in the 000-odd sector 0^- has actually a lower energy than the scalar glueball, an effect that also can be seen from the perturbative evaluation of the energy levels. This we expect to be a consequence of the strong finite size effects that are visible at small values of f.

When f grows, we see the effect of the boundary conditions in field space set in. For even larger f, the wave function has spread out over the entire (r_c, r_d) plane, and the model has lost its validity. It is however possible that this already happens before this point because of a break down of the adiabatic approximation. In order for the adiabatic approximation to be valid, the wave function for the transverse modes must still be in its ground state. To check this for the modes outside the (c, d) space is hard, but transverse to the tunneling path we can examine the transverse modes within the (c, d) space. Fig. 5-6 and 5-12 do not only show the localization of the transverse wave function at the sphaleron, but also indicate that this transverse wave function is in its ground state. We therefore assume that the adiabatic approximation is valid, and that values of the coupling constants for which our effective model is useful are determined by the spreading out over the (r_c, r_d) plane.

From these considerations, we derive the following windows in the coupling constant. For the lowest order hamiltonian, the interesting window is between $f = 0.3$ and $f = 0.5$. For the one-loop case, it is between $f = 0.2$ and $f = 0.3$.

One of the issues raised above was the level of localization of the wave function around the sphaleron. This is related to the question whether the assumption is true that only the boundary conditions at and near the sphalerons are felt. We argued that this was determined by the rise of the potential in the transverse directions. The one-loop correction to the $\mathrm{tr}(Y)$ term in the potential at the c sphaleron, which can be expressed in κ_1, κ_7 and κ_8, is such that it results in a lesser degree of localization. In both the lowest order and the one-loop case, a strong localization of the wave function around the sphaleron is not realized and the boundary conditions are not felt *exclusively* at the sphalerons. This should not come as a big surprise since it is unnatural for an eigenvalue problem that the spectrum is determined by boundary

conditions at a finite number of points. Typically the conditions at a boundary with codimension one determine the spectrum. This is illustrated by our problem: we feel the conditions at a finite part of the boundary, determined by the localization potential in the transverse directions. As long as the coupling is low enough, our assumption that the boundary conditions are only felt close to the sphalerons is true and the results are valid.

For a fuller discussion of the results and a comparison with the results on the torus, the reader is referred to chapter 6.

6 Conclusions

6.1 Summary

The goal of this thesis was to calculate the glueball spectrum on S^3. In particular, we set out to study the effects of the topology of the configuration space on the spectroscopy. These effects can be seen as the results of the presence of instantons. To this end we developed the effective theory of the low-energy modes in chapter 2. Using a Born-Oppenheimer approximation, we integrate out the fast modes of the full theory and are left with an effective quantum mechanical problem for the slow modes. We used the hamiltonian method to argue the validity of this approach, although a lagrangian method was used to calculate the influence of the high-energy modes.

Chapter 3 focused on the intersection of the fundamental domain with the space of low-energy modes. We can impose gauge invariance on the theory by restricting the dynamics to this fundamental domain. When choosing explicit coordinates in the configuration space of a gauge theory, one encounters various coordinate singularities. The Gribov horizon is the locus in configuration space where these coordinate singularities first, in the sense of perturbation theory, show up. The fundamental domain screens most parts of the Gribov horizon from the dynamics, so that we need not resolve the singularities that occur there by choosing other coordinates. There are however so-called singular boundary points: here the boundary of the fundamental domain and the Gribov horizon touch. Using bounds on the fundamental domain, we explicitly constructed singular boundary points. We argued that in the dynamical region we are interested in, these points will not influence the dynamics.

The influence of large gauge transformations, Gribov copies and the θ parameter is taken into account by imposing boundary conditions at the boundary of the fundamental domain. Dynamical arguments showed that we had some freedom in choosing the boundary conditions.

In chapter 4 we performed the calculation of the one-loop effective lagrangian. After renormalization, one can extract the correction to the lowest order effective hamiltonian. Our renormalization scheme, defined by eq. (4.5.1), can be related to other schemes like the MS or $\overline{\text{MS}}$ scheme.

In chapter 5 we calculated the spectra of both the lowest order (or truncated) hamiltonian and of the one-loop corrected hamiltonian. The method consisted of defining proper boundary conditions and constructing a basis of functions that respect these conditions. The matrix of the hamiltonian with respect to a truncation of this basis was subsequently diagonalized numerically. Using the Rayleigh-Ritz method we determined the spectra of the effective hamiltonians.

Summarizing the results, we can conclude that we managed to calculate the low-lying glueball states on the three-sphere in the effective model accurately.

6.2 Discussion

It is important to emphasize one should not expect our results for the spectrum to be accurate for large volumes. For large volumes the effects of the non-trivial topology and geometry (curvature of the configuration space, not to be confused with the curvature of S^3) become too strong to be described by the effective theory. Within the effective theory we clearly observe that at large coupling the wave functional will start to feel more of the boundary of the fundamental domain than just the neighbourhood of the sphaleron. However, it has been the main aim of this study to demonstrate that instanton effects on the low-lying spectrum are large, but calculable as long as energies remain close to the sphaleron energy, where nevertheless semiclassical techniques will completely fail.

The fact that $m_{0^+}R$ is decreasing, down from $m_{0^+}R = 4$, is what should be expected for the following reason. A rough estimate for where one should expect instantons to become relevant, based on what one finds on T^3, would be $m_{0^+}R \simeq 1.4$. Here we equate the largest geodesic distance on a torus of size L, $\sqrt{3}L/2$, to its value on S^3, πR, or

$$L = \frac{2\pi}{\sqrt{3}}R, \tag{6.2.1}$$

and we use that on T^3 instantons are relevant for $z \equiv m_{0^+}L > 5$ [36,37]. Furthermore, we assume that the scalar glueball masses are roughly equal in both geometries at these volumes. These low values of $m_{0^+}R$ are not reached in the tree level approach, but we do reach them in the one-loop case which shows that it was necessary to include the one-loop corrections. This regime of masses occurs for values of the coupling where we expect our model to still be valid. Specifically, $m_{0^+}R = 1.4$ corresponds to $f = 0.28$. At larger couplings, we clearly see that the wave functional feels too much of the boundary of the fundamental domain. For $f = 0.4$ this is dramatically clear from fig. 5-12, where the wave function is seen to probe unacceptable regions of the boundary of the fundamental domain to remain a good approximation to the full wave function. From fig. 5-9 we see that the scalar and tensor mass even cross around $f = 0.33$, which is certainly unacceptable for the full theory. Clearly we have pushed the model passed its region of validity for $f > 0.3$.

Of course, at some point $m_{0^+}R$ has to start to rise again, and when m_{0^+} reaches its asymptotic infinite-volume value, $m_{0^+}R$ grows linearly with R. Both the truncated and the one-loop results show that $m_{0^+}R$ exhibits a minimum, after which it starts to rise again. It rises linearly in f for $f \to \infty$, as follows from the strong coupling results in fig. 5-4, which are also valid for the one-loop case. This however does not mean that we are approaching the infinite-volume limit, because our effective model is certainly not fit to describe this regime. Moreover, it is clear that no statements can be made on the R dependence of f for these large couplings and volumes.

Other indications that our results are in the domain of expected validity are that at $f = 0.25$ the tensor to scalar mass ratio is given by 1.5, rising from 1 at zero coupling to 1.8 at $f = 0.28$, see fig. 5-10. For a torus geometry one finds a similar

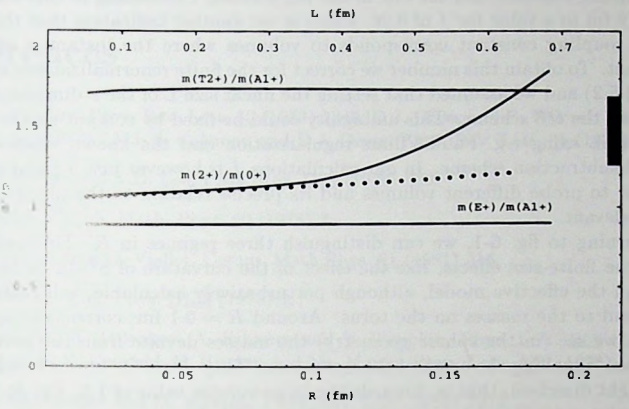

Figure 6-1. Comparison of the tensor to scalar mass ratio m_{2^+}/m_{0^+} as obtained on the three-sphere to the relevant ratios on the torus. The dotted line denotes the perturbative expansion, the bar on the right indicates the range of lattice Monte Carlo values at $L = 1$ to $L = 1.5$ fm.

range. Below $z = m_{0^+}L = 5$ the tensor is split into a doublet at $\sim 0.9m_{0^+}$ and a triplet at $\sim 1.7m_{0^+}$ [36,38] (due to breaking of rotational to cubic invariance), whereas these states seem to merge at $z > 7$ into a degenerate quintet with $m_{2^+} = 1.5m_{0^+}$.

We assume that in intermediate volumes the two-loop β function can be used to convert the dependence on the relevant coupling constants to the dependence on the radius R or the size L. Thus, for R we have ($f \equiv g^2/(2\pi^2)$)

$$(\Lambda_R R)^2 = \left(\beta_1 g^2\right)^{-\frac{\beta_2}{\beta_1^2}} e^{-\frac{1}{\beta_1 g^2}}, \quad \beta_1 = \frac{11}{24\pi^2}, \quad \frac{\beta_2}{\beta_1^2} = \frac{102}{121}, \tag{6.2.2}$$

and the same formula holds for $\Lambda_L L$ in terms of the minimal subtraction coupling $g_{\overline{\rm MS}}$. If we, as usual, set the scale by a string tension of $\sigma = (425\text{MeV})^2$ and use that $\sqrt{\sigma}/m_{0^+} \approx 0.3$ for T^3, we have that in physical units $z = m_{0^+}L = 5$ corresponds to $L = 0.7$ fm and hence, using eq. (6.2.1), to $R = 0.19$ fm. As derived earlier, this corresponds to $f = 0.28$ on the three-sphere, and eq. (6.2.2) gives $\Lambda_R = 1.3$ fm^{-1}. On the torus, $z = 5$ corresponds to $g_{\overline{\rm MS}} = 2.42$ [9]. Relating this to $L = 0.7$ fm gives $\Lambda_L = 0.39$ fm^{-1}. In this way we can compare our result for m_{2^+}/m_{0^+} as a function of the volume to the doublet E^+ and the triplet T_2^+ on the torus, as is shown in fig. 6-1. The vertical bar on the right indicates the range of lattice Monte Carlo values [38] for the E^+ and T_2^+ masses (equal within errors) at $L = 1$ to 1.5 fm.

Another way to relate the length scales above to a value of the coupling constant uses the definition of the running coupling constant in [39] and the relation between

this coupling constant and the one in the MS scheme. Proceeding in this way relates $R = 0.19$ fm to a value for f of 0.26, which is yet another indication that this regime for the coupling constant corresponds to volumes where the instanton effects are important. To obtain this number we correct for the finite renormalizations appearing in eq. (4.5.2) and we assumed that setting the linear size L of the ε-dimensional torus to R gives the MS scheme. This ambiguity could be fixed by computing the effective hamiltonian using e.g. Pauli-Villars regularization and the known relation to the minimal subtraction scheme. In our calculations f is however just a parameter that allows us to probe different volumes and its precise relation to the physical scale is not so relevant.

Returning to fig. 6-1, we can distinguish three regimes in R. For small R, we expect the finite-size effects, like the effect of the curvature of S^3, to be large. The masses in the effective model, although perturbatively calculable, will therefore not correspond to the masses on the torus. Around $R = 0.1$ fm, corresponding to $L = 0.36$ fm, we see (in the sphere geometry) the masses deviate from the perturbative expansion, signalling the onset of the instantons. They drive the tensor to scalar ratio in the right direction, that is, towards the large-volume value of 1.5. For $R > 0.2$ fm, our effective model is no longer valid, as discussed before.

Finally, an important goal of this project was to get results for glueball masses as a function of θ. The truncated results showed a pronounced dependence on θ in the regime where boundary effects are appreciable (see fig. 5-5). Quite remarkably, and unexpectedly, this strong dependence disappears when adding the one-loop corrections. In particular, at $\theta = 0$ and $\theta = \pi$, where boundary conditions can be implemented most accurately, the masses do not differ significantly (see fig. 5-11). Caution needs to be applied in concluding that the same will hold at large volumes, but in any case it would be interesting if glueball masses could be measured at $\theta = \pi$ on the lattice as comparison.

In conclusion, we should expect our one-loop corrected result to be a relatively accurate representation of the true masses on S^3 up to $f = 0.28$ corresponding to a circumference of approximately 1.3 fm, up to where also the variational basis does not exhibit too much of the problems with the Temple bound (cf. fig. 5-9). The approach to infinite-volume values (see also section 3.5 of chapter 3) of results on the three-sphere, as compared to torus results, is slow. We typically have a dependence on powers of $1/R$ as compared to an exponential behaviour in L [13]. As our results should not be expected to be already in the asymptotic domain, the rough agreement we find with results on the torus is gratifying.

When comparing the truncated and one-loop corrected results, the results for the θ dependence show that strong non-linear and non-perturbative effects influence the spectrum. We have shown there is a small, but finite window from $R = 0.1$ fm to $R = 0.2$ fm (at smaller volumes everything can be described perturbatively) where these effects can be included reliably, showing convincingly how important the global properties of the field space are for the non-perturbative dynamics of non-abelian gauge theories.

References

[1] H.D. Politzer, Phys. Rev. Lett. 30 (1973) 1346; D.J. Gross and F. Wilczek, Phys. Rev. Lett. 30 (1973) 1343; S. Coleman and D.J. Gross, Phys. Rev. Lett. 31 (1973) 851.

[2] N.M. Christ and T.D. Lee, Phys. Rev. D22 (1980) 939.

[3] I. Singer, Comm. Math. Phys. 60 (1978) 7.

[4] O. Babelon and C. Viallet, Comm. Math.Phys. 81 (1981) 515.

[5] V. Gribov, Nucl. Phys. B139 (1978) 1.

[6] A. Belavin, A. Polyakov, A. Schwarz and Y. Tyupkin, Phys. Lett. B59 (1975) 85; M. Atiyah, V. Drinfeld, N. Hitchin and Yu. Manin, Phys. Lett. A65 (1978) 185.

[7] F.R. Klinkhamer and M. Manton, Phys. Rev. D30 (1984) 2212.

[8] M. Lüscher, Nucl. Phys. B219 (1983) 233.

[9] J. Koller and P. van Baal, Nucl. Phys. B302 (1988) 1; P. van Baal, Acta Phys. Pol. B20 (1989) 295.

[10] A.S. Kronfeld, P. van Baal, Nucl. Phys. B (Proc. Suppl.) 9, (1989) 227.

[11] M. García Pérez et al, Nucl. Phys. B413 (1994) 535.

[12] P. van Baal and N.D. Hari Dass, Nucl. Phys. B385 (1992) 185.

[13] M. Lüscher, Comm. Math. Phys. 104 (1986) 177.

[14] R.E. Cutkosky, J. Math. Phys. 25 (1984) 939; R.E. Cutkosky and K. Wang, Phys. Rev. D37 (1988) 3024; R.E. Cutkosky, Czech. J. Phys. 40 (1990) 252.

[15] M.A. Semenov-Tyan-Shanskii and V.A. Franke, Zapiski Nauchnykh Seminarov Leningradskogo Otdeleniya Matematicheskogo Instituta im. V.A. Steklov AN SSSR, 120 (1982) 159. Translation: (Plenum Press, New York, 1986) p. 1999.

[16] D. Zwanziger, Nucl. Phys. B412 (1994) 657.

[17] G. 't Hooft, Phys. Rev. D14 (1976) 3432.

[18] R. Jackiw, in *Current algebra and anomalies*, (World Scientific, Singapore, 1985) p. 211.

[19] P. van Baal, Nucl. Phys. B351 (1991) 183.

[20] A.O. Barut and R. Raczka, *Theory of group representations and applications*, (Polish Scientific Publishers, Warsaw, 1977).

[21] P. van Baal, in *Probabilistic Methods in Quantum Field Theory and Quantum Gravity*, ed. P.H. Damgaard et al, (Plenum Press, New York, 1990) p. 131.

[22] G. Dell'Antonio and D. Zwanziger, in *Probabilistic Methods in Quantum Field Theory and Quantum Gravity*, ed. P.H. Damgaard et al, (Plenum Press, New York, 1990) p. 107; G. Dell'Antonio and D. Zwanziger, Comm. Math. Phys. 138 (1991) 291.

[23] P. van Baal, Nucl. Phys. B369 (1992) 259.

[24] S. Donaldson and P. Kronheimer, *The geometry of four manifolds*, (Oxford University Press, Oxford, 1990); D. Freed and K. Uhlenbeck, *Instantons and four-manifolds*, M.S.R.I. publ. Vol. I (Springer, New York, 1984).

[25] P. van Baal and R.E. Cutkosky, Int. J. Mod. Phys. A (Proc. Suppl.) 3A (1993), 323.

[26] S. Wolfram et al, *Mathematica*, (Addison-Wesley, New York, 1991).

[27] R.E. Cutkosky, private communication, November 1992.

[28] D. Zwanziger, Nucl. Phys. B378 (1992) 525.

[29] M. Lüscher, Ann. Phys. 142 (1982) 359.

[30] J.A.M. Vermaseren, *Symbolic manipulation with FORM*, (Computer Algebra Nederland, Amsterdam, 1991).

[31] C. Bloch, Nucl. Phys. 6 (1958) 329.

[32] A.R. Edmonds, *Angular momentum in quantum mechanics*, (Princeton University Press, Princeton, 1957).

[33] M. Reed and B. Simon, *Methods of modern mathematical physics*, vol. 4 (Academic Press, New York, 1978).

[34] T. Kato, J. Phys. Soc. Japan 4 (1949) 334.

[35] M. Abramowitz and I.A. Stegun, *Handbook of mathematical functions*, (Dover publications, New York).

[36] P. van Baal, Acta Phys. Pol. B20 (1989) 295.

[37] J. Hoek, Phys. Lett. B219 (1989) 92.

[38] B. Carpenter, C. Michael and M.J. Teper, Phys. Lett. B198 (1987) 511; C. Michael, G.A. Tickle and M.J. Teper, Phys. Lett. B207 (1988) 313.

[39] M. Lüscher, R. Narayanan, P. Weisz, U. Wolff, Nucl. Phys. B384 (1992) 168; M. Lüscher, R. Sommer, U. Wolff and P. Weisz, Nucl. Phys. B389 (1993) 247.

Nederlandse samenvatting

Niet-perturbatieve verschijnselen voor ijktheorieën op de drie-bol

Hoge-energiefysica is die tak van wetenschap die poogt de interacties tussen de elementaire bouwstenen der materie te verklaren. Er zijn vier fundamentele krachten in de natuur. In volgorde van oplopende sterkte zijn dit de zwaartekracht, de zwakke kracht, de elektromagnetische kracht en de sterke kracht. Van deze zijn de elektromagnetische kracht en de zwaartekracht het best bekend. De sterke kracht houdt atoomkernen bij elkaar, de zwakke kracht treedt op bij bepaalde soorten radioactief verval. Bij de vier krachten horen deeltjes die deze krachten overbrengen, de zogeheten krachtvoerende deeltjes. Dit zijn respectievelijk de gravitonen, de W- en Z-bosonen, de fotonen en de gluonen. Alle overige materie bestaat uit krachtvoelende deeltjes. Deze kunnen onderverdeeld worden in leptonen en hadronen: de hadronen zijn per definitie gevoelig voor de sterke kracht, de leptonen (bijv. elektronen, neutrino's) niet.

Van de leptonen neemt men aan dat het elementaire deeltjes zijn, terwijl men hadronen beschrijft als samengestelde deeltjes, opgebouwd uit quarks. Zo bestaan mesonen (bijv. pionen) uit een quark-antiquark paar, terwijl de zwaardere baryonen (bijv. protonen, neutronen) uit drie quarks bestaan. De sterke kracht houdt de quarks bijeen in de hadronen: een relatief zwakke restkracht is verantwoordelijk voor de samenklontering van protonen en neutronen tot atoomkernen. Dit is analoog aan de Van der Waals kracht tussen moleculen, die een overblijfsel is van de elektromagnetische kracht die de atomen binnen het molecule bindt.

Het grootste probleem binnen de theorie van de sterke wisselwerking is het opsluitingsprobleem. Dit is de observatie dat de quarks, in tegenstelling tot de leptonen, niet als vrije deeltjes in de natuur voorkomen, maar altijd opgesloten zitten binnen hadronen. Als men de hadronische toestanden in het deeltjesspectrum opbouwt uit quarks, is het noodzakelijk een nieuw quantumgetal in te voeren om aan het uitsluitingsprincipe van Pauli te voldoen. Dit quantumgetal noemt men kleur: het neemt de waarden rood, groen en blauw aan. De opsluitings- of confinement-eigenschap kan nu geherformuleerd worden door te stellen dat slechts kleurloze toestanden op kunnen treden als fysische deeltjes.

Algemeen wordt aangenomen dat quantumchromodynamica (QCD) de correcte theorie is voor de sterke wisselwerking. Deze theorie is een generalisatie van de theorie die op zeer nauwkeurige wijze elektromagnetisme beschrijft: de quantumelektrodynamica (QED). In beide theorieën zijn de fundamentele materievelden fermionvelden (elektronen resp. quarks) die wisselwerken met de bosonische ijkvelden (fotonen resp. gluonen). De ijkvelden zijn geassocieerd met een lokale symmetrie. In QED is de

lokale symmetriegroep U(1), corresponderend met elektrische lading. In QCD is SU(3) de lokale symmetriegroep, die met de kleurlading van de quarks correspondeert.

Een manier om voorspellingen te doen met QCD berust op storingsrekening. Dit is de methode die in het geval van QED zeer succesvol was. Men neemt aan dat de koppeling tussen gluonen en quarks zwak is, en voert vervolgens storingsrekening uit rond vrije quarks en gluonen. Hoewel quarks en gluonen niet in vrije toestand voorkomen, kan men zo toch op bevredigende wijze voorspellingen doen voor hoogenergetische botsingsprocessen met hadronen. De reden hiervoor is het verschijnsel van asymptotische vrijheid: bij hoge energie is de aanname van zwakke koppeling juist. Het opsluitingsprobleem en het berekenen van het hadronspectrum zijn echter zaken die niet binnen perturbatieve QCD aangepakt kunnen worden.

Een niet-perturbatieve aanpak van QCD is de roostermethode, waarbij de ruimtetijd gediscretiseerd wordt. Dit maakt de euclidische padintegraal voor de theorie goed gedefinieerd en men kan vervolgens de eigenschappen van het spectrum bestuderen door middel van methoden uit de statistische fysica. Met betrekking tot het opsluitingsprobleem heeft men de quark-antiquark potentiaal voor statische bronnen uitgerekend. Deze blijkt lineair te groeien met de afstand tussen de twee quarks, wat sterk wijst op opsluiting. Het beeld dat ontstaat is dat van een koord van gluonen tussen de twee quarks met een energie per lengte, of string tension, σ. Als de afstand tussen de twee quarks te groot wordt, breekt het koord. Hierbij wordt echter op het breekpunt een nieuw quark-antiquark paar gevormd, zodat de eindtoestanden weer kleurloos zijn.

Rooster-QCD heeft de laatste tien jaar veel successen gekend, maar veel problemen zijn nog niet opgelost. Zo vereist het simuleren van de volledige theorie (d.w.z. met dynamische quarks) nog steeds extreem veel computertijd. Bij het toepassen van roostermethoden op elektrozwakke processen stuit men op het probleem dat een eenvoudige beschrijving van chirale fermionen op het rooster nog niet gevonden is.

Het niet-abelse (niet-commutatieve) karakter van de ijkgroep SU(3) in QCD leidt tot zelf-interacties van de gluonen. Dit staat in schril contrast met de abelse theorie QED waar de fotonen geen (directe) zelf-wisselwerking hebben. Het gegeven dat gluonen onderling wisselwerken opent de mogelijkheid van een gebonden toestand van gluonen, een zogeheten glueball. Een andere manier om te zeggen dat gluonen behalve krachtvoerend ook krachtvoelend zijn, is om te zeggen dat ook zij kleurlading dragen. Een geschikte combinatie van gluonen kan een kleurloos object en dus een fysisch deeltje of resonatie vormen. Het bestaan van glueballs is derhalve ook een manifestatie van kleur-opsluiting. Hoewel er resonanties in het hadronische spectrum zijn die goede kandidaten zijn voor glueballs, kan men nog niet beweren dat glueballs in de natuur werkelijk bestaan.

In dit proefschrift wordt een systeem van wisselwerkende gluonen in een eindig volume bestudeerd. Aannemende dat confinement veroorzaakt wordt door het ijkgedeelte van QCD, kan men beginnen met de quarkvelden uit de theorie weg te laten. Dit betekent dat men de dynamica van het pure niet-abelse ijkveld (of Yang-Mills

veld) bestudeert. Het zich beperken tot een eindig volume geeft analytische mogelijkheden om niet-perturbatieve verschijnselen te bestuderen. Het mechanisme van asymptotische vrijheid maakt dat de koppeling klein is voor hoge energieën oftewel voor kleine afstanden. Door ijktheorie in een klein volume te bestuderen, blijft de koppeling klein en kunnen we storingsrekening toepassen. Door het vergroten van het volume kunnen we niet-perturbatieve effecten waaronder, hopelijk, confinement zien inzetten.

De dynamica van het ijkveld kan gezien worden als quantummechanica voor oneindig veel vrijheidsgraden. We reduceren de volledige theorie tot een effectieve theorie met slechts eindig veel vrijheidsgraden. Het idee achter deze effectieve theorie is de Born-Oppenheimer benadering uit de molecule-fysica. Men denke hier bijv. aan het waterstofmolecule H_2. Omdat de massa van de elektronen veel kleiner is dan die van de protonen, kunnen we de tijdschalen scheiden. Men lost eerst het Schrödingerprobleem op voor de twee elektronen in de potentiaal van de statische protonen. De verkregen energieniveau's hangen parametrisch af van de posities van de protonen. Deze energieniveau's dragen bij aan de potentiaal voor het Schrödingerprobleem van de protonen. Men zegt dat we de snelle modes (de elektronen) hebben uitgeïntegreerd en een effectief probleem in de langzame modes (de protonen) hebben overgehouden. De term 'uitintegreren' vindt zijn oorsprong in de formulering van de quantummechanica in termen van padintegralen.

De Born-Oppenheimer benadering kan in de veldentheorie gebruikt worden om een effectieve theorie te verkrijgen in een eindig aantal langzame modes. Hiertoe moet een oneindig aantal snelle modes uitgeïntegreerd worden. De effectieve theorie neemt de vorm aan van een Schrödingerprobleem, hetgeen betekent dat we van een quantummechanische hamiltoniaan op een zekere configuratieruimte het spectrum dienen uit te rekenen. Voor een niet-abelse theorie heeft de configuratieruimte een gecompliceerde topologische structuur: er kunnen niet-samentrekbare gesloten cirkels optreden.

Ter vergelijking met roosterresultaten is het verstandig voor het eindig volume dat van een torus te kiezen, d.w.z. een kubus met periodieke randvoorwaarden. Voor deze geometrie heeft men in het verleden de roosterresultaten kunnen reproduceren, waarbij de effectieve theorie een aantal niet-perturbatieve effecten meenam. De volgende stap zou zijn om de invloed van instantonen mee te nemen. Dit zijn configuraties van het ijkveld die samenhangen met tunnelingsprocessen tussen ijkkopieën van het vacuum. Alternatief kan men zeggen dat we de topologische structuur, in het bijzonder gesloten cirkels, van de configuratieruimte in rekening wil brengen.

In de torusgeometrie zijn deze effecten zeer moeilijk mee te nemen, reden waarom in dit proefschrift de geometrie van de drie-bol bestudeerd wordt. Dit betekent dat we voor het eindig volume het drie-dimensionale oppervlak van een bol in vier dimensies nemen. Ondanks het feit dat dit verder afstaat van roostersimulaties, kunnen we in deze geometrie wel de invloed van de instantonen, en in het bijzonder van de θ-hoek, bestuderen. Deze θ-hoek hangt samen met de niet-samentrekbare cirkels gesloten cirkels in de configuratieruimte. De θ-hoek is een vrije parameter van de theorie, en

we bestuderen met deze methode voor het eerst zijn invloed op de massa's van de glueballs. Voor de oneindig-volume limiet mag de keuze van het eindig volume, torus of drie-bol, niet uitmaken. Hierbij moet gezegd worden dat we binnen het huidige model deze limiet nog zeker niet kunnen nemen.

Hoofdstuk 1 bevat een introductie en een uitgebreidere omschrijving van de inhoud van dit proefschrift. In hoofdstuk 2 ontwikkelen we de nodige machinerie voor de analyse van ijktheorie op de drie-bol en we construeren daar in laagste orde de effectieve theorie voor de dynamica. In hoofdstuk 3 onderzoeken we de complicaties van het feit dat de ijkgroep niet-abels is. We leggen de ijkvrijheid vast via het gebruik van een fundamenteel domein. Voor de effectieve theorie betekent dit dat er zekere randvoorwaarden in de configuratieruimte worden opgelegd: deze randvoorwaarden bevatten de θ-afhankelijkheid.

In hoofdstuk 4 wordt de een-lus correctie op de laagste orde effectieve hamiltoniaan uitgerekend. Het bovengenoemde uitintegreren van de snelle modes wordt in dit hoofdstuk expliciet uitgevoerd. In hoofdstuk 5 worden met behulp van variationele methoden de spectra van zowel de laagste-orde als van de een-lus gecorrigeerde effectieve hamiltoniaan bepaald. De resultaten zijn de massa's van de diverse typen glueballs. Hoofdstuk 6 bevat een samenvatting en een bespreking van de resultaten. We beargumenteren dat de invloed van de instantonen groot, maar berekenbaar is. We bakenen het regime van geldigheid van de effectieve theorie af en laten zien dat de resultaten redelijk overeenstemmen met de resultaten die op de torus verkregen zijn.

List of publications

- B.M. van den Heuvel,
  Energy-momentum conservation in gauge theories,
  J. Math. Phys. 35 (1994) 1668.

- P. van Baal and B.M. van den Heuvel,
  Zooming-in on the SU(2) fundamental domain,
  Nucl. Phys. B417 (1994) 215.

- B.M. van den Heuvel and P. van Baal,
  Dynamics on the SU(2) fundamental domain,
  Nucl. Phys. B (Proc. Suppl.) 42 (1995) 823.
  Based on a talk presented at the 1994 Lattice Conference (Bielefeld, Germany, 26 Sept.-1 Oct. 1994).

- B.M. van den Heuvel,
  Glueball spectroscopy on S^3,
  Phys. Lett. B368 (1996) 124.

- B.M. van den Heuvel,
  One-loop effective action for SU(2) gauge theory on S^3,
  hep-lat/9604017, accepted for publication in Phys. Lett. B.

- B.M. van den Heuvel,
  Glueballs on the three-sphere,
  in preparation.

Curriculum vitae

Op 4 november 1969 werd ik geboren te Dubbeldam, thans Dordrecht. In 1987 behaalde ik aan het Christelijk Lyceum te Dordrecht het diploma VWO, waarna ik aan de studies wiskunde en natuurkunde aan de Rijksuniversiteit Leiden begon. In augustus 1988 behaalde ik beide propaedeutische examens. Mijn experimentele stage heb ik afgelegd in de groep quantumvloeistoffen o.l.v. prof.dr. G. Frossati. In augustus 1992 slaagde ik (cum laude) voor de doctoraalexamens wiskunde en natuurkunde. Het afstudeeronderzoek voor natuurkunde werd uitgevoerd o.l.v. prof.dr. F.A. Berends aan het onderwerp: "The process $e^+e^- \to W^+W^-Z$: an application of the Weyl-Van der Waerden formalism". Mijn afstudeeronderzoek voor wiskunde werd verricht aan het onderwerp "Energy-momentum conservation in gauge theories" o.l.v. dr. C.A.M. Peters. Tijdens mijn studie heb ik als student-assistent bij de subfacultateit wiskunde diverse werkcolleges verzorgd.

Per 1 september 1992 trad ik in dienst als assistent-in-opleiding bij de Rijksuniversiteit Leiden om bij prof.dr. P.J. van Baal promotieonderzoek te verrichten aan ijktheorieën in hamilton-formulering. Ik heb een werkcollege bij het vak "Quantumtheorie II" verzorgd en geassisteerd bij de werkgroep "Gravitatie". Tijdens mijn promotieperiode heb ik de volgende hoge-energiefysica scholen bezocht: de AIO-winterschool te Dalfsen (twee maal), de workshop "Strong interaction study days on topics in field theory" te Erlangen (Duitsland) en de zomerschool "Fluctuating geometries in statistical mechanics and field theory" te Les Houches (Frankrijk). Hiernaast heb ik drie maal deelgenomen aan de "International Conference on Lattice Field Theory" en wel te Amsterdam, Bielefeld (Duitsland) en St. Louis (Verenigde Staten).

Stellingen

1. Zij G een Lie groep met $\mathfrak{g}$ de bijbehorende Lie algebra. Zij k een Ad-invariante metriek op de algebra met geïnduceerde metriek g op de groep. Als $\{X_i\}$ een basis is van $\mathfrak{g}$, vormen de bijbehorende linksinvariante vectorvelden $\bar{X}_i$ op G een oneindigdimensionale representatie van $\mathfrak{g}$. Nu geldt dat de Laplace-operator Δ op G gelijk is aan de tweede Casimir-operator van deze representatie:

$$\Delta \equiv \frac{1}{|g|^{1/2}} \partial_\alpha \left(|g|^{1/2} g^{\alpha\beta} \right) \partial_\beta = k^{ij} \bar{X}_i \bar{X}_j.$$

Hiermee kunnen zonder keuze van lokale coördinaten uitdrukkingen voor de laplaciaan afgeleid worden.

R. Gilmore, Lie groups, Lie Algebras, and some of their applications, 1974. Hoofdstuk 2 van dit proefschrift.

2. Beschouw de harmonische oscillator met quasi-periodieke randvoorwaarden op $[-a, a]$:

$$\mathcal{H} = \frac{\hat{p}^2}{2m} + \frac{1}{2} m\omega^2 x^2, \quad \psi(a) = e^{-i\theta}\psi(-a), \quad \psi'(a) = e^{-i\theta}\psi'(-a).$$

De energieniveau's worden gegeven door $E = (\nu + \frac{1}{2})\hbar\omega$, met ν de oplossingen van de vergelijking

$$\psi_1'^{(\nu)}(\tilde{a})\psi_2^{(\nu)}(\tilde{a}) + \sin^2(\frac{\theta}{2}) = 0, \quad \text{met } \tilde{a} = \sqrt{m\omega/\hbar}\, a,$$

waarbij ψ_1 en ψ_2 zijn gegeven door

$$\psi_1^{(\nu)}(z) = e^{-\frac{1}{2}z^2} {}_1F_1(-\frac{\nu}{2}, \frac{1}{2}, z^2), \quad \psi_2^{(\nu)}(z) = z e^{-\frac{1}{2}z^2} {}_1F_1(\frac{1-\nu}{2}, \frac{3}{2}, z^2),$$

met ${}_1F_1$ de confluente hypergeometrische functie. Voor $\theta = 0, \pi$ zijn $\psi_1(\tilde{x})$ en $\psi_2(\tilde{x})$ (met $\tilde{x} = \sqrt{m\omega/\hbar}\, x$) de eigenfuncties, voor de overige waarden van θ wordt de eigenfunctie gegeven door

$$\cos(\frac{\theta}{2})\psi_2^{(\nu)}(\tilde{a})\psi_1^{(\nu)}(\tilde{x}) - i\sin(\frac{\theta}{2})\psi_1^{(\nu)}(\tilde{a})\psi_2^{(\nu)}(\tilde{x}).$$

3. Het gebruik van trial functies met beperkte drager bij een Rayleigh-Ritz berekening zoals voorgesteld door Burden en Faires, is af te raden.

R.L. Burden and J.D. Faires, Numerical Analysis, 1985.

4. Definieer de volgende integraal

$$F_d = \int_{-\pi}^{\pi} \frac{d^d\vec{l}}{(2\pi)^d} \frac{1}{2\sum_{i=1}^{d}(1-\cos(l_i))}.$$

Dan heeft F_d de volgende asymptotische expansie voor $d \to \infty$

$$F_d = \frac{1}{2d}\left(1 + \frac{1}{2d} + \frac{3}{4d^2} + \frac{3}{2d^3} + \frac{15}{4d^4} + \cdots\right).$$

5. Beschouw Yang-Mills ijktheorie met ijkgroep G en ijkinvariante actie $S[A]$. Na afsplitsing van het volume van de groep van ijktransformaties geldt voor de partitiefunctie

$$Z = \int DA \frac{e^{-S[A]}}{Z_{GF}[A]},$$

met $Z_{GF}[A]$

$$Z_{GF}[A] = \int Dg \exp\left\{\frac{1}{\alpha}\int d^4x \,\mathrm{tr}\left[g^\dagger \partial_\mu \partial^\mu g + 2g^\dagger A_\mu \partial^\mu g\right]\right\}.$$

Voor $G = \mathrm{SU}(2)$ kan Z_{GF} gezien worden als de partitiefunctie van een niet-linear σ-model.

D. Zwanziger, Nucl. Phys. B345 (1990) 461.
C. Parrinello and G. Jona-Lasinio, Phys. Lett. B251 (1990) 175.

6. Zij ψ een variationeel gevonden benadering van een eigentoestand van een hamiltoniaan H. Laat $\gamma = \langle\psi|H|\psi\rangle$ de bijbehorende bovengrens zijn voor de eigenwaarde E en $\eta = \langle\psi|(H-\gamma)^2|\psi\rangle$ een schatting voor de nauwkeurigheid. Hoewel bij een eindige uitbreiding van het aantal variationele basisfuncties γ gegarandeerd kleiner wordt of gelijk blijft, is het niet uitgesloten dat η groeit.

M. Reed and B. Simon, Methods of modern mathematical physics,vol. 4, 1978.

7. Bij het berekenen van de energie-impulstensor voor een ijktheorie met Diracvelden moet niet de metriek, maar de onderliggende spinstructuur gevarieerd worden. Dit kan op bevredigende wijze in het bundelformalisme beschreven worden.

S. Weinberg, Gravitation and Cosmology, 1972.
B.M. van den Heuvel, J. Math. Phys. 35 (1994) 1668.

8. Een onderzoeker dient zich met betrekking tot zijn inspanningen bewust te zijn van de wet van de afnemende meeropbrengsten.

9. Het hebben van uitgesproken meningen duidt op een geringe belangstelling voor nuancering.

10. Het huidige topvolleybal laat zien dat lichaamslengte ook voor spelverdelers van doorslaggevend belang is geworden.

11. Het muziekgenre 'progressive rock' is bijzonder behoudend.

12. Het stelen van fietsen zou verboden moeten worden.

Bas van den Heuvel
11 september 1996